Republic of Iraq
Ministry of Higher Education
And Scientific Research
University of Babylon
College of Engineering

Design of Dual-Band a Wearable patch Antenna for 5G Applications

A Thesis
Submitted to College of Engineering / University of Babylon in Partial Fulfillment of the Requirements for the Degree of master's in Electrical Engineering \ Communications

By
Shahlaa Yaseen Younis Alebady

Supervised by
Prof. Dr. Mohammed Taih Gatte

2023 A.D **1444 A.H**

يَرْفَعِ اللَّهُ الَّذِينَ آمَنُوا مِنكُمْ وَالَّذِينَ أُوتُوا الْعِلْمَ

دَرَجَاتٍ وَاللَّهُ بِمَا تَعْمَلُونَ خَبِيرٌ ﴿ 11 ﴾

سورة المجادلة

Supervisor Certification

I certify that this thesis entitled **"Design of Dual-Band a Wearable patch Antenna for 5G Applications"** is prepared by Shahlaa Yaseen Younis Alebady under my supervision at the Department of Electrical Engineering, College of Engineering, University of Babylon, as a partial fulfilment of the requirement for the degree of master's in Communications Engineering.

Signature:

Name: Prof. Dr. Mohammed Taih Gatte

(Supervisor)

Date: / / 2023

In view of the above recommendation I am forward this thesis for discussion by the Examination Committee.

Head of Department

Signature:

Name: Prof. Dr.

Date: / / 2023

Acknowledgements

First, I praise ALLAH Almighty for providing me this opportunity and granting the capability to proceed this thesis.

I would like to warmly thank and gratitude my father, my mother, brothers, sisters, and husband for their spiritual support in all aspects of my life.

I would like to express my profound gratitude and my respect to my supervisor: Assist. Prof. Dr. Mohammed Taih Gatte for his supervision, guidance and constant support.

I would like to thank all my friends for their friendship and encouragement during the period of the study. I also appreciate the help and support from all persons who are directly or indirectly involved in my project

Dedication

To my first supporter and Source of strength, which I always find in front of me, helping me in everything ……. My Father.

To Source of love and tenderness and the most incredible woman in my life ……. My Mother.

To my beloved, my supporter, and whoever has the great credit for my presence in this place ……. My Husband

My Jewels in Life……. My Sisters and Brothers.

To all my friends and people close to me who have a significant role.

I Dedicate This Work.

SHAHLAA

Table of Contents

List of Tables

List of Figures

List of Abbreviations

Abbreviation	Definition
AC	Aperture Coupling
BANs	Body Area Networks
CM	Cavity Model
CP	Coaxial Probe
CPW	Coplanar Waveguide
CST	Computer Simulation Technology
FWM	Full Wave Model
GPS	Global Positioning System
HFSS	High Frequency Simulation Software
HIPERLAN	High-Performance Radio Local Area Network
IoT	Internet Of Things
LAN	Local Area Network
ML	Microstrip Line
MS	Microstrip
PC	Proximity Coupling
PCB	Printed Circuit Board
PC-MSPA	Proximity-Coupled Microstrip Patch Antenna
RT	Return Loss
SL	Strapline
SMA	Subminiature Version A
TLM	Transmission Line Model
VSWR	Voltage Standing Wave Ratio
WBAN	Wireless Body Area Network
WLAN	Wireless LAN

List of Symbols

Item	Description
C	Speed Of Light
Dir	Directivity
fr	Frequency Resonance
G	Gain
P_{rad}	Radiated Power
S11	The Absolute Value Of Return Loss
Γ	Return Loss
η	Radiation Efficiency
ηr	Radiation Efficiency
λ	Resonance Wavelength

ABSTRACT

The rapid development of wearable applications based on 5G networks has led to an urgent need for specific antenna types. These antennas must have low power consumption, small size, great flexibility, and other features. Thus, the microstrip antenna is the best choice for these applications. In this thesis, a dual band antenna has been presented for 5G wearable applications. The proposed antenna operates in 6GHz and 28GHz frequencies, which are within the 5G frequency bands. The antenna design is simulated and validated by two-simulation softwares: Computer Simulation Technology (CST-Studio) and High-Frequency Simulation Software (HFSS).

The Arlon AD 250C, Rogers RT/droid 5880(tm), and FR4 materials are used as substrates, in addition to the copper as a patch and ground. The simulation results show that the Rogers RT/droid 5880(tm) material has the better performance compared to other materials. However, the FR4 material is used in the fabrication process due to the unavailability of the Rogers RT/droid 5880(tm) in the Iraqi materials.

The propose antenna has been designed with four feeding methods: Microstrip line, Coaxial (coplanar feed), Proximity coupled, and Aperture coupled. The simulation results shows that the Aperture coupled method has the best results over the other methods. Where, the antenna parameters with the Aperture coupled method are determined as follows: S11 values are -69.2dB and 23.2dB at 6GHz and 28 GHz, respectively, in addition, VSWR values are 1.006 dB and 1.14 dB at 6GHz and 28 GHz, respectively. Furthermore, the gain and efficiency values are (3.72 dB & 65.7%) and (7.07 dB & 97.5%) for 6GHz and 28 GHz, respectively. These results and other are compared with some literature results and this

comparison shows that the proposed antenna outperforms the previous works.

The folding ability of the proposed antenna has been tested by bending it on cylinders with different radii. Where, the simulation results show that the folded antenna versions have the same performance as the original one. Finally, the fabrication results show the fabricated antenna has a problem due to the air gap between the antenna's substrates, which left because the hardiness of the FR4 material. However, the performance of the fabricated antenna has been corrected by compressing the both substrates during the test process.

Chapter One

Introduction

CHAPTER ONE

INTRODUCTION

1.1 Background

In wireless signal propagation, the microstrip antenna is an important component in data communication that can be transmitted by sending the signal from one antenna to another using airspace, as shown in Figure (1.1). wearable devices are one of the leading technologies used in the development of our lives. The main characteristic of a microstrip patch antenna is compact, lightweight, low cost, easy to fabricate, and suitable for flexible applications [1] . The concept of the flexible antenna is to replace the solid substrate associated with the copper layer with a flexible substrate that can be folded easily. Using materials substrates like polymer, rubber, paper, plastic, etc., gives flexibility to the fabricated antennas based on these materials. The antenna offers attractive solutions in various fields, such as health, entertainment, and sports [2] .

In health, for example, Wearable devices can collect patient information (steps, blood pressure, temperature, heart rate, calories, and even glucose)and send to nearby terminal (extracorporeal communication between a device on the patient and any other communication device on the other end) via body area networks (BANs), A wearable patch antenna provides an essential component of a wireless body area network (WBAN). the Most applications of the wearable antenna are 5G Communication Systems, Wireless Communication, Medical, Internet of Things (IoT), High-Performance Radio Local Area Networks (HIPERLAN), Military Applications, Global Positioning Systems (GPS), and Wireless LAN (WLAN)[3] .

The advent of 5G has allowed data to be transmitted in larger quantities, that recently considered the best option for wireless communications. This technology has provided many opportunities, as it will work to advance the current communication technology even further. The 5G has two bands of frequencies, microwaves and millimetre waves, which leads to different characteristics and advantages [4].

Figure 1.1: How to transmit the signal from one antenna to another

1.2 Problem Statement

The recent applications in medicine and IOT require high data rate communication, which can be achieved via using of the dual bands of 5G technologies, which employ higher frequencies (millimetre wave), besides the frequencies that are used in the lower generations(GSM, 3G, and 4G).

1.3 Objectives

I. To design an antenna for medical and IOT applications
II. Design a dual bands antenna operating at 6GHz and 28GHz frequencies.
III. To study the effect of the feeding method on the proposed antenna
IV. To study the effect of the folding on the proposed antenna design using different radii
V. To fabricate the proposed antenna, test the manufactured one, and compare the measured with the simulated performance parameters.

1.4 Organization of the Thesis

Chapter 1: An introduction to the thesis, including the main vital problems and the objectives that must be addressed in this thesis.

Chapter 2: presents a review of the related literature of the previous works and a comprehensive review of the microstrip antenna and its analysis, as well as clarifying the main equations for calculating the dimensions. Besides, antenna feeding is also presented and compared between the feeding methods; this chapter also explains the most critical parameters.

Chapter 3: explains the methodology of design, the algorithm of work, and the dimensions of the proposed antenna using three feeding methods, as well as the shape of the antenna after bending with different radii, besides the manufacturing process.

Chapter 4: Shows the simulation results, the practical side, and a discussion of the most critical parameters, such as S11, VSWR, gain, and directivity. This chapter also shows the results of the manufacturing process and compares them with the simulation results.

Chapter 5: presents conclusions and suggestions for future work to enhance scientific research.

References

Appendix

Chapter Two

THEORY AND LITERATURE REVIEW OF 5G ANTENNAS

CHAPTER TWO

THEORY AND LITERATURE REVIEW OF PATCH ANTENNAS

2.1 Introduction

Due to the requirements of the existed and planned applications, 5G networks have attracted substantial attention. Radars, scanners, higher band 5G networks, short-range wireless networks, and many other applications are examples of these current and future applications. Due to the rising popularity of social media, the current need for high-quality multimedia material, and the requirement for networks that can manage very high data rates, 5G networks are now necessary [5]. To meet the demands of 5G networks, small antennas with wideband and improved beam shaping are needed. Planar dual-band antenna architectures like coplanar waveguide (CPW), strapline (SL), and microstrip (MS) have thus become very popular antennas in comparison to conventional wire antennas (yagi-Uda, helical, and spiral) [6].

Additionally, there is much interest in creating a powerful microstrip patch antenna to achieve the required performance at the effective operating frequency within millimeter wave systems[7]. The Microstrip patch antenna offers many advantages with good results compared to other antennas. Microstrip patch antennas have replaced conventional antennas in many applications due to their lightweight, wearability, ease of fabrication, and small size [8]. Before implementing a prototype antenna mounted on a strip, the substrate of any proposed design can be validated using simulation software like Computer Simulation Technology (CST-Studio) and High-Frequency Simulation Software (HFSS). The microstrip antenna

design depends on the operating frequency and the theory of antenna design parameters [9].

2.2 Microstrip Antenna

The microstrip antenna considers an ideal choice for good performance, lightweight, small size, and cheap manufacturing cost. Moreover, the microstrip antenna is suitable for planar or nonplanar surfaces, as shown in Figure 2.1. The simplest form of this antenna consists of two parallel layers of conductive material separated by a thin layer of dielectric material of thickness h, permeability μ_o (usually μ_o=1), and relative dielectric permittivity ε_r. The lower conductor acts as a ground plane, and the upper conductor acts as a radiator; the primary function of the bottom metal layer is to work as a shield, preventing antenna radiation from being reflected off structures around it. In most cases, the system is not restricted to a single layer; instead, additional layers can be placed below the ground plane layer to provide support for the feed network[3].

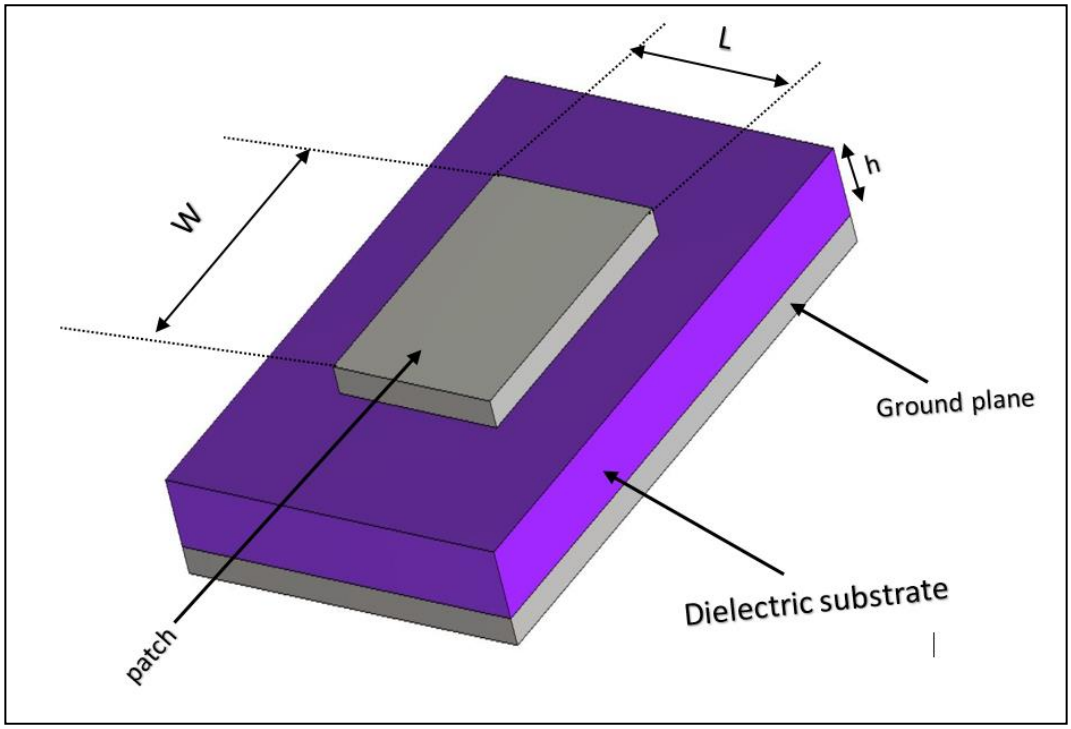

Figure 2.1: Structure of microstrip patch antenna[10]**.**

Where (L) is the length of the patch, (h) is the height of the substrate,(W) is the width of the patch .

There are many shapes of radiating patch such as square, rectangular, circular ,and so on. The radiating patch can be designed in any shape and it has no limitation. Figure 2.2 shows the various types of geometric structures of the microstrip patch antenna [11].

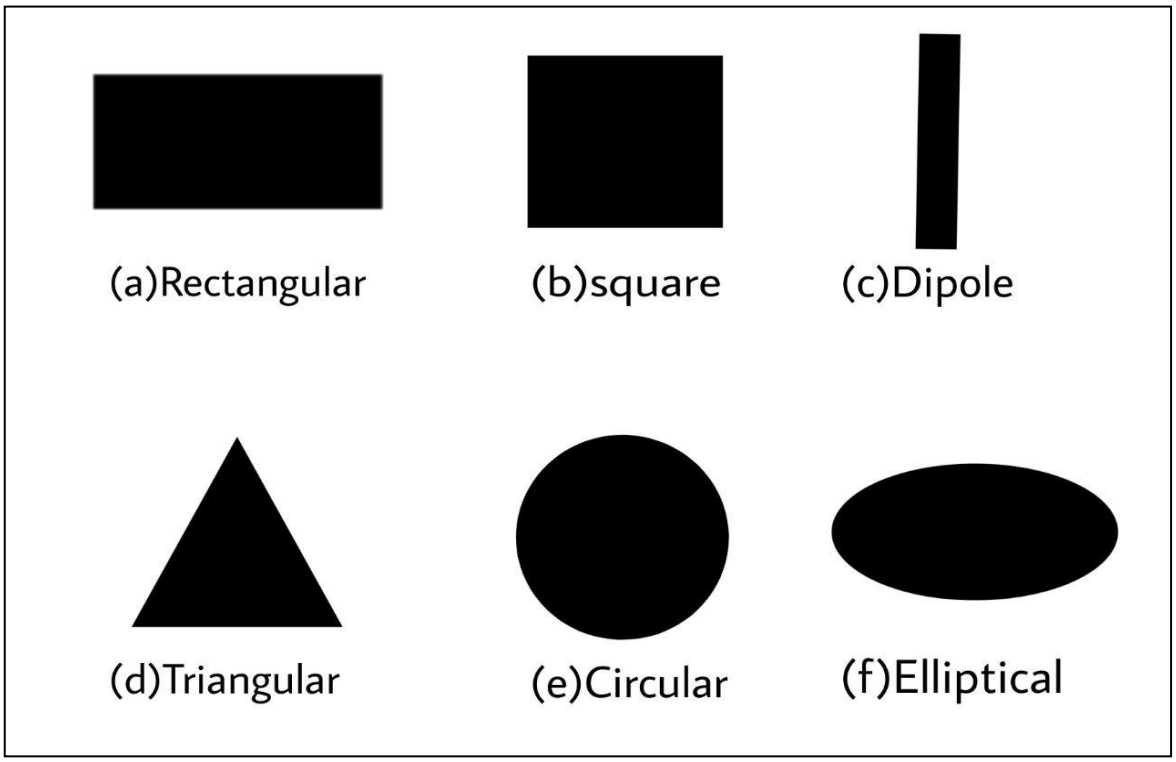

Figure 2. 2: The Conventional shapes of microstrip patch elements

2.3 Antenna Analysis

There are many methods of analysis for microstrip antennas. The most popular models are the transmission line model (TLM), cavity model(CM) , and full wave model(FWM). The transmission-line model is the easiest of all, it gives good physical insight, but is less accurate and it is more difficult to model coupling . Compared to the transmission-line model, the cavity model is more accurate but at the same time more complex. However, it also gives good physical insight and is rather difficult to model coupling. the full-wave models are very accurate, very versatile, and can

treat single elements, finite and infinite arrays, stacked elements, arbitrary shaped elements, and coupling. However they are the most complex models and usually give less physical insight[12].

In figure 2.3 the non-homogeneous electric field lines are shown. As can be seen, most of the field lines reside in the substrate and parts of some lines exist in air. Fringing in this case makes the microstrip line look wider electrically compared to its physical dimensions. Since some of the waves travel in the substrate and some in the air, an effective dielectric constant ε_{reff} is introduced to account for fringing and the wave propagation in the line.[13].

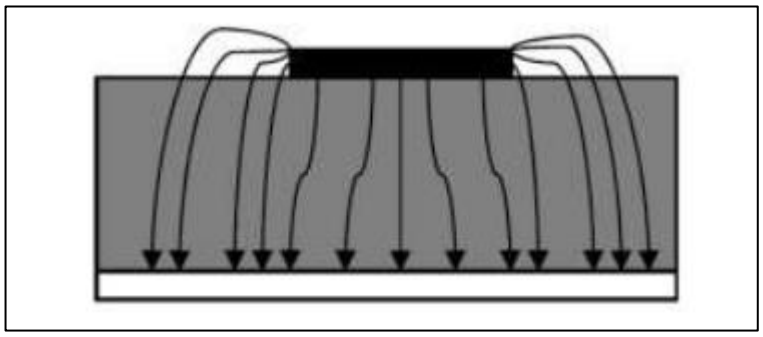

Figure 2. 3: Dielectric Field Lines

The value of ε_{reff} is slightly smaller than ε_r since the fringing fields around the periphery of the patch are not confined in the dielectric substrate, but also spreading the as shown in Figure 2.6[14].

The effective dielectric constant is calculated as shown in the equation below [9]:

$$\boldsymbol{\varepsilon_{reff} = \frac{\varepsilon_r+1}{2} + \frac{\varepsilon_r-1}{2}\left[1 + 10\frac{h}{w}\right]^{-0.5}} \qquad \boldsymbol{\ldots\ldots\ldots\ldots 2\text{-}1}$$

Where:

ε_r = relative permittivity

h= the patch substrate thickness

W= width of the patch

The main dimensions to analyze are the L and W of the patch and the thickness of the substrate material. Because the patch dimensions are limited to the width and length of the patch, as in Figure 2.4.

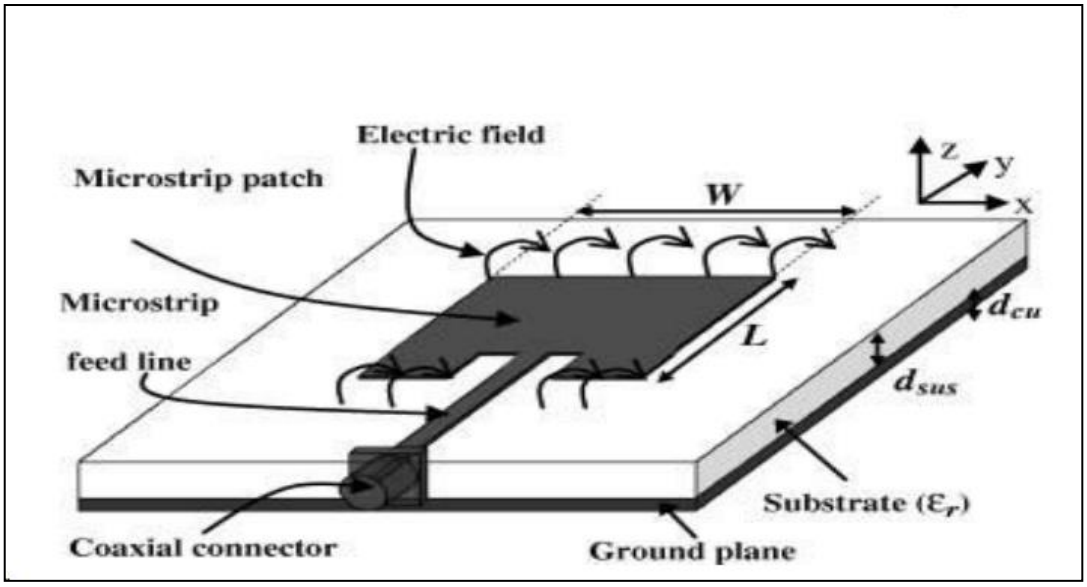

Figure 2.4: Microstrip antenna [10]

The fringing is the length-to-height ratio of the patch (*L*/*h*), and this ratio is better to be much larger than one, which reduces the fringing of the field, This aspect must be taken into account because it affects the frequency of the antenna.

Because of the fringing effects, electrically the patch of the microstrip antenna looks greater than its physical dimensions, as shown in Figure 2.5. The extra length is called Length Extension (ΔL). The equation below shows how to calculate ΔL [14]:

$$\Delta L = \mathbf{0.412H}\frac{[\varepsilon_{reff}+0.3][\frac{W}{h}+0.264]}{[\varepsilon_{reff}-0.258][\frac{W}{h}+0.8]} \qquad \ldots\ldots\ldots\ldots \mathbf{2\text{-}2}$$

Where:

h= the patch substrate thickness

W= width of the patch

ε_{reff} = effective dielectric constant

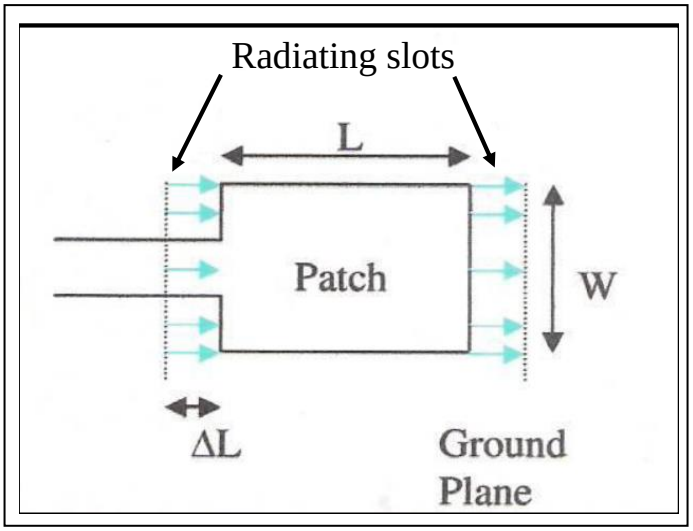

Figure 2.5: Radiating edges of microstrip patch antenna.

As mentioned previously, the length of the patch increased by ΔL, so the effective length (L_{eff}) that can be calculated via the following equation [11]:

$$\mathbf{L_{eff} = L + 2\Delta L} \qquad \text{..... 2- 3}$$

For a given resonant frequency, the effective length can be calculated using the equation below: [9]

$$\mathbf{L_{eff} = \frac{C}{2f_r\sqrt{\varepsilon_{reff}}}} \qquad \text{..... 2- 4}$$

Where f_r = Operating frequency

C = The speed of light in vacuum

The correction width can be calculated as shown in the equation below [15]:

Patch Width (W)

$$W = \frac{1}{2f_r\sqrt{\mu_0\varepsilon_0}}\sqrt{\frac{2}{\varepsilon_r+1}} \qquad \text{..... 2- 5}$$

Where f_r = Resonant frequency

μ_0 = Permeability in free space

ε_0 = permittivity in free space

ε_r = relative permittivity

2.4 Materials of Substrates

In the design process of a microstrip antenna, one of the important factors is the selection of substrate that mainly depends on the features like cost, dielectric constant, ease of manufacturing (easy cutting, drilling, and forming), thermal conductivity, expansion, and dielectric loss [3].

The operating temperature affects the substrate's dimensions and dielectric constant, which must be considered when making any microstrip patch antenna. The main physical properties in the antenna manufacturing process are chemical resistance, bending ability, formability, shock resistance, structural strength, elastic mechanical power, and substrate properties when coated [13].

There are two common types of substrates: flexible and Rigid. Flexible substrates are easy to manufacture yet have a higher coefficient of thermal expansion. Due to these flexible materials, wearables have become a reality. flexible substrate enables printed circuitry to insert into tight areas and flexible materials also reduce the weight antenna. One benefit to flexible substrates is that they can survive in hazardous environments. There are many flexible substrates, such as RT Duroid (ε_r = 2.3), RT Duroid 6010.5 (ε_r = 10.5), and RT Duroid 5880 (ε_r = 2.2). Rigid substrates are more expensive but are characterized by better reliability and a lower thermal expansion coefficient. Rigid substrates are best to use in situations where you want to pursue easy maintenance and repairs. Their clearly marked components make it easy to identify the affected areas. There are many examples of Rigid substrates, such as Alumina (ε_r = 9.7), quarts (ε_r = 3.8), FR4 (ε_r = 3.4), Gallium Arsenide (ε_r = 12.3), and Sappier (ε_r = 11.7)[3].

The thicker substrate with a lower dielectric constant is better, providing better efficiency and higher bandwidth, leading to larger antenna sizes. Moreover, using a thinner substrate with a higher dielectric constant leads to a smaller antenna size, lower efficiency, and smaller bandwidth. Therefore, there is a tradeoff between the performance and length of a good antenna.[16].

2.5 Feeding Techniques of Patch Antenna

There is more than one way to feed a microstrip antenna, but there are four most common ways, a direct method (the Coaxial Probe(CP), Microstrip Line(ML)) and an indirect method (Aperture Coupling(AC), and Proximity Coupling(PC)), and each process will be explained in simplified[8] [14] .

Feeding methods are essential to match the feed line impedance and the rectifying antenna impedance. The patch resistance must match the feed line resistance. The maximum power will not be transmitted if there is no matching impedance between the antenna and the feed line[17] .Antenna impedance can be matched depending on the design impedance[18].

2.5.1 Coaxial Feed (Coplanar Feed)

This method is done by coupling the patch and conductor into the coaxial cable, which passes through the patch-bearing substrate. In contrast, the outer conductor connects to the ground plane of the same substrate, as shown in Fig. 2.6. The input impedance mainly depends on the feed's location, so the feed line impedance can be matched when the patch is placed correctly. The main advantage of this feed is that it can be placed anywhere inside the patch to check its input impedance. This feeding method is also characterized by ease of fabrication and has low spurious radiation. However, the disadvantage of this method is the narrow

bandwidth and difficulty to design because the internal conductor must pass through the substrate and protrude beyond the ground plane [3].

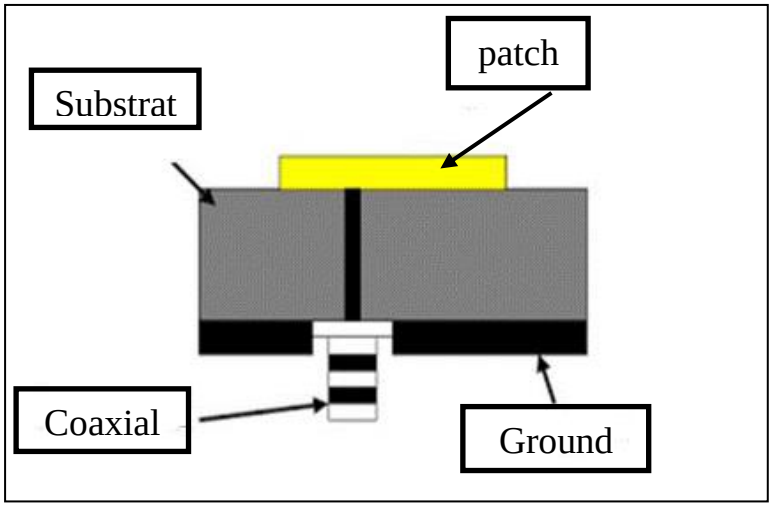

Figure 2.6: Coaxial Feed (Coplanar Feed)[10]

2.5.2 Microstrip Line Feed

In this method, the conductive line is attached directly to one of the patch edges of the microstrip antenna. As shown in Fig. 2.7, the conductive line's width is very small compared to the patch's width. A benefit of this method is that the feed line and patch are attach onto a single substrate, providing a flat surface[19].

The primary purpose of the cut-in patch is to match the patch resistance to the feed-line impedance without the need to add any additional matching element. The input impedance of the patch antenna depends slightly on the thickness of the substrate material and the permittivity. Still, it depends more firmly on the contact location between the feed and the patch.[14]. Feeding the microstrip line is the most straightforward in antenna printing and assortment, and it is inexpensive. In addition, it is easy to match the resistance through internal position control [20].

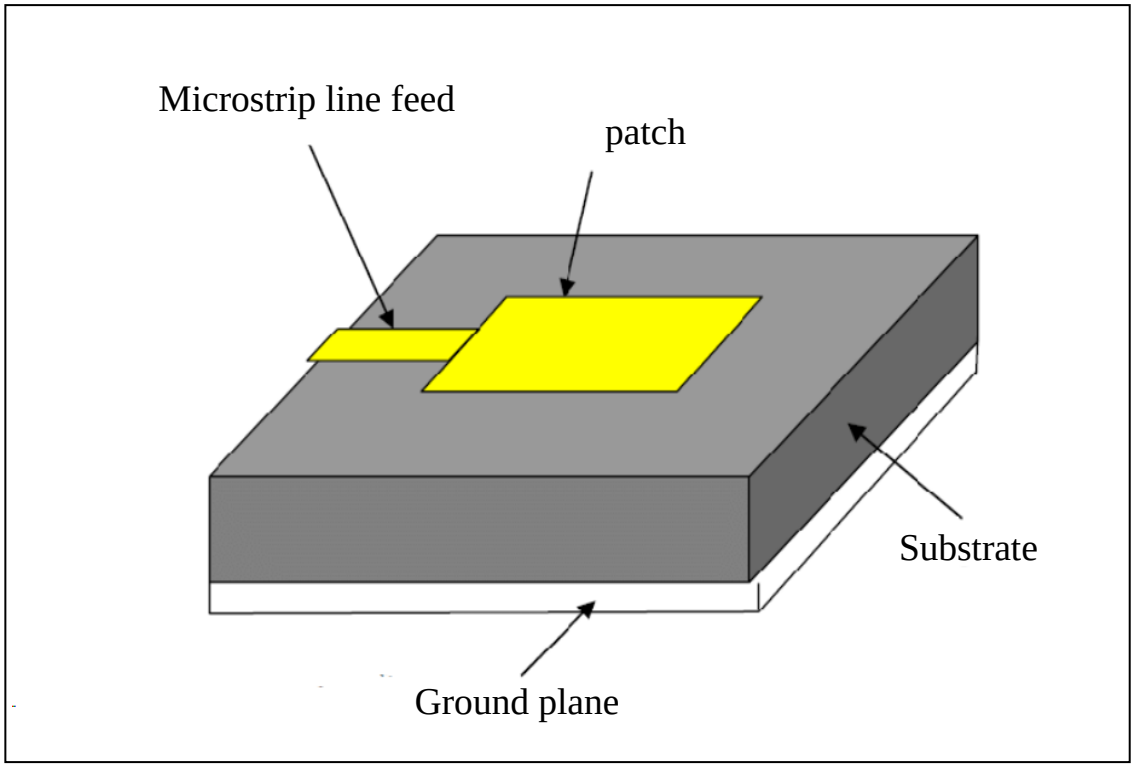

Figure 2.7: Microstrip Line Feed[21]

2.5.3 Proximity Coupled Feed

As shown in Figure 2.8, this type of feeding consists of two dielectric substrates. The feed line is buried between the two substrates, the patch is printed at the top of the first substrate, and electromagnetic coupling is between the feed line and the patch. The matching is controlled by changing the dimensions of the feed line. This feed is characterized by providing high bandwidth of up to 13% due to the increased thickness of the antenna, besides less spurious radiation compared to Microstrip Line Feed and coaxial feed. However, the main drawback of this method is that it consists of two layers of substrates, which leads to the difficulty of manufacturing and increasing antenna thickness[22].

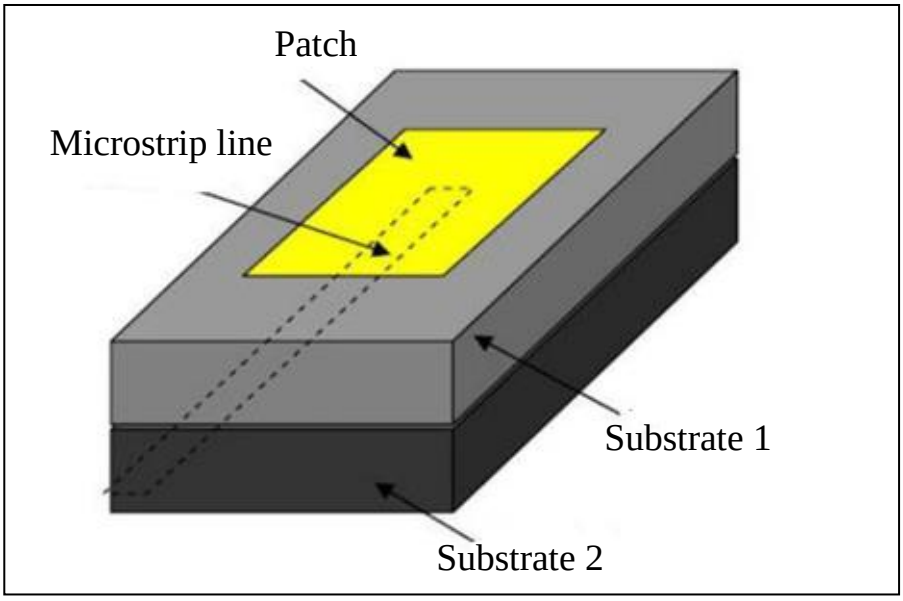

Figure 2.8: Proximity Coupled Feed[21]

2.5.4 Aperture Coupled Feed

This feeding method consists of two dielectric substrates separated by a ground plane containing a coupling slot parallel to and directly below the patch, as shown in figure 2. 9. The feed line connects to the bottom of the lower substrate, and the patch is printed on the top of the upper substrate. At the same time, the ground plane separates the upper and the lower substrates (patch and the feed line), thus reducing the spurious radiation. Moreover, the separation of two substrates via the ground layer prevents the effect of the first substrate dielectric constants on the second substrate dielectric constants. The thick substrate with a low dielectric constant usually assigns to the patch layer, while a thin substrate with a high dielectric constant assigns to the feed layer[23].

The coupling process between the patch and the feed line process is done by a slot located at the ground level, which can be performed with different shapes, rectangular or circular, etc., and the impedance matching controls via the dimensions (width and length) of the coupling slot. This feeding method is similar to the Proximity Coupling method in its

drawbacks, which are the difficulty of manufacturing because it contains two substrates[24].

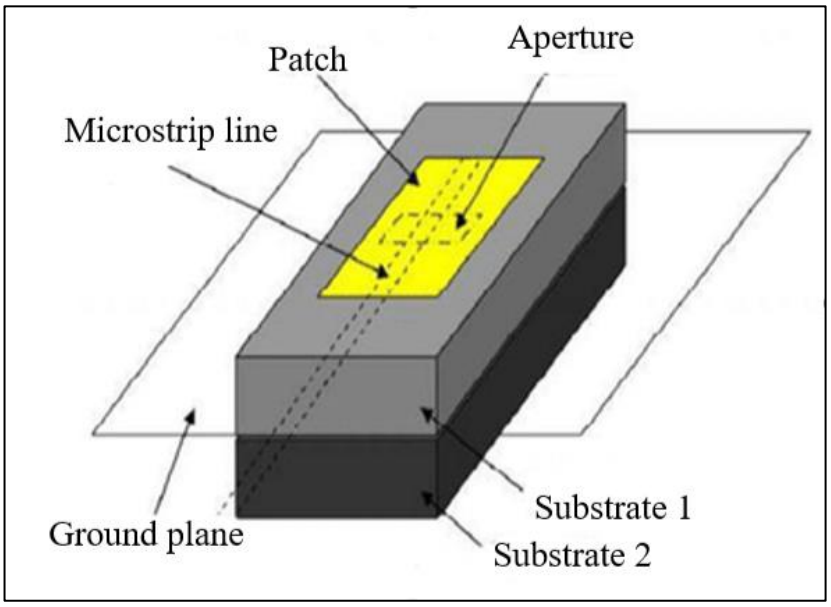

Figure 2.9: Aperture Coupled Feed[21]

2.6 Literature Review

The microstrip antenna has great literature works in terms of frequencies ranges and feeding methods. In this section, some of the works are presented, as follows:

2.6.1 Microstrip Antenna

M. A. A. Rahim et al., 2017 [27], used CST program for simulation , and Rogers Duroid RT5880 as a substrate. This antenna has a frequency of 28 GHz with the S11 of -52.522 dB and a bandwidth of 1.12 GHz. The antenna is intended to operate in the KA band. The antenna is designed with 32 patch elements, and the group results are better than the single patch results. The shape of the antenna is shown in Figure 2.10.

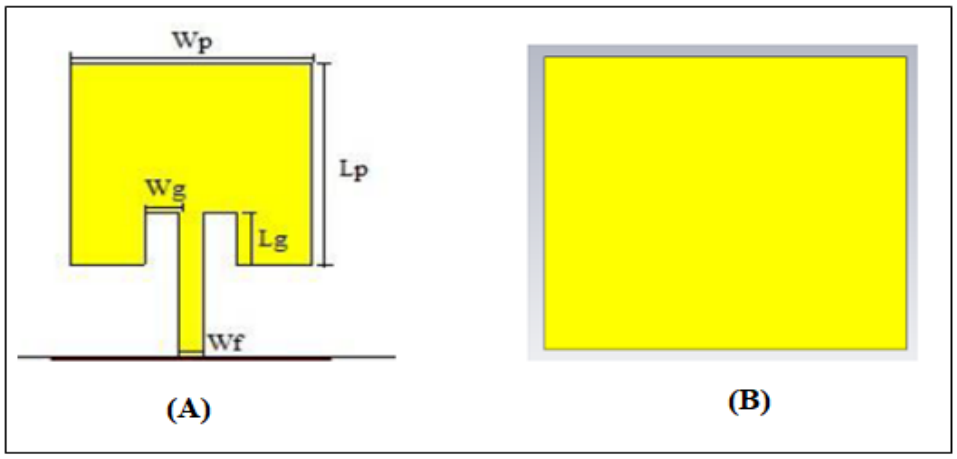

Figure 2.10:(A)top image(B)The back view of the single patch antenna [27].

A. S. B. Mohammed et al.,2021, [25] explained The effect of substrate and conductive material thicknesses on the antenna's. Practically, explained the effect of these thicknesses on the centre frequency.The size of the antenna is 5.43 * 4.54 * 0.5 mm3. This antenna has a frequency of 28GHz, which supports 5G applications. The results of the conclusion in this research are that the thickness and type of the conductive material have minimal effect on the centre frequency. Still, it dramatically affects the return loss, bandwidth, and gain. Thus, choosing the optimal type of conductive material and its thickness in designing the microstrip patch antenna is essential. The shape of the antenna is shown in Figure 2.11.

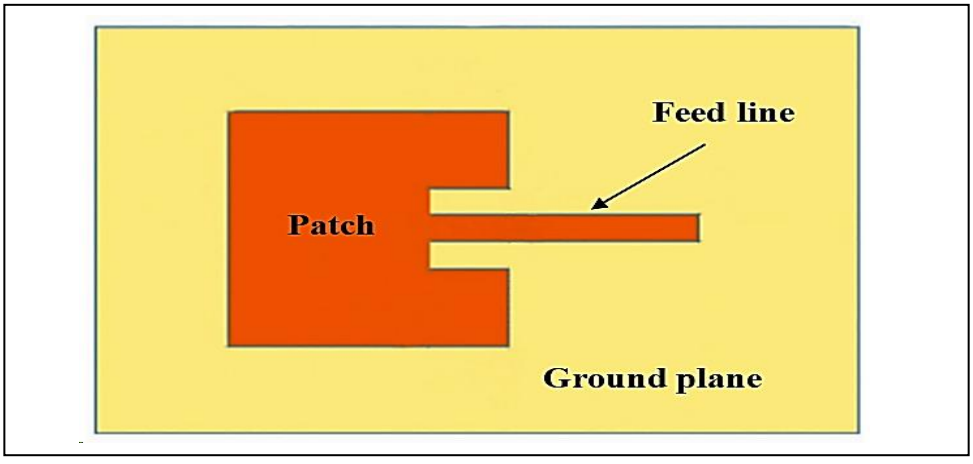

Figure 2. 11: The proposed antenna shape [25].

R. Hussain et al., 2022 [26] used HFSS program for simulation and Rogers RO-4350 as a substrate. The proposed antenna consists of two multi-input and output elements. Each piece consists of four concentric pentagonal holes and a distance of 49 mm separates the two aspects. The proposed antenna covers the 6 GHZ wave band and the millimeter wave band (1.5, 1.9, 2.7, 3.6, 4.2, and 28), where the bandwidth of each frequency is respectively 0.18, 0.32, 0.42, 0.7, 0.5, and 0.5GHz. The maximum gain is 8.5%, and the maximum efficiency is obtained—91%. The shape of the antenna is shown in Figure 2.12.

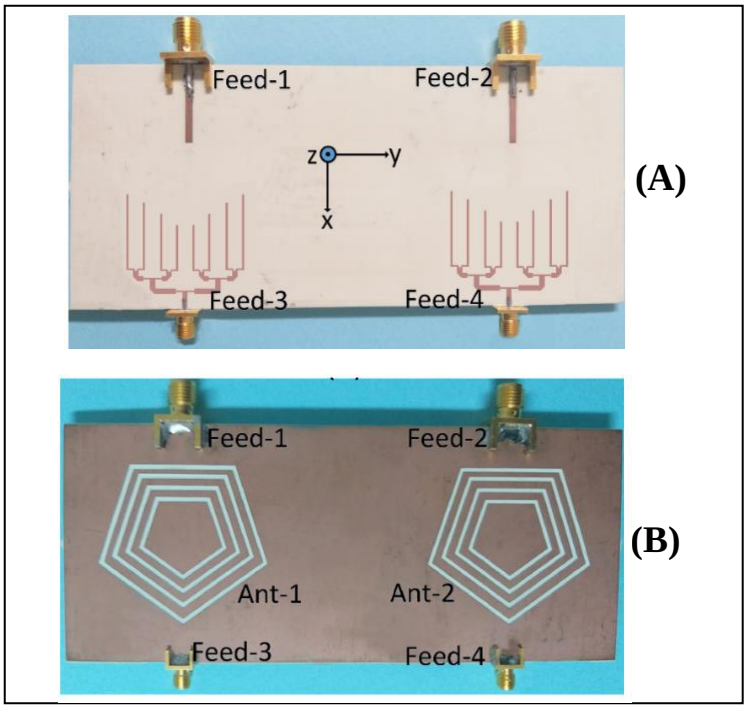

Figure 2. 12: (A) Top image (B) Bottom image [26]**.**

2.6.2 Microstrip Line Feed

M. Buravalli et al., 2020 [28], used HFSS program for simulation [28], and it is designed to operate at a frequency of 30 GHz. Initially, the single-patch antenna is prepared as in Figure 2.10 (A), but the input impedance is 42.70 ohms, which does not match well with the 50-ohm power line impedance amount of S11 is -19.03 dBm, and VSWR equals

1.25. When using a set of monolayer antennas to design a 2 x 3 antenna array as in Figure 2.13 (B), an input impedance of 54.03 ohms is obtained, plus an amount of S11 of -26.52 and a VSWR of 1.09 [28].

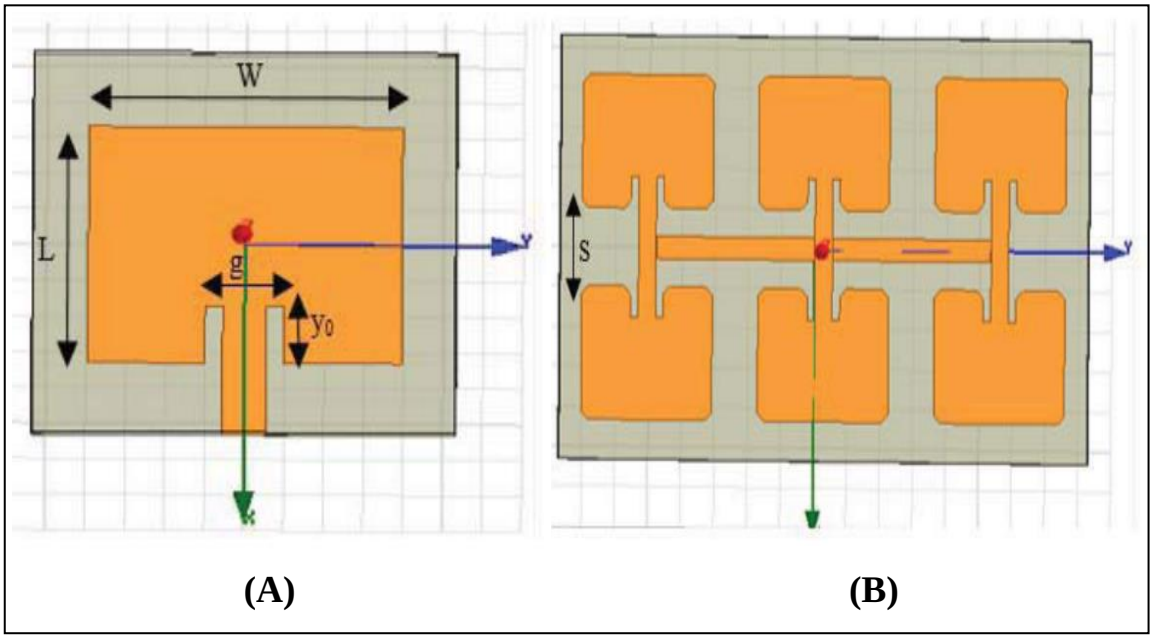

Figure 2. 13: (A) single-patch antenna,(B) 2x3 antenna array[28]

J. O. Abolade et al., 2021 [29], used HFSS program for simulation, and Duroid 5880 as a substrate. This antenna works at multiple frequencies (six-band): (2.37, 3.06, 3.52, 4.28, 4.88, and 6.0GHz) with antenna dimensions 0.35 d x 0.14 λd and λd is the wavelength for the lowest frequency. The shape of the antenna patch is inspired by nature in the form of a grape leaf, and then five incisions are inserted into the patch to produce multiple bands. The antenna is manufactured, and the most important parameters are calculated. The shape of the antenna is shown in Figure 2.14.

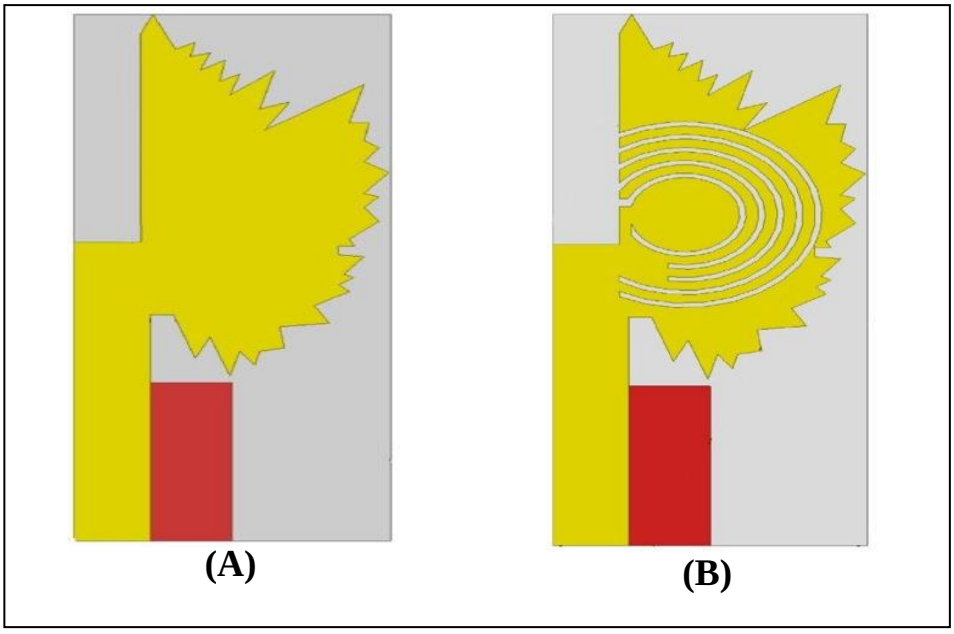

Figure 2.14:(A)rudimentary antenna image(B)Antenna after drilling brackets [29]

2.6.3 Coaxial Feed

M. V. Mokal et al., 2017 [31]**,** used CADFEKO Suite 7.0 program for simulation, and FR4 as a substrate, the rectangle patch antenna is analyzed using two feeding techniques, coaxial feeding technique and microstrip line feeding technique, where the resonant frequency of the antenna is 2.4GHz, in the microstrip line feeding method the return losses are -16.5 As for the coaxial feeding method, it is -26.8, as well as the VSWR and the rest of the parameters proposed antenna in the coaxial feeding method are the best. The shape of the antenna is shown in Figure 2.15.

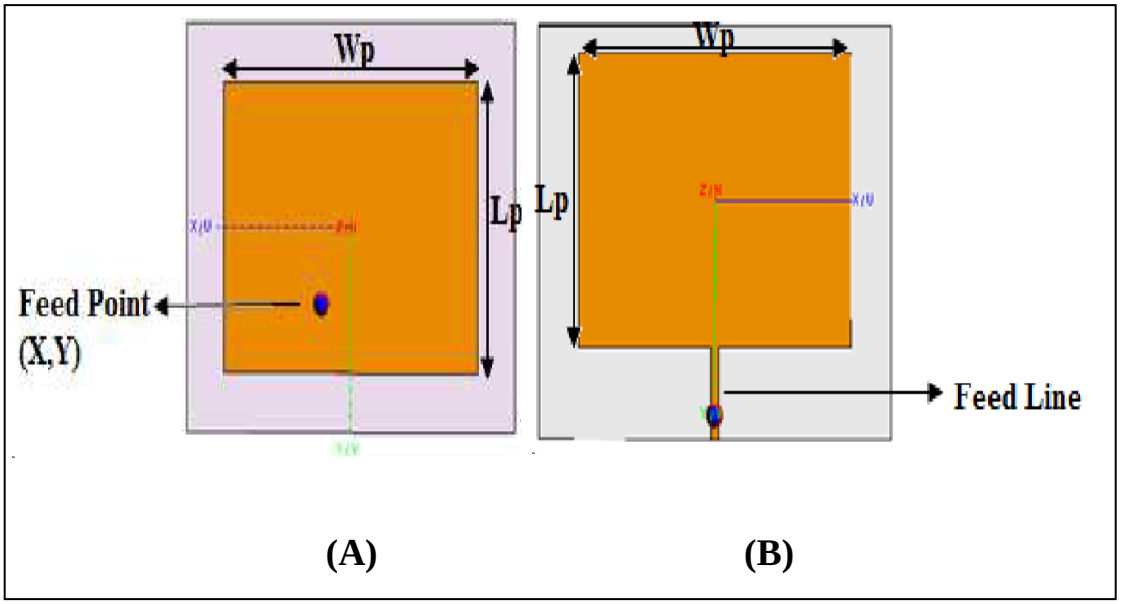

Figure 2. 15: (A) coaxial feeding technique,(B) micro strip line feeding technique[31]

V. L. Pham et al., 2022 [30], in Figure 2.16, Demonstrates a dual-band antenna that consists of one or more pairs of rectangular spots as show in Figure 2.13. The antenna is printed on the top surface of the Roger RO4003 substrate. In addition, These patch antenna dimensions were chosen to be suitable for generating dual-band radiation. This antenna is a transparent radiator ideal for applications requiring transparent radiators. Although no transparent substrate is used in this research, this theory and design are the same for transparent and opaque substrates. The frequency ratio is 1.12 in the c band, and the antenna produces an S11 < -10 dB value. It resonates at two resonant frequencies, 5 GHz and 6.5 GHz, with a bandwidth (4.82-5.03), i.e. 210 MHz at 5 GHz, with a gain of 9 and (5.49-5.78). That is, 290 MHz at 6.5 GHz, with an increase of 6.8 [30].

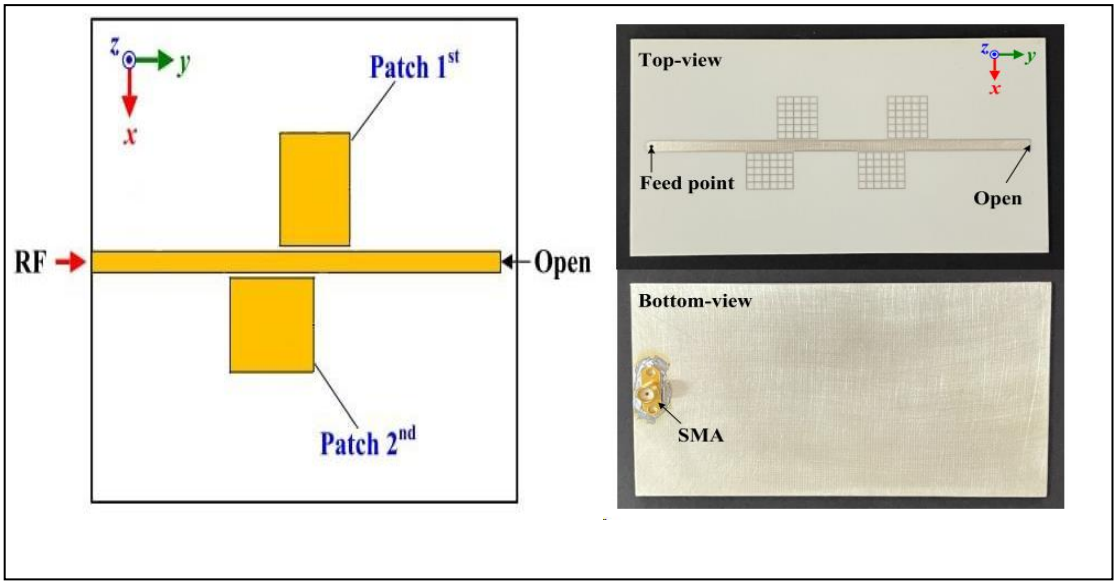

Figure 2. 16: (A)The frontal shape of the antenna at simulation (B) The front and back shape of the antenna after manufacturing[30]

2.6.4 Proximity Coupled Feed

N. Aboserwal et al., 2020 [33], used HFSS program for simulation, and Rogers TM 5880 Duroid, Rogers TM 4350B and Rogers TM 6006 as a substrates. The research aims to develop for calculating the bandwidth, as this is done by using the different parameters and the relationship between them and conclude the bandwidth equation more accurately. Antenna frequency in different bands, namely X, C and S. Figure 2.17 show a picture of the proposed antenna [33].

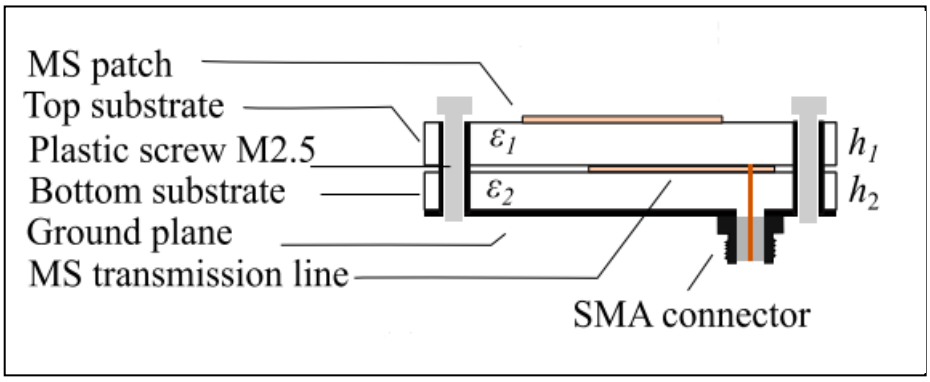

Figure 2.17: Side view of the antenna [33]

S. N. Ariffah et al., 2020[34], used CST program for simulation , and FR4 material is as a the substrate. Designed by cutting the edges of the patch, the antenna at 5.8GHz has a return loss of -10.015 dB, a gain of 3.551 dB, and a directivity of 5.97 dB. Figure 2.18 shows a picture of the proposed antenna[34].

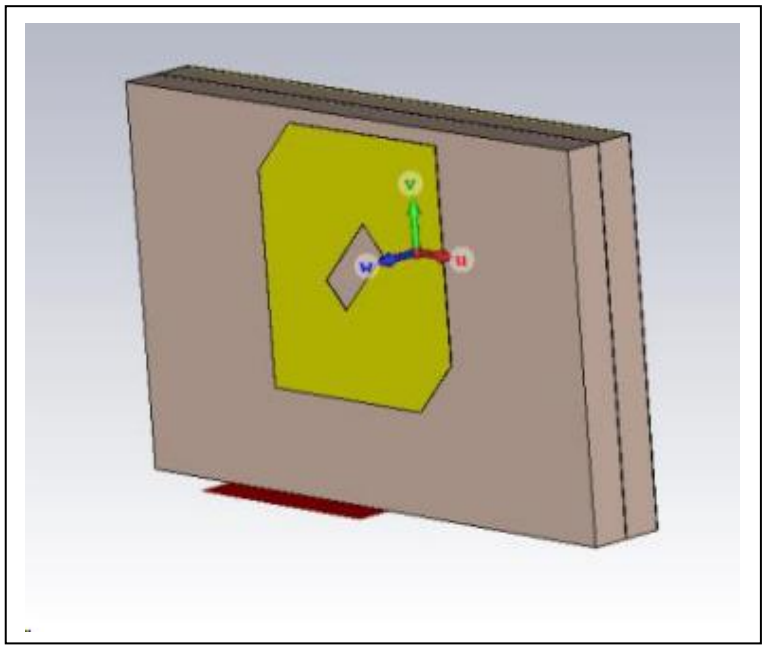

Figure 2. 18: proposed antenna [34]

D. K. Kong et al., 2021 [32], used CST program for simulation,. In this antenna, a rectangular microstrip feed line open at one end is inserted into the cavity of the proximity coupled microstrip patch antenna (PC-MSPA) between the two substrate layers, and this step helps to obtain a wide bandwidth of 7GHz at a frequency of 9GHz and a lower VSWR value from 2. The shape of the antenna is shown in Figure 2.19.

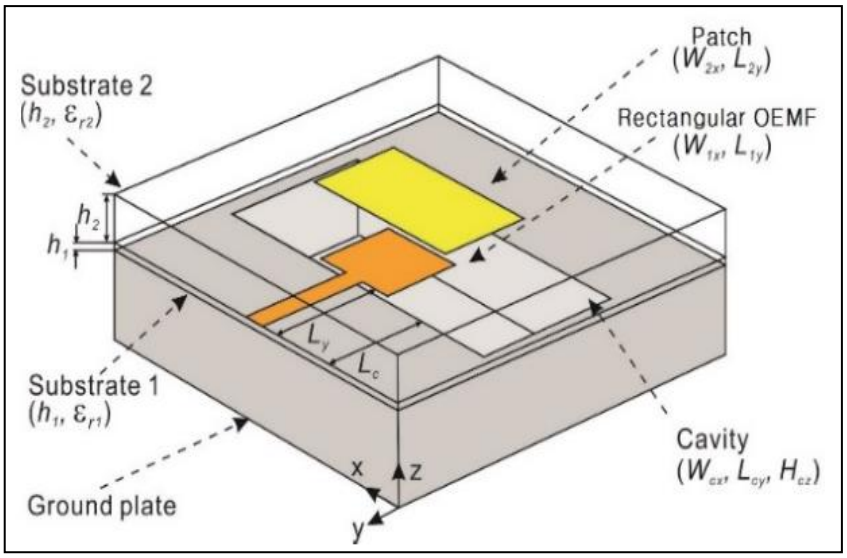

Figure 2.19: proposed antenna [32]

2.6.5 Aperture Coupled Feed

C. Hertleer et al., 2007[24], used ADS-Momentum program for simulation, wool and felt as a substrates and conductive textile materials in the patch, microstrip line and ground level. The antenna frequency is at 2.45GHz as this antenna operates in the ISM band with a bandwidth of 0.0835 GHz and an efficiency of 63%. The antenna is tested when bent on a cylinder of radius 8 mm, and the results are compared with the planar design. Figure 2.20 shows a picture of the proposed antenna in this paper.

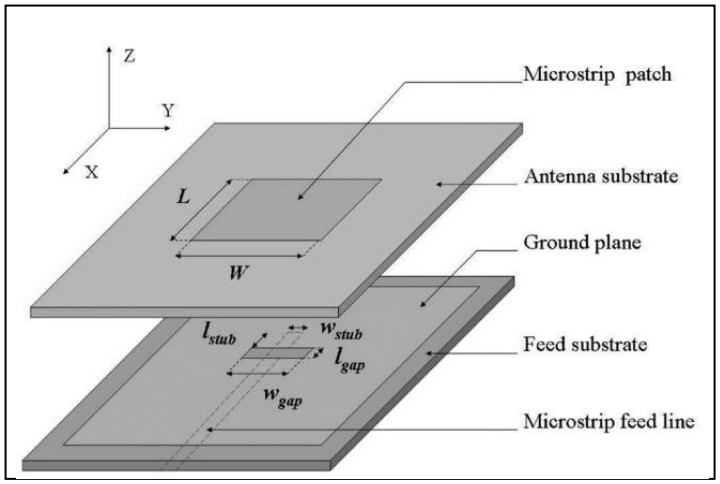

Figure 2.20: proposed antenna [24]

K. A. Malar et al.,2017 [23], used CST program for simulation, PCB as a substrates . This antenna is a frequency of 2.45 GHz with a size of 10 * 10 mm where. The feed line in this antenna is designed in the shape of the letter T, and the patch is fed through a hole in the ground surface. This antenna achieved a gain of 5.6 dB, an efficiency of 47%, and 0.0835GHz bandwidth from 2.22 to 2.4835 GHz. The antenna is also tested when bending with different radii and compared with the planar design. Figure 2.21 shows a picture of the proposed antenna in this paper.

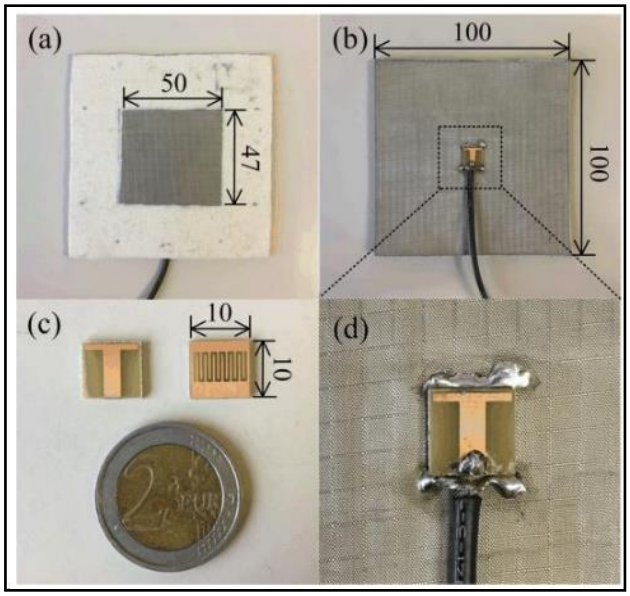

Figure 2.21: (a) Top image,(b) Bottom image ,(c) Feeding network ,and (d) Enlarged image of connection dimensions in mm [23].

C. Hertleer et al., 2022 [35], used HFSS program for simulation, wool and felt as a substrates . and used copper for the patch, ground plane and microstrip line. This antenna operates at 2.4 GHz on the body and 5.8 GHz outside. The antenna is designed from flexible substrates, which are bendable and used in wearable applications. has calculated the important parameters for bending design and compared them with the planar design. The antenna frequency is at 28 GHz. The shape of the antenna is shown in Figure 2.22.

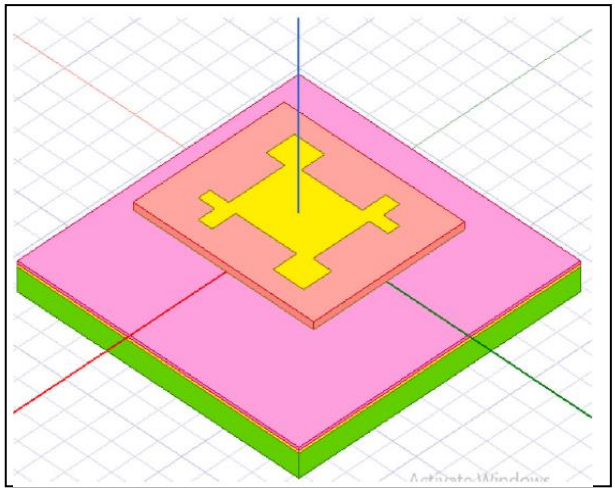

Figure 2.22: proposed antenna [35]

2.7 Basic Antenna Parameters

This section presents The basic communication parameters to have a better idea about wireless communication using antennas. Wireless communication is done in the form of waves. Hence, we need to have a look at the properties of waves in communications.

2.6.1 Reflection Coefficient (Γ)

Reflection is a prominent phenomenon that must be considered, whereas the reflection coefficient is the ratio of the back reflected power to the transmitted power. If the transmitted power is PT and the reflected power is PR, then the equation below can calculate the reflection coefficient [36]:

$$\boldsymbol{\Gamma = \frac{Z_L - Z_0}{Z_L + Z_O} = \frac{P_R}{P_T}} \qquad \ldots\ldots\ldots\ldots \textbf{2- 6}$$

Where $\Gamma = reflection\ coefficient$

$Z_L =$ The load impedance

$Z_O =$ characteristic impedance of TL

The best antenna performance is when the value of the reflection coefficient approaches zero, which means that the load matching to the line feeding and there is no reflected wave. To obtain this result, the load impedance must be matched with the impedance of the line. The antenna

mismatch leads to not delivering all the power to the antenna from the feed line. Such loss is called return loss (RL)[3].

The following equation can calculate return loss (RL):

$$\mathbf{RL = -20\ log|\Gamma|} \quad \text{..... 2- 7}$$

Return loss is expressed in decibels and for maximum power transfer the reflected signal should be small. Where 30 dB return loss is better than 20 dB[37].

2.6.2 Directivity

The antenna's directivity is the ratio of the radiation intensity in one direction to its average intensity in all directions. This definition can be clarified through the equation below[6][19].

$$\mathbf{D = \frac{4\pi U}{P}} \quad \text{..... 2- 8}$$

Where D =Directivity of the antenna

U = Is the radiation intensity of the antenna.

P = Is the total power radiated.

Since the directivity is the ratio of the intensity of two radiations, it is a dimensionless quantity. It is generally expressed in dB. If the direction is not specified, it indicates the highest radiation intensity.

2.6.3 Gain

gain of an antenna takes the directivity of the antenna into account along with its effective performance. As mentioned earlier, directivity is the ratio of the radiation intensity in one direction to its average power in all orders, so the gain is the ratio of the radiation intensity scattered in these directions to the radiation intensity that would be obtained if the power accepted by the antenna, which can be expressed mathematically by the following equation[38]:

$$\mathbf{gain} = \frac{\mathbf{4\pi P_r}}{\mathbf{P_i}} \qquad \ldots\ldots\ldots\ldots\ldots \mathbf{2\text{-}9}$$

Where P_r = power radiated per unit solid angle

P_i = Input (accepted) power

2.6.4 Bandwidth

Bandwidth is another main parameter that must be taken into account that defines the range in which the antenna can correctly receive or radiate energy. It also defines the range of frequencies that are near the center frequency where all parameters such as directivity, gain and return losses are close to the values of the center frequency. The bandwidth can be calculated by the equation below[36][39]:

$$\mathbf{BW = F_H - F_L} \qquad \ldots\ldots\ldots\ldots\ldots \mathbf{2\text{-}10}$$

Where BW = is bandwidth

F_H = Is higher frequency

F_L = Is lower frequency

While the percentage of bandwidth can be calculated from the following equation:

$$\mathbf{BW\%} = \frac{\mathbf{F_H - F_L}}{\mathbf{F_c}} \times \mathbf{100\%} \qquad \ldots\ldots\ldots\ldots\ldots \mathbf{2\text{-}11}$$

Where $\mathbf{F_c}$ = is center frequency

2.6.5 Voltage Standing Wave Ratio (VSWR)

To transmit or receive power correctly via the antenna, the feeder and transmission line impedance must match the antenna's impedance. VSWR is a measure that numerically describes how well the antenna is impedance matched to the radio or transmission line it is connected to. VSWR is an essential parameter for all microwaves. The ideal amount is when VSWR equal one, which occurs at Γ equal zero, which means there is no reflection and all the energy is transferred to the antenna. For some applications, the

acceptable value of the VSWR is less or equal to two. The following equation can calculate the VSWR[39]:

$$\mathbf{VSWR} = \frac{\mathbf{1}+|\boldsymbol{\Gamma}|}{\mathbf{1}-|\boldsymbol{\Gamma}|} \qquad \ldots\ldots\ldots\ldots\ldots \textbf{2- 12}$$

Where $\Gamma =$ reflection coefficien

We can calculate the reflected power percentage from the equation below[40].

$$\mathbf{p = 100 * \Gamma^2} \qquad \ldots\ldots\ldots\ldots\ldots \textbf{2- 13}$$

Chapter Three

Methodology

CHAPTER 3

METHODOLOGY

3.1 Introduction

The rapid development of wireless communications has become commonplace in everyday life. Wireless applications have been widely expanded in the last decades due to the domination of the internet, mobile technologies (3G, LTE, 4G and 5G) and wireless body area networks (WBAN)[41].

5G is the best path in wireless communications [42]. 5G represents a significant evolution of the 4G network and its predecessors, giving many previously unavailable features. It offers massive connectivity, a higher data rate, low latency, and high reliability than its predecessors [43]. 5G systems can also use the millimeter wave band for the first time in communication networks, where an antenna is designed to operate at various frequency bands in 6GHz,and 28GHz, where the higher frequency bands considered millimeter-wave frequency that can be increased the bandwidth [26].

Furthermore, advancing manufacturing technologies and materials with elastic properties lead to new trends in flexible electronics [44]. The flexible antenna is considered the most significant invention in the flexible electronics industry, where the applications of wearable antennas go far beyond traditional wireless communications [45].

wireless body area networks are employed with various applications, such as medical applications, global positioning systems (GPS), and military applications. WBAN medical applications show great promise in improving the quality of life of people and satisfying many requirements of

elderly people by enabeling them to live safely, securely, healthily and independently [46] [47].

Textile materials, used as an antenna substrate, are an advanced technology for man-machine interfaces, where fabric antennas can be easily implemented into clothing because textile materials make attractive substrate[48]. Textiles typically have a low dielectric constant [49].

The recently developed antennas adopted the lower frequency ranges (433.95, 867, 915, 2380, 2450, and 5800) MHz However, the majority of these antennas are single band [23], [50]–[53], and some of them are multiband, while the rest are dual-band, besides another antenna targeting the band of higher frequency [54]–[58]. In this work, the proposed antenna has two rounds of operation, the lower frequency bands (6 GHz),the higher frequency bands (28 GHz) .

3.2 Computer Simulation Technology (CST)

The design and evaluation of the proposed antenna are performed with the assistance of this simulation software, an electromagnetic field simulation program that is simple to operate and combines an unprecedented level of simulation performance with ease of use [59] [60].

A key feature of CST Studio Suite is the Complete Technology approach which gives the choice of simulator or mesh type that is best suited to a particular problem, seamlessly integrated into one user interface.

Since no one method works equally well for all applications, the software contains several different simulation techniques (time domain solvers, frequency domain solvers, integral equation solver, multilayer solver, asymptotic solver, and eigenmode solver) to best suit various applications.[61].

3.3 The Proposed Antenna Design

The antenna model used in this research works in two resonance frequencies, 6 GHz and 28 GHz. The main design is based on research which operates at frequency 28 [3], that updates to include two bands at 28 and 6 GHz, making it more suitable for 5G applications.

The proposed system is shown in figure 3.1. Where, the proposed antenna is fed with four feeding methods, namely (Microstrip Line Feed(MLF)[18], Proximity Coupled Feed(PCF), Aperture Coupled Feed(ACF)[35], and Coaxial Probe(CP)). The aperture coupled feed is adopted in system design because it offers the best performance results. Furthermore, the coaxial feeding method was not suitable for this design and it didn't give any results.

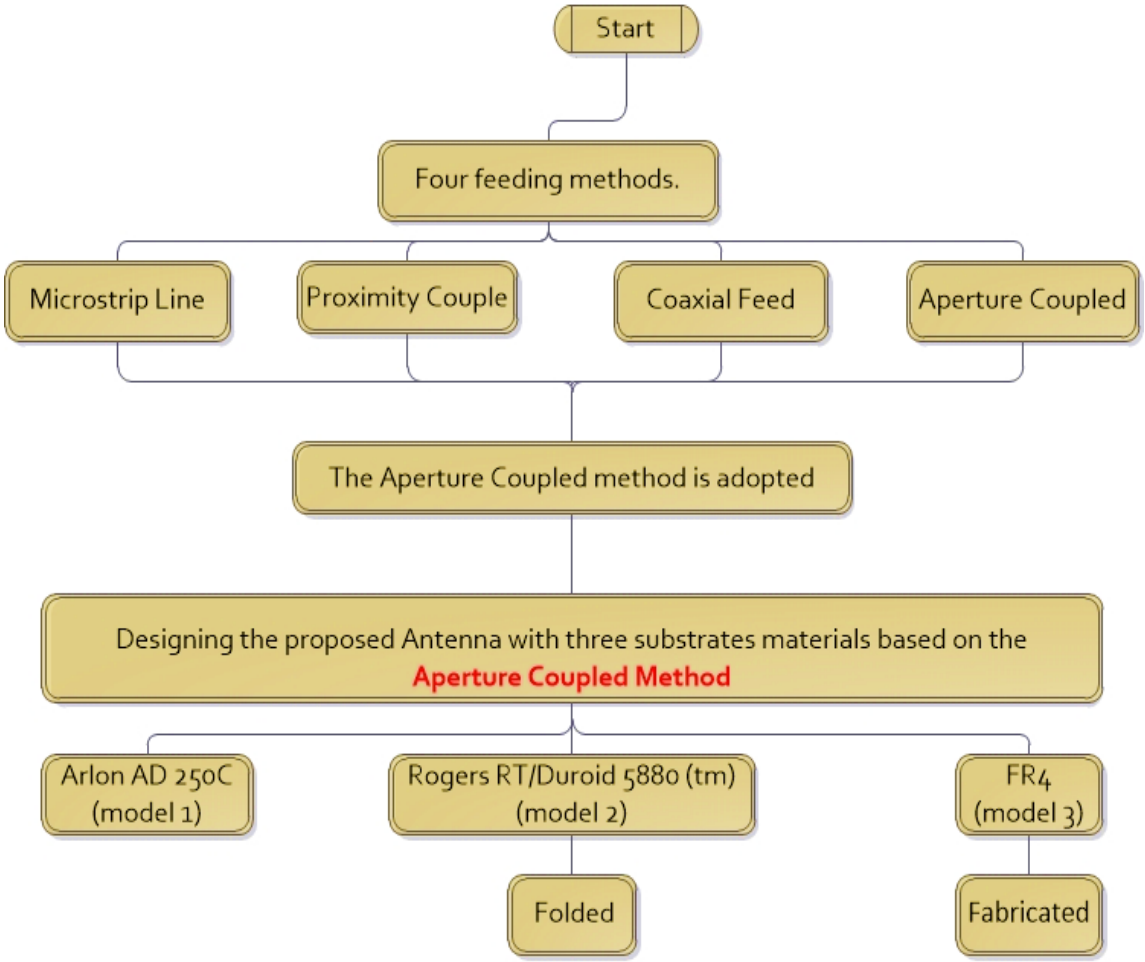

Figure 3.1: The proposed System.

The proposed antenna with the ACF method is designed with three substrates materials: Arlon AD 250C, Rogers RT/droid 5880(tm), and FR4 materials. The Rogers RT / duroid 5880 (tm) is used as a substrate in all of these feeding methods where (ε_r = 2.2 and tangent = 0.0009).

3.3.1 Microstrip Line Feed

This method is the direct method, which means to feed the patch using the feed line that attaches to the patch directly, Table 3.1 proposed Antenna Dimensions in Microstrip Line Feed Method. The proposed model consists of an T-shaped patch design , as well as The dimensions of the ground plane led to the best possible impedance match being achieved. Figure 3.2 shows the shape of the antenna from front and back.

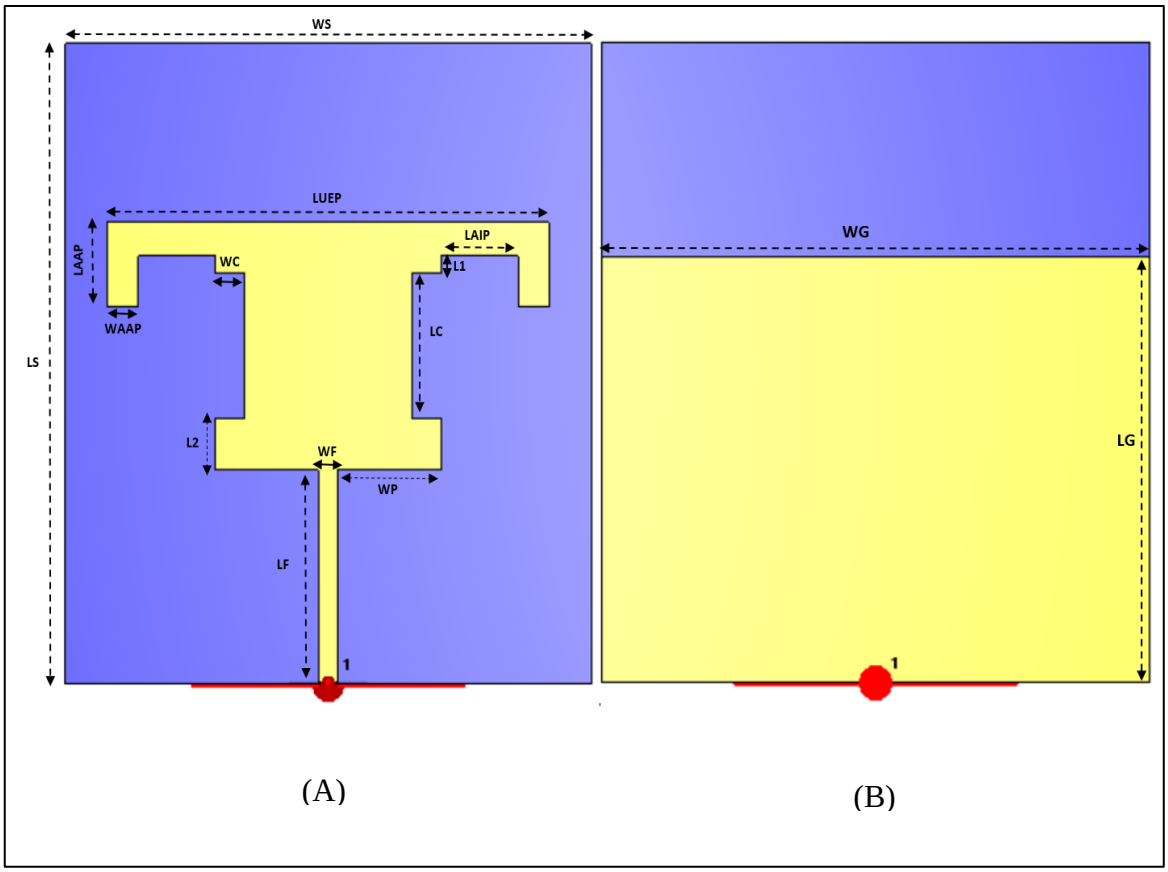

Figure 3. 2: (A) Front view of the proposed antenna (B) The shape of the antenna in the back.

Table 3.1: Proposed Antenna Dimensions in Microstrip Line Feed Method

The Sample	mm	The Sample	mm
LS	22	LUEP	16.62
WS	19.8	LAAP	2.9
L1	0.59	WAAP	1.16
L2	1.75	LAIP	2.9
WF	0.C	WC	1.1
LF	7.3	LC	5
WG	19.8	copper thickness	0.035
LG	14.63	substrate thickness	0.22
WP	3.9		

3.3.2 Proximity Coupled Feed

This method feeds the patch indirectly using a feed line buried between the two substrates, where the patch is indirectly stimulated. This method is distinguished by the fact that the antenna has two substrates with T-shaped patch design. To get the best resistance match, we changed the dimensions of the feed line and ground level.

Figure 3.3 shows the antenna's shape and the feed line's location and Table 3.2 shows the antenna dimensions suggested in this method.

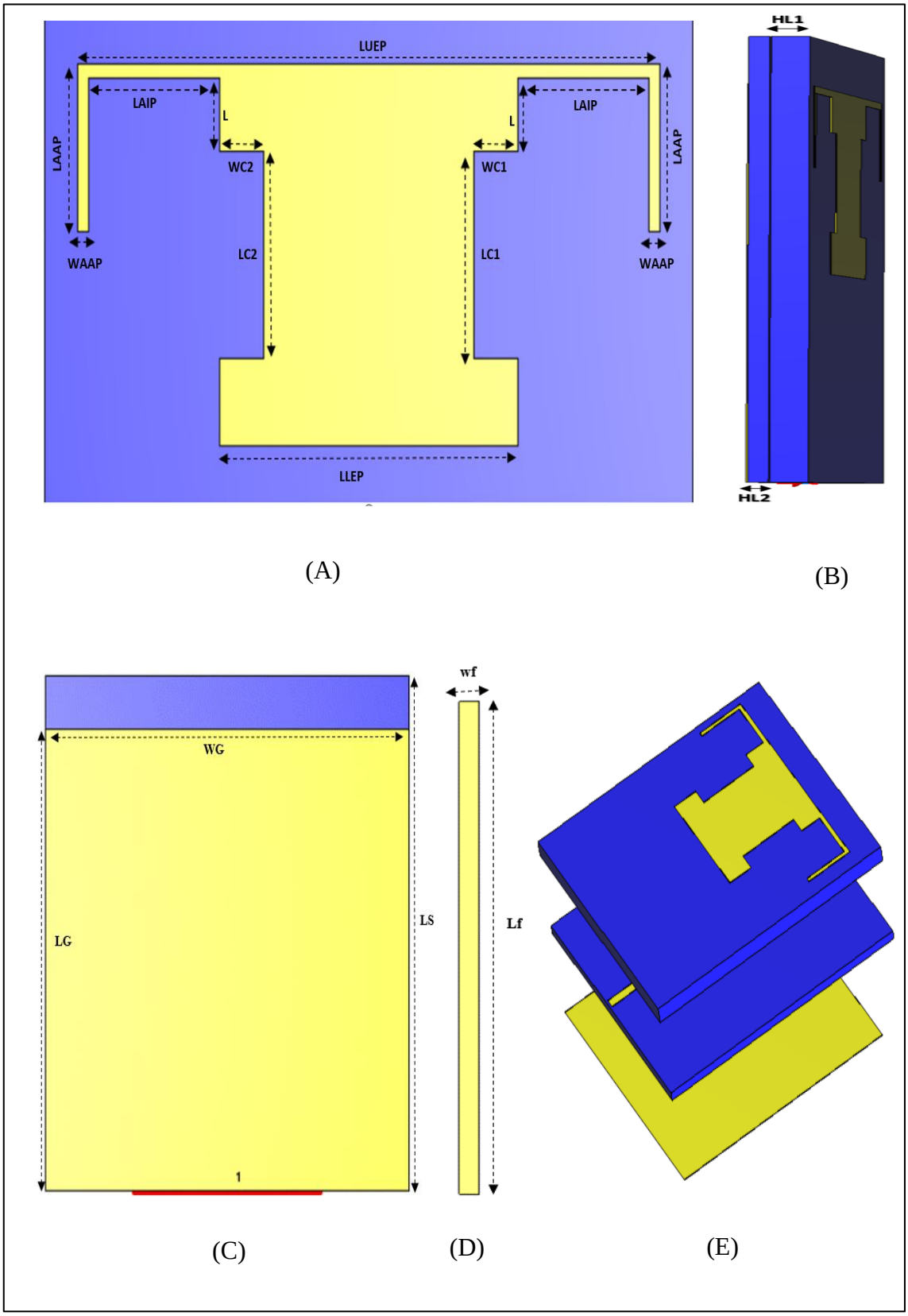

Figure 3. 3: The proposed antenna shape in the Proximity Coupled Feed method. (A) Front (B) Side image (C) Back (D) Feed line (E) Illustration of the layers

Table 3.2: Proposed Antenna Dimensions in Proximity Coupled feed **Method**

The Sample	mm	The Sample	mm
LG	19.70	LAAP	4.04
WG	20	WAAP	0.34
LS	22	LAIP	4.04
L	1.76	WC1=WC2	1.35
WF	0.72	LC1=LC2	5
LF	17.8	LLEP	9.20
HL1	1.1	copper thickness	0.035
HL2	0.6	LUEP	17.96

3.3.3 Aperture Coupled Feed

The proposed model consists of a T-shaped patch design with two substrates, which are excited by drilling a rectangular-shaped hole at ground level through a microstrip line printed below the bottom substrate as shown in Figure 3.4.

Figure 3.4 shows the antenna design proposed to operate at 6 GHz and 28 GHz bands. The antenna has two parts of a conductive layer made of metal the first layer works as a radiator which is the top layer of the first substrate The other layer works as a reflector ground which is placed below the first substrate and on the top of the second substrate besides this substrate contains a hole slot, that stimulate radiation from the line microstrip, which is printed n the back of the second substrate, which is also made from the same material of the patch. Moreover, differoent types of substrates are chosen to work on, besides the different types of feeding that makes many models according to the type of substrate material used and feeding method:-

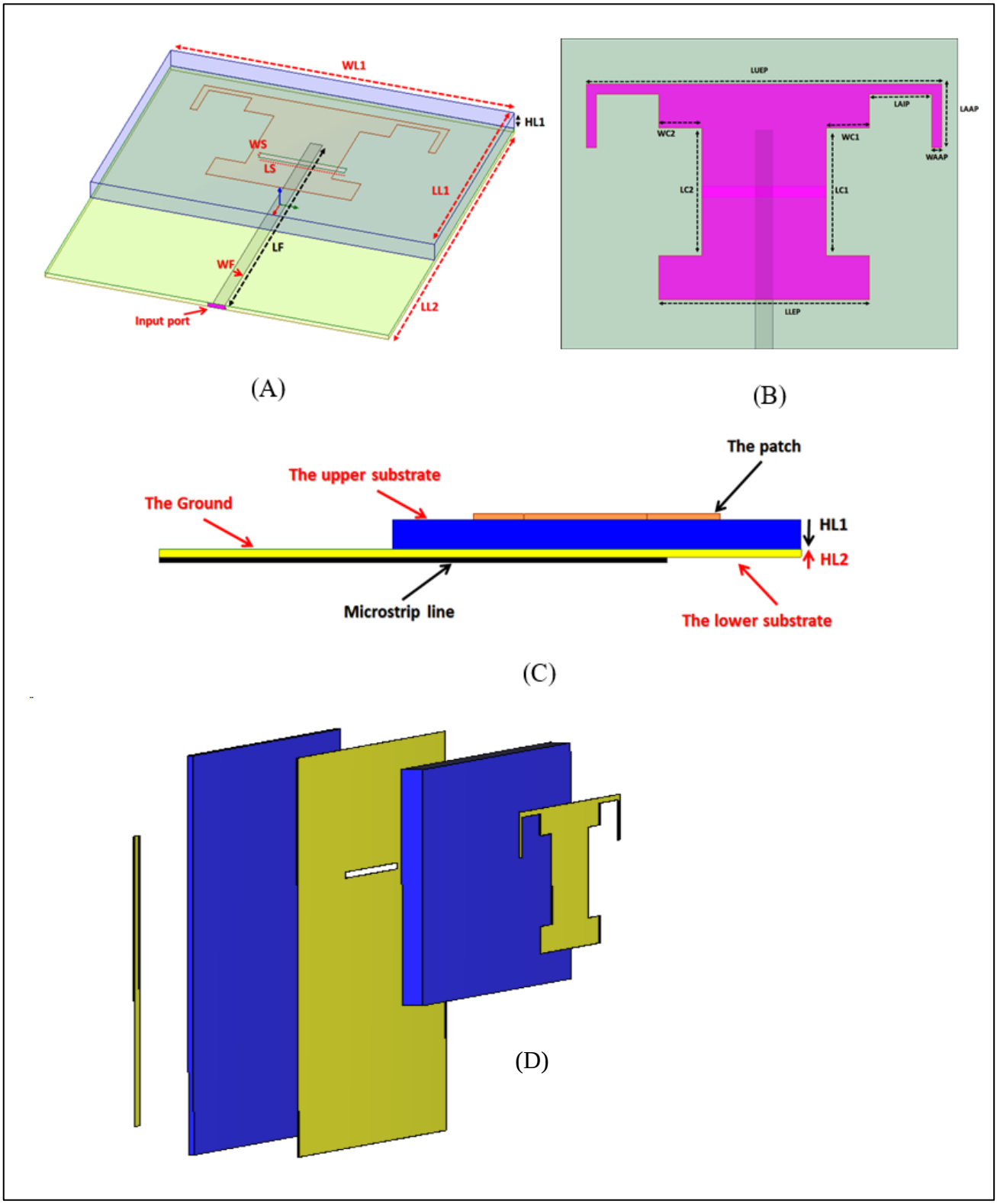

Figure 3.4: (A) 3D view for proposed antenna (B) Top view (C) side view (D) A clear picture of the layers

3.3.3.1 Model 1

The first model used the Arlon AD 250C as a substrate, which has good results at the higher frequency (millimeter wave band), but the result of the gain at frequency 6 GHz is not good. Therefore, this substrate is not adopted because of the bad results of gain at low frequency, and for this reason, Rogers is used in the second model. Dimensions of the model are shown in Table 3 .3.

Table 3.3: Proposed Antenna Dimensions in Aperture Coupled Feed Method used the Arlon AD 250C as a substrate

The Sample	Mm	The Sample	mm
LL1	14	LUEP	15.5
HL1	0.5	LAAP	3.16
WL1	20	WAAP	0.36
LL2	22.02	LAIP	3.16
WF	0.7	WC1=WC2	1.73
LF	17.21	LC1=LC2	5
WS	0.32	LLEP	8.46
LS	5		
HL2	0.25		

3.3.3.2 Model 2

The second model used Rogers RT / duroid 5880 (tm) as a substrate, shows the best performance in terms of basic antenna parameters results. The model is developed twice to reach a good result in all aspects.Table 3.4 presents the dimensions of the first design before development using Rogers RT / duroid 5880 as a substrate.

Table 3.4: Proposed Antenna Dimensions in Aperture Coupled Feed Method used Rogers RT / duroid 5880 (tm) as a substrate.

The Sample	mm	The Sample	mm
LL1	14	LUEP	14.26
HL1	1	LAAP	2.5
WL1	20	WAAP	0.4
LL2	22.02	LAIP	2.5
WF	0.7	WC1=WC2	1.73
LF	17.42	LC1=LC2	5
WS	0.32	LLEP	8.46
LS	5.2		

This model is improved by adjusting the dimensions of the patch antenna design, where the value of S11 is improved, as well as the bandwidth at the frequency of 28 GHz, which represents the first improvement. Table 3.5 presents the dimensions of the antenna after the first improvement.

Table 3.5: The dimensions of the proposed antenna in the double-aperture feed method after the first optimization process

The Sample	mm	The Sample	mm
LL1	14	LUEP	14.26
HL1	1.075	LAAP	2.5
WL1	20	WAAP	0.4
LL2	22.02	LAIP	2.5
WF	0.7	WC1=WC2	1.73
LF	17.42	LC1=LC2	5.01
WS	0.32	LLEP	8.46
LS	5.2	Copper thickness	0.035
HL2	0.238		

The other improvement has been done to cancel the third frequency. this antenna is suitable for bending, that section will be explained later. Table 3.6 shows the dimensions of the antenna after the last improvement, which will be mainly adopted in the simulation process.

Table 3.6: The dimensions of the proposed antenna in the double-aperture feed method after the final optimization process

The Sample	mm	The Sample	mm
LL1	13	LUEP	13.6
HL1	1	LAAP	2.5
WL1	20	WAAP	0.3
LL2	22	LAIP	2.5
WF	0.7	WC1=WC2	1.5
LF	16	LC1=LC2	5
WS	0.33	LLEP	8
LS	7	Copper thickness	0.035
HL2	0.25		

3.3.3.3 Model 3

In this model, FR4 is used as a substrate that has a $\varepsilon_r = 4.3$. Table 3.7 shows the dimensions of this model of an antenna where FR4 is the material of antenna substrate.

3.4 Steps Designing of the Proposed Patch Antenna

In the first step, the patch antenna rectangular is used as a radiator, giving two responses, one at 28 GHz and 2nd at 10 GHz, as shown in figure 3.5. Therefore, by shifting the lower frequency to 6 GHz some parts are cut from the centre patch, which made the 2nd frequency at 7 GHz. The basic reason leads for shifting the band from 10 GHz to 7 GHz is that when parts are removed from the patch lead to the spacing between the edges.

Finally, two metal pieces are added on top of the patch as shown in figure 3.5, to make the peak response at an indeed frequency of 6 GHz.

Table 3.7: Proposed Antenna Dimensions for Aperture Coupled Feed Method using FR4 as a substrate

The Sample	mm	The Sample	mm
LL1	13	LUEP	16.6
HL1	1	LAAP	3.8
WL1	20	WAAP	0.5
LL2	23	LAIP	3.8
WF	0.7	WC1=WC2	1.5
LF	16	LC1=LC2	5
WS	0.43	LLEP	8
LS	8.49	copper thickness	0.035
HL2	0.77		

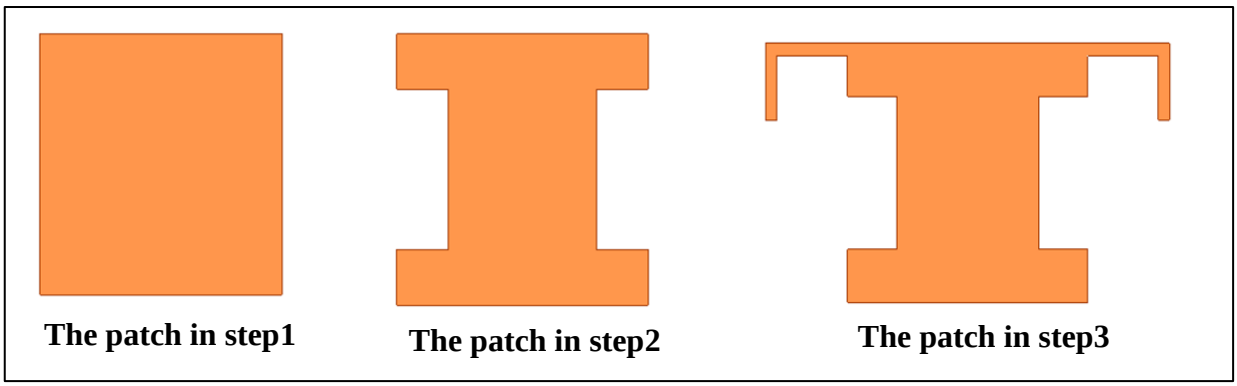

Figure 3. 5: The design steps for excited dual bands.

3.5 Antenna Bending

In this part, the performance of the antenna is explained after it is bent using Rogers RT / duroid 5880 as a substrate, which employs the second model after improvement. This model has an appropriate substrate that makes the proposed model suitable to operate in the higher frequencies,

dependent on the Aperture Coupled Feed Method to feed the antenna, and it is simulated via CST software and bent on the surface of a cylinder. The antenna is tested on different cylindrical radii, (5, 10, 15, and 20) mm. Figure 3.6 shows the direction of the bend towards the cylindrical surface. Figure 3.7 shows the shape of the proposed design after bending with radii (5, 10, 15, and 20) mm. The VSWR and radiation efficiency are calculated via simulation, and the rest of the parameters, such as gain and directivity, are also calculated and the results after bending are compared to the results of the planar design.

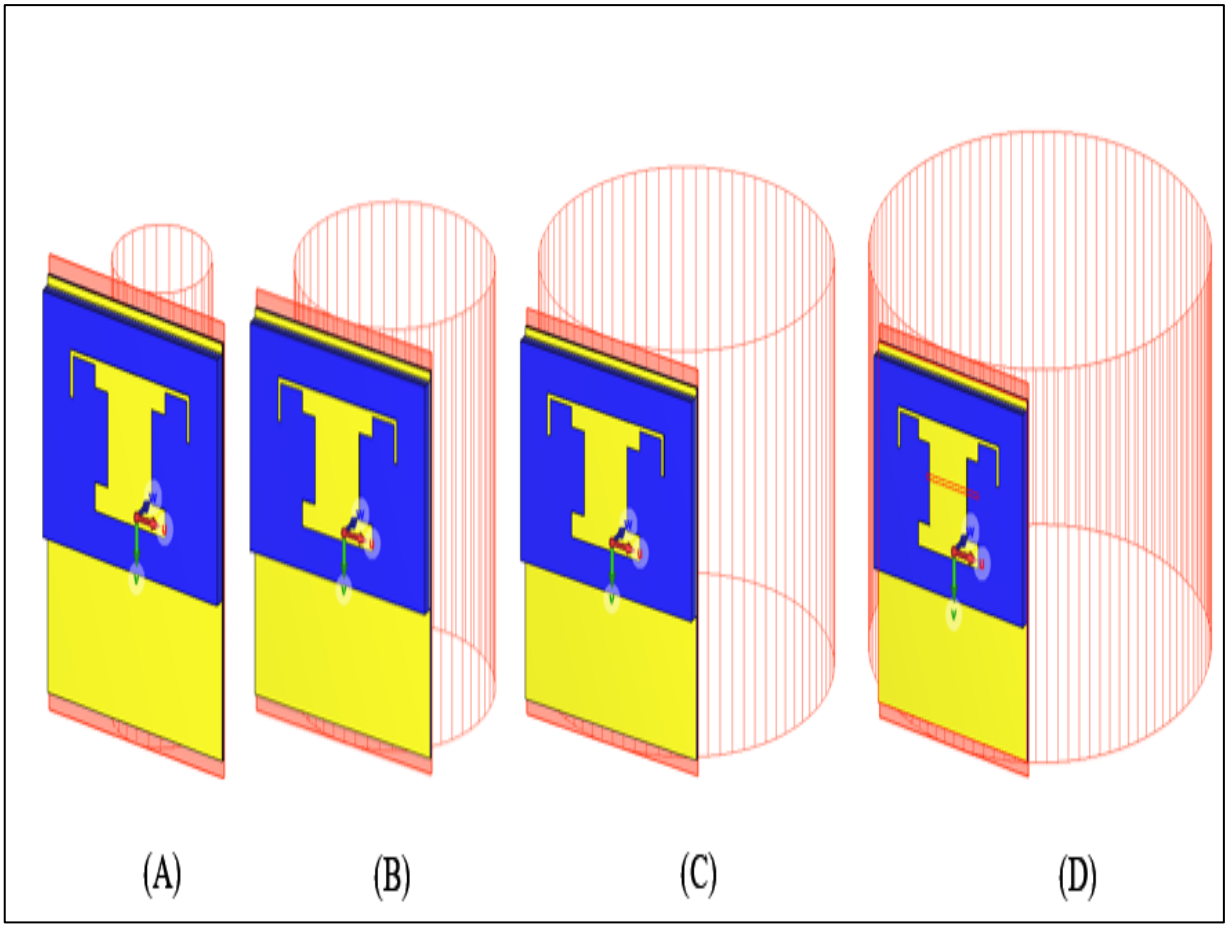

Figure 3. 6: proposed design shape after bending (A) R =5 millimeter (B) R=10 millimeter (C) R=15 millimeter (D) R=20 millimeter

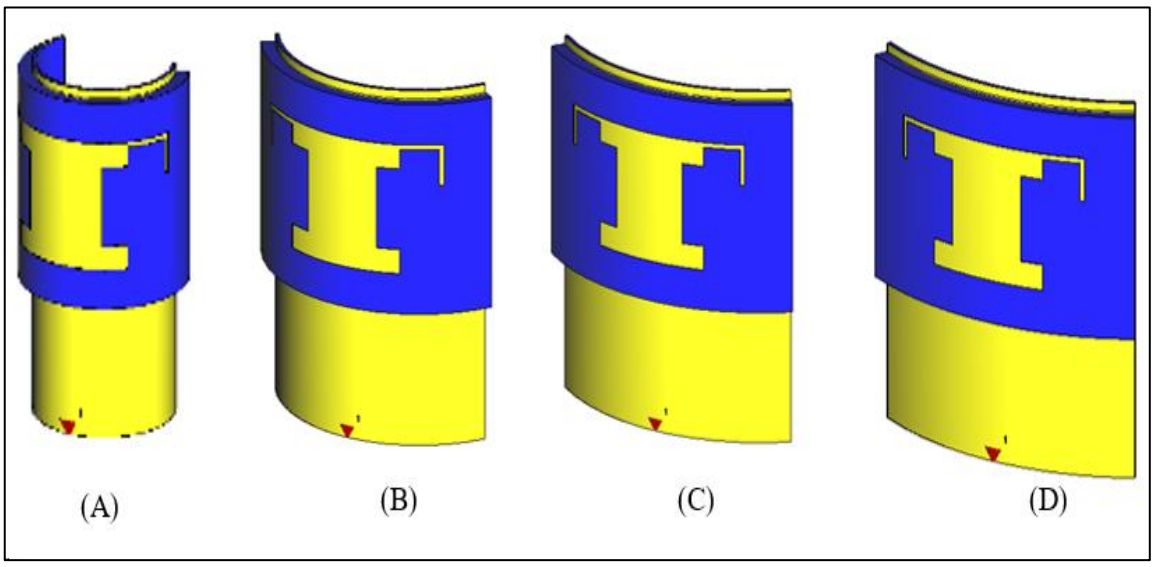

Figure 3. 7: Different radii of the cylinder (A) R =5 millimeter (B) R=10 millimeter (C) R=15 millimeter (D) R=20 millimeter

3.6 Antenna Fabrication

The fabrication process of the proposed design is carried out on an FR4 substrate that has a dielectric constant ε_r = 4.3, the design includes two parts, and each part has to be printed on one of the substrates. Then, the two substrates of the proposed design are glued by using a glues material on the outer sides of both substrates of the antenna, as shown in Figure 3.8, and depending on the dimensions in Table 3.7.

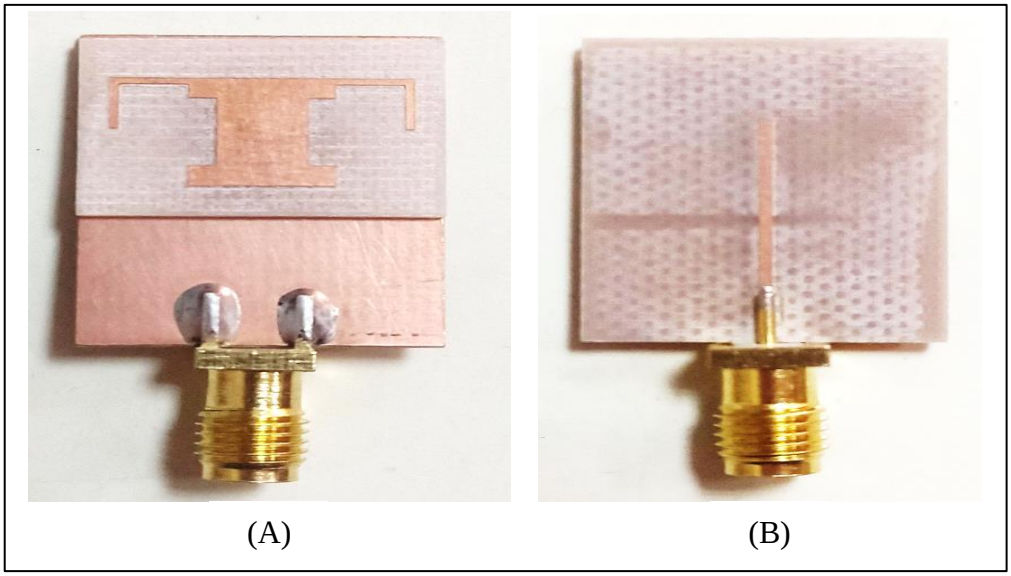

Figure 3. 8: Antenna shape after manufacturing (A) front (B) back

Since the substrate material is solid, the two substrates cannot be attached together without an air gap (a space between the two substrates when they are glued to each other). This gap should be reduced to the minimum possible distance by pressing the two substrates during the gluing process. For this reason, a tool is used to compress the two substrates to get the minimum gap between them. Figure 3.9 shows the shape of the antenna during the test. The vector network analyzer (VNR) uses in the testing of the proposed antenna design to calculate the main performance parameters.

(A)

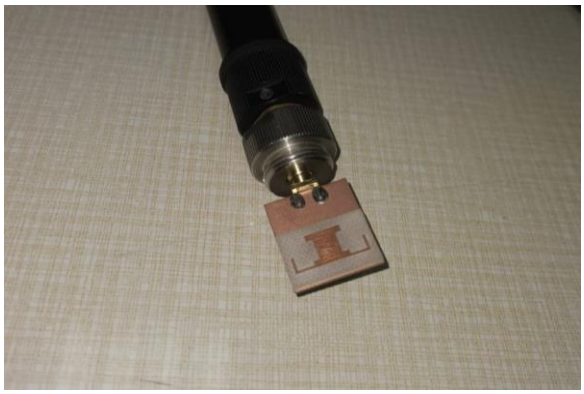

(B)

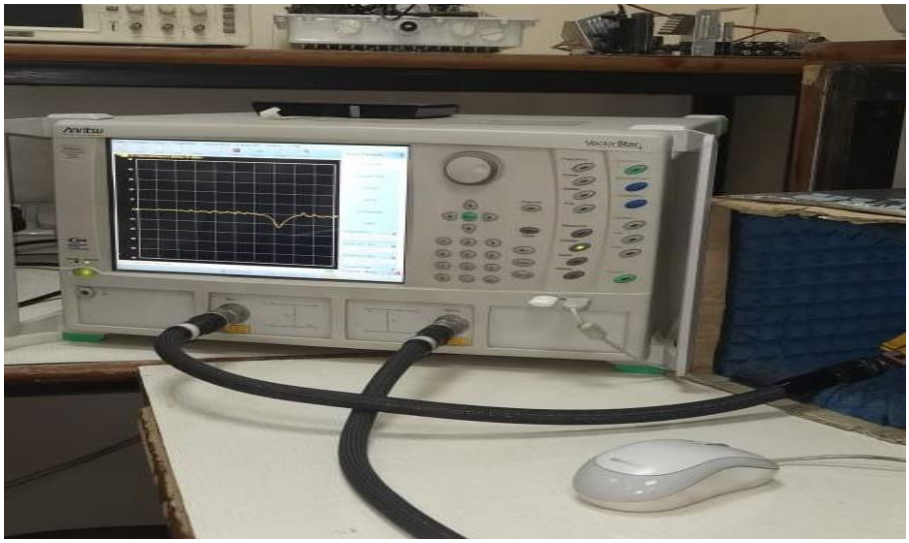

Figure 3.9: Pictures of the antenna after manufacturing (A) without pressure (B) during the examination process.

In the manufacturing process, SMA connectors of 50 ohms are used, which are semi-precise units that are developed to act as a connector for the coaxial cable with a screw coupling mechanism, as shown in figure 3.10.

SMA is initially providing electrical performance from DC to 12 GHz, but it is developed to provide good performance from DC to 34 GHz, and thus it is suitable for frequencies that It is being worked on in this research. It also has high mechanical durability. The most important features of these connectors are that they are made of brass or stainless steel, as well as a lightweight, high-strength. The SMA connector is used in microphone systems, mobile phone antennas, Wi-Fi antenna systems, and PC/LAN.

Figure 3.10: Subminiature version A.

With the rapid development of wireless communication technologies, the need for more effective and efficient devices for testing ideas and analyzing results for communication designs has increased. For this reason, wireless network analysts have been turned to give a clear vision of the operation and performance of radio frequency networks. The network analyzer provides a monitoring process for the response, where the process and performance can be seen, and thus their suitability can be evaluated. In this manufacturing process, an Anritsu device is used in the process of analyzing the results of the antenna, as shown in Figures 3.9 and 3.11.

Figure 3.11: The vector network analyzer (VNR).

Chapter Four

Results and Discussion

CHAPTER 4

RESULTS AND DISCUSSION

4.1 Introduction

This chapter presents the results of the proposed antenna, besides the results of its bent model, using Computer Simulation Technology (CST) software. It covers the results of the proposed antenna model and bending model with a comparison to the results of the planar antenna. Parameters such as return losses, voltage standing wave ratio, gain, antenna efficiency and directivity are presented. The results of the proposed antenna parameters are calculated according to the three feeding methods Microstrip Line Feed (MLF), Proximity Coupled Feed (PCF), and Aperture Associated Feed (ACF); the results of these techniques will be presented, explained, and discussed besides a comparison of the real techniques results.

4.2 Proposed Antenna Feeding Methods

In this section, the results of the feeding methods are presented as follows:

4.2.1 Microstrip Line Feed(MLF)

In the MLF method of feeding, the calculated values of return loss for both frequencies are (-35 dB at 6 GHz and -24.9 dB at 28GHz), and the amount of percentage bandwidth is 2.7% (6.49-5.32 GHz) at 6 GHz and 1.23% (28.98 - 28.63) at 28 GHz as shown in Figure 4.1. Moreover, the VSWR for this feeding method is 1.03 dB and 1.12 dB at 6 GHZ and 28 GHZ, respectively, as shown in Figure 4.2.

On the other side, the values of the gain and directivity at 6GHz are not good enough, while, they are well at 28GHz. Where the gain values are 1.75 dB and 7.81 dB at 6 GHz and 28GHz, respectively, as shown in Figure 4.3. In addition, the directivity values are 2.7 dB and 8.27 dB at 6 GHz and 28GHz, respectively, as shown in Figure 4.4. Moreover, the efficiency of the MLF method is 64% at 6 GHz and 94% at 28 GHz.

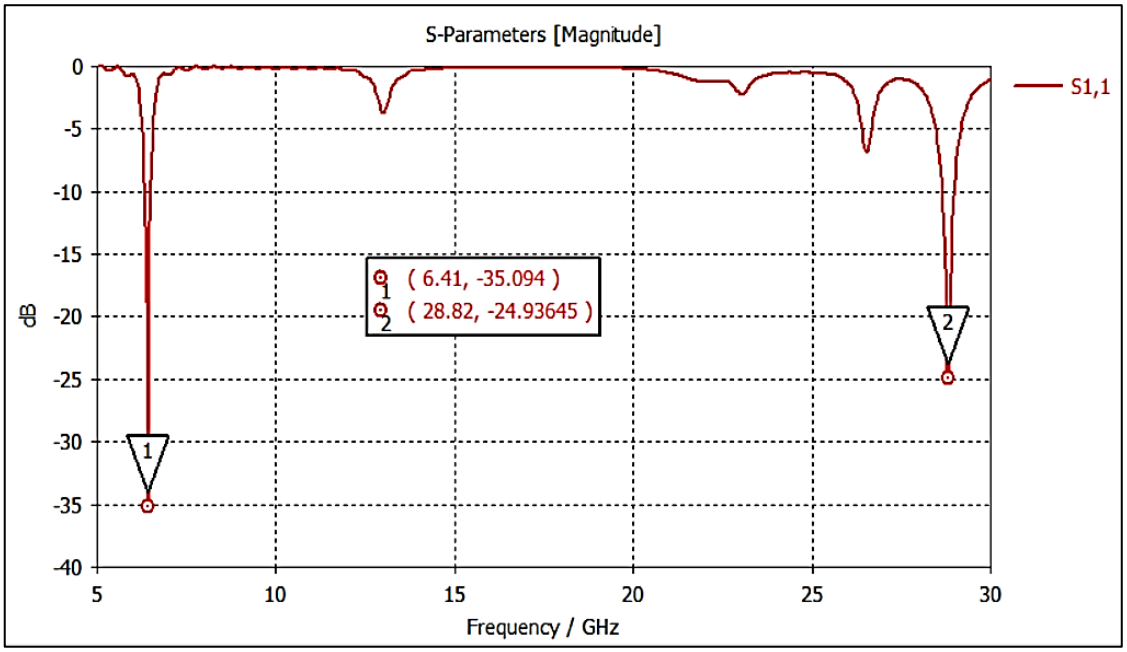

Figure 4.1: S11 of the proposed antenna using MLF method.

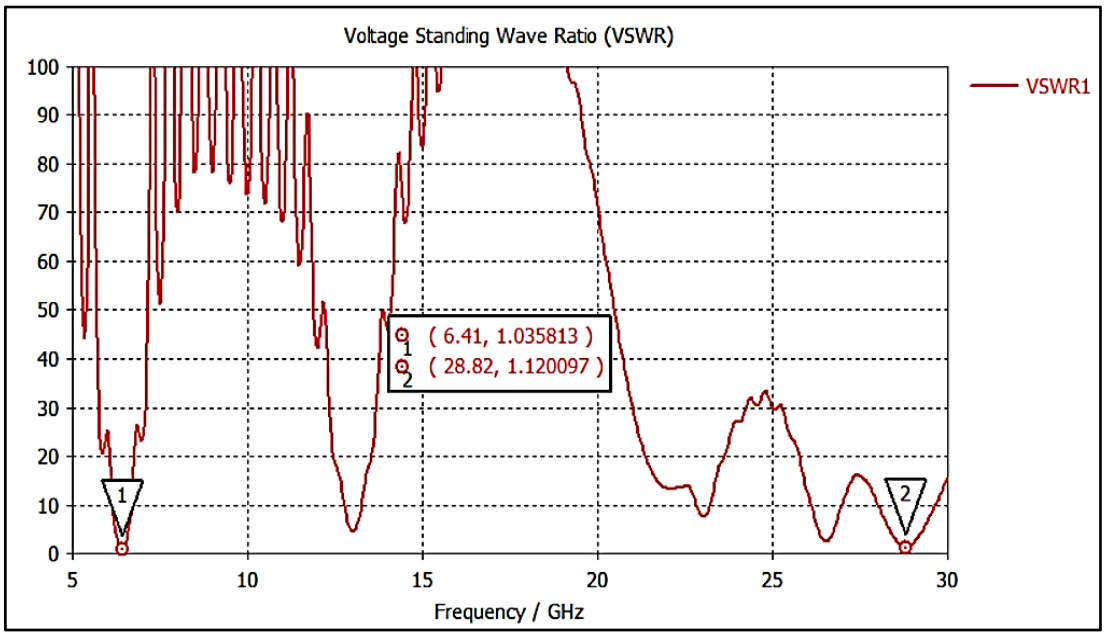

Figure 4.2: VSWR of the proposed antenna using MLF method.

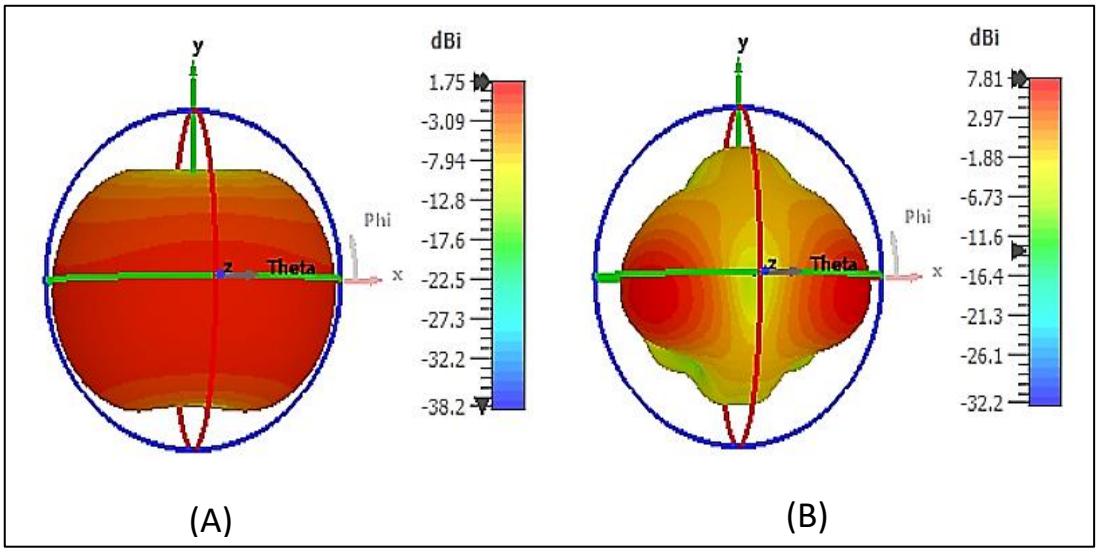

Figure 4.3: The gain (A) The gain at frequency 6 GHz, (B) The gain at frequency 28 GHz, using MLF method.

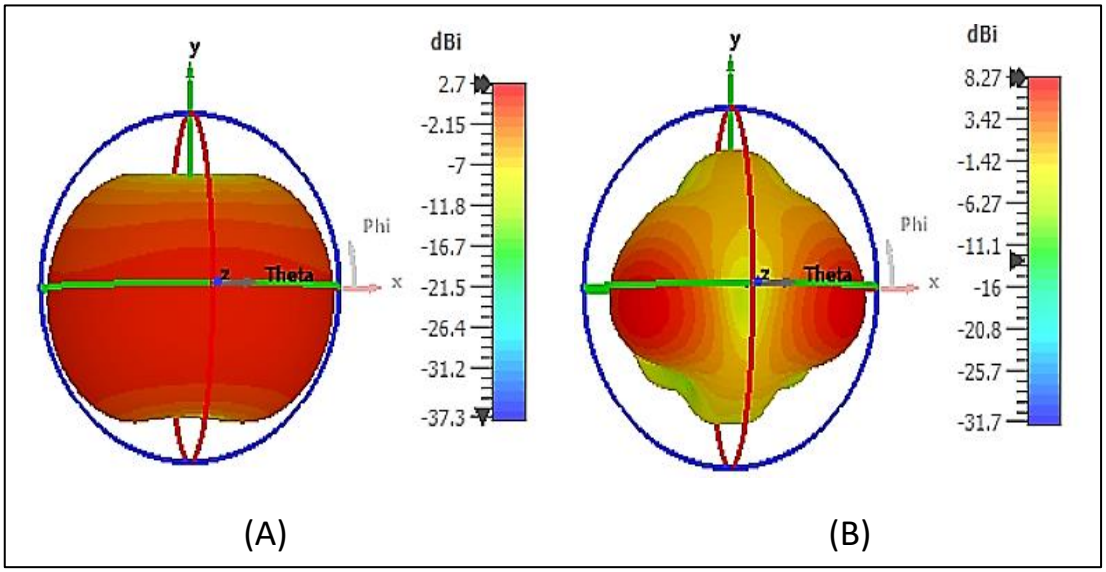

Figure 4.4: (A) The directivity at frequency 6 GHz, (B) The directivity at frequency 28 GHz, using MLF method.

4.2.2 Proximity Coupled Feed

In this feeding method, the return losses are -45.33 dB and -25.7 dB at 6 GHz and 28GHZ, respectively, which have percentage bandwidths of 3.2% (6-6.2) at 6 GHz and 2.76% (28.5 - 29.3) at 28 GHz as shown in Figure 4.5. The VSWR in this method is 1.01 dB and 1.1 dB at 6 GHZ and 28 GHZ, respectively, as shown in Figure 4.7.

On the other side, the values of the gain and directivity at 6GHz are not good enough, while, they are well at 28GHz. Where the gain values are 2.77 dB and 7.02 dB at 6 GHz and 28GHz, respectively, as shown in Figure 4.6. In addition, the directivity values are 5.1 dB and 7.17 dB at 6GHz and 28GHz, respectively, as shown in Figure 4.8 and the obtained efficiencies are 64% at 6GHz and 94% at 28GHz.

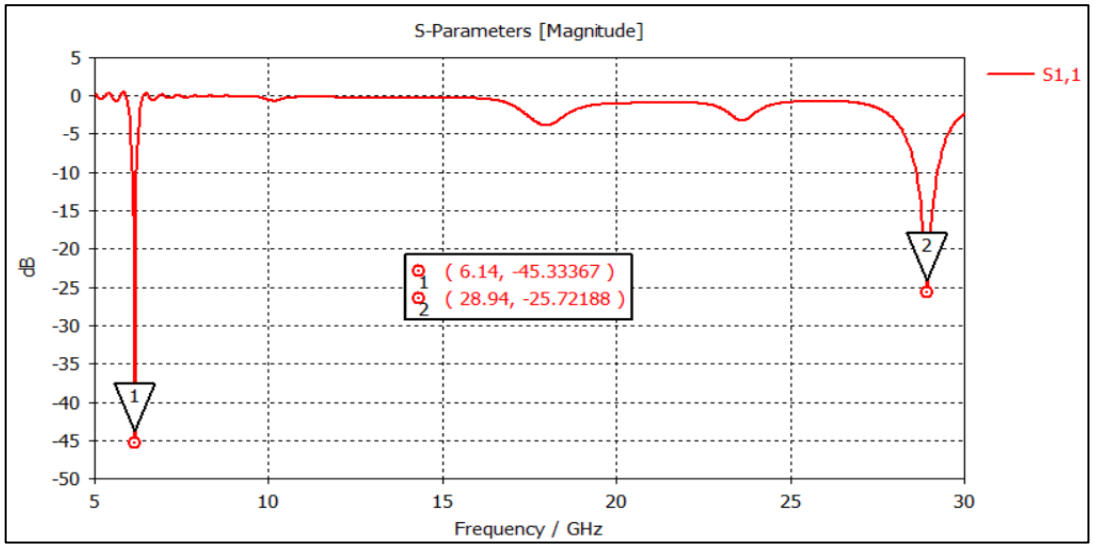

Figure 4.5: S11 for the proposed antenna using PCF method.

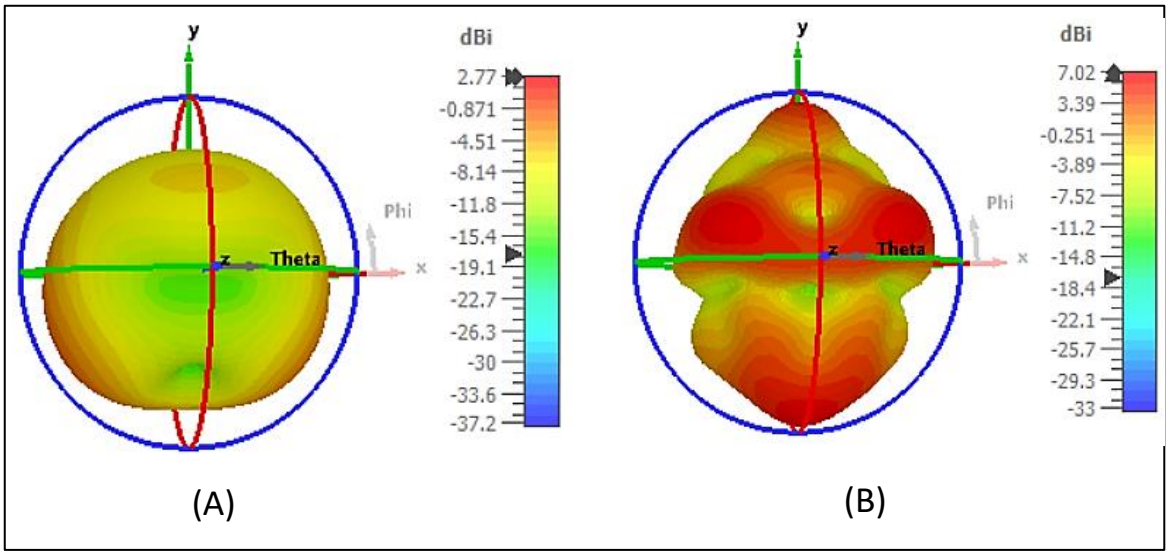

Figure 4.6: (A) The gain at frequency 6 GHz, (B) The gain at frequency 28 GHz, using PCF method.

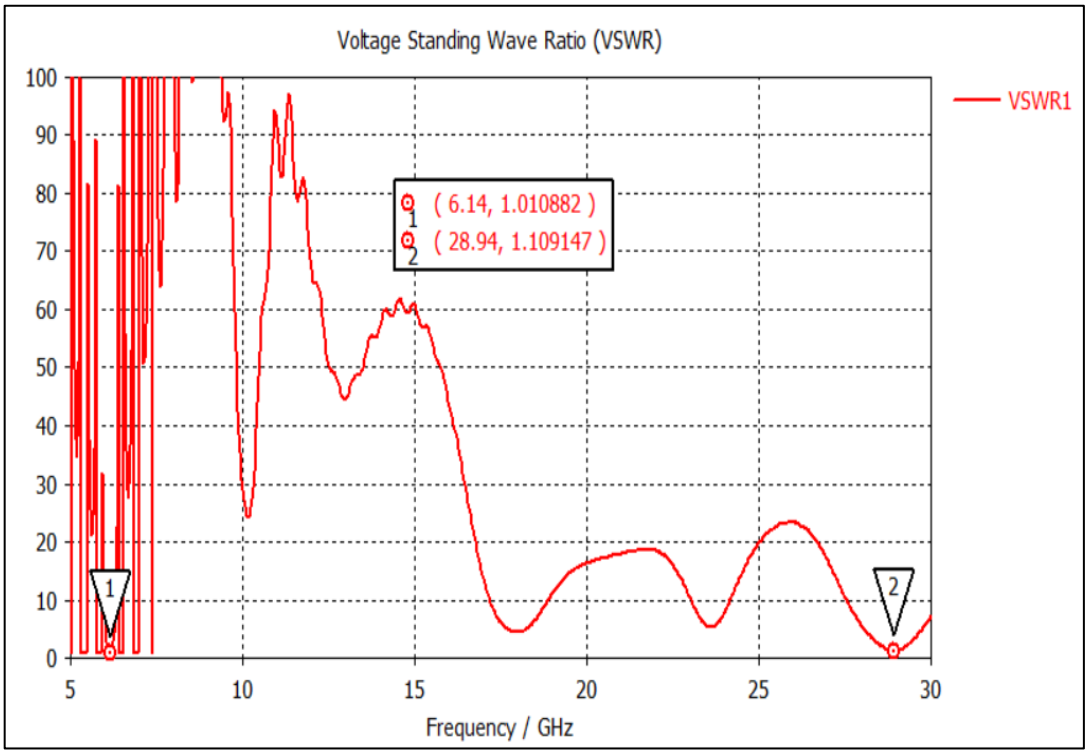

Figure 4.7: VSWR for the proposed antenna using PCF method.

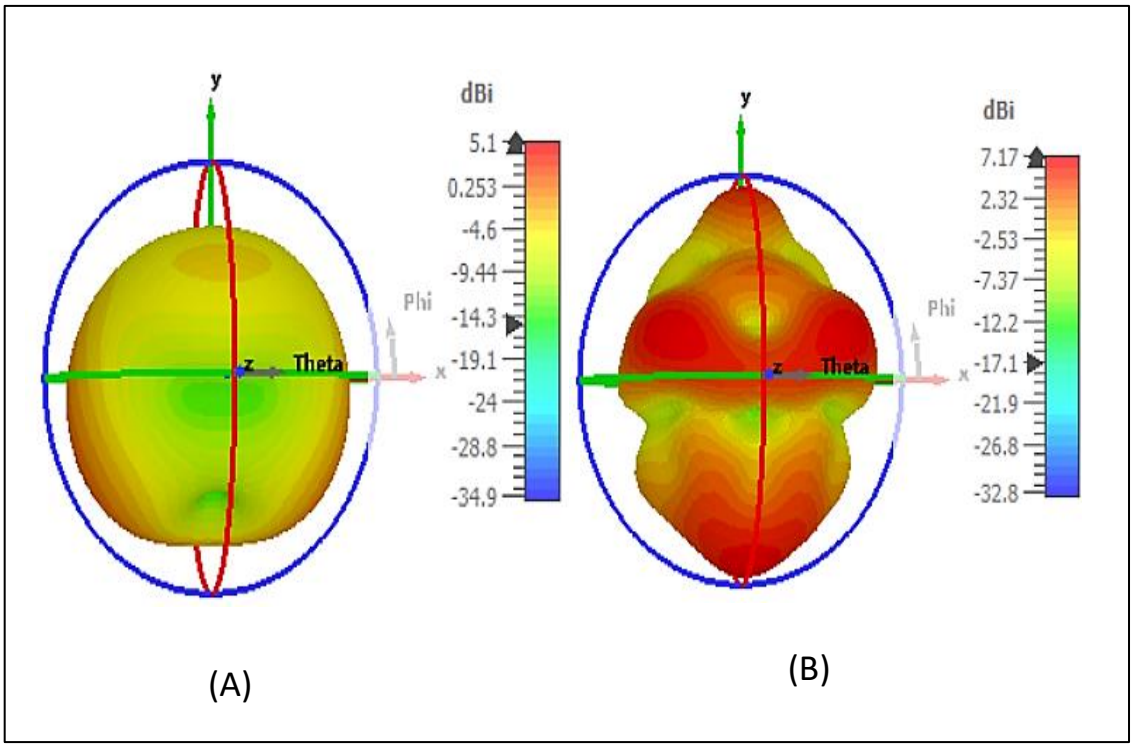

Figure 4.8: (A) The directivity at frequency 6 GHz, (B) The directivity at frequency 28 GHz, antenna using PCF method.

4.2.3 Aperture Coupled Feed

The simulation results of this technique with the proposed antenna are very well and they are superior to those of the other feeding methods. So the ACF method has been adopted to design the proposed antenna with three models. These models are designed based on different substrate types.

4.2.3.1 Model 1

In this model, Arlon AD 250C is used as a substrate, as mentioned earlier in the third chapter. the simulation results of this model show that the gain value is not good and the values of bandwidth 2.07% (6.126-6) at 6 GHz and 5.3% (28.6 - 27.1) at 28 GHz as presented in Figure 4.9. Figure 4.10 shows that the VSWR of the proposed antenna model is 1.1 at 6 GHz and 1.005 at 28 GHz. The gain are -0.062 dB and 10 dB at 6 GHZ and 28GHZ, respectively, as shown in Figure 4.11. In addition, the directivity valus is 3.9 dB and 10.2 dB at 6 GHZ and 28 GHZ, respectively, as shown in Figure 4.12.

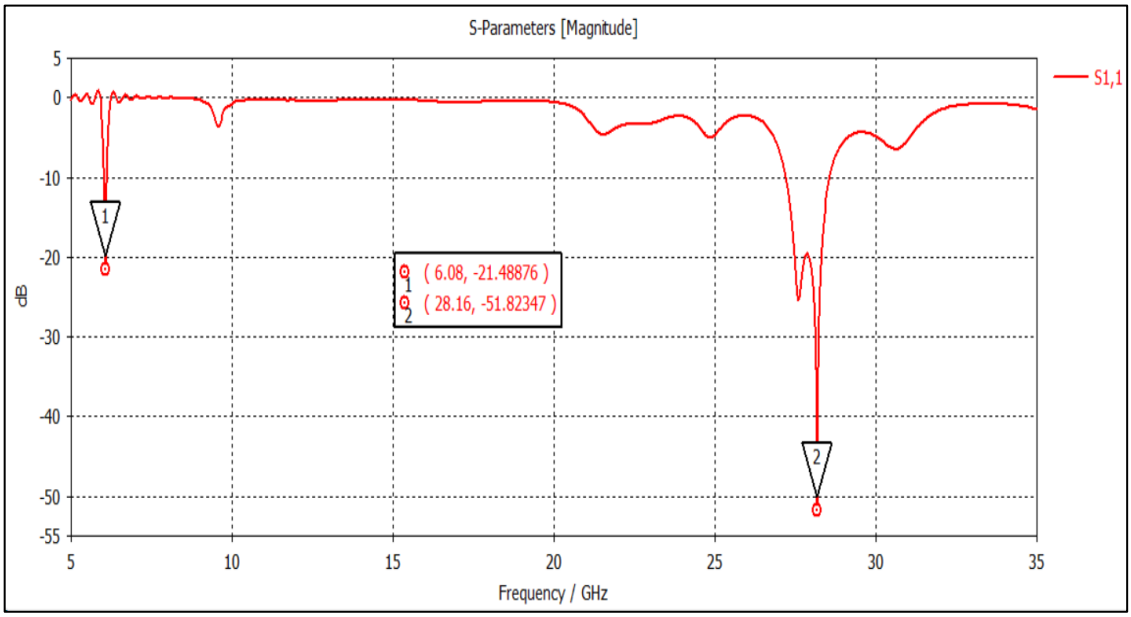

Figure 4.9: S11 for the proposed antenna using Arlon AD 250C as substrate

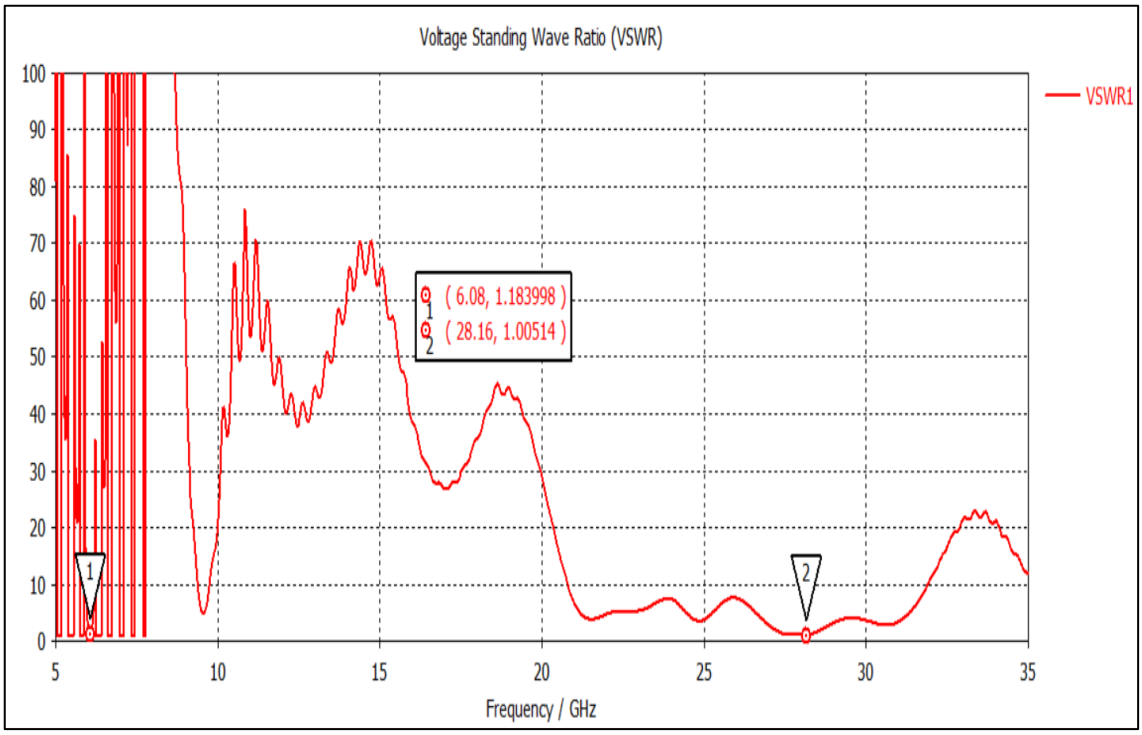

Figure 4.10: VSWR for the proposed antenna using Arlon AD 250C as substrate

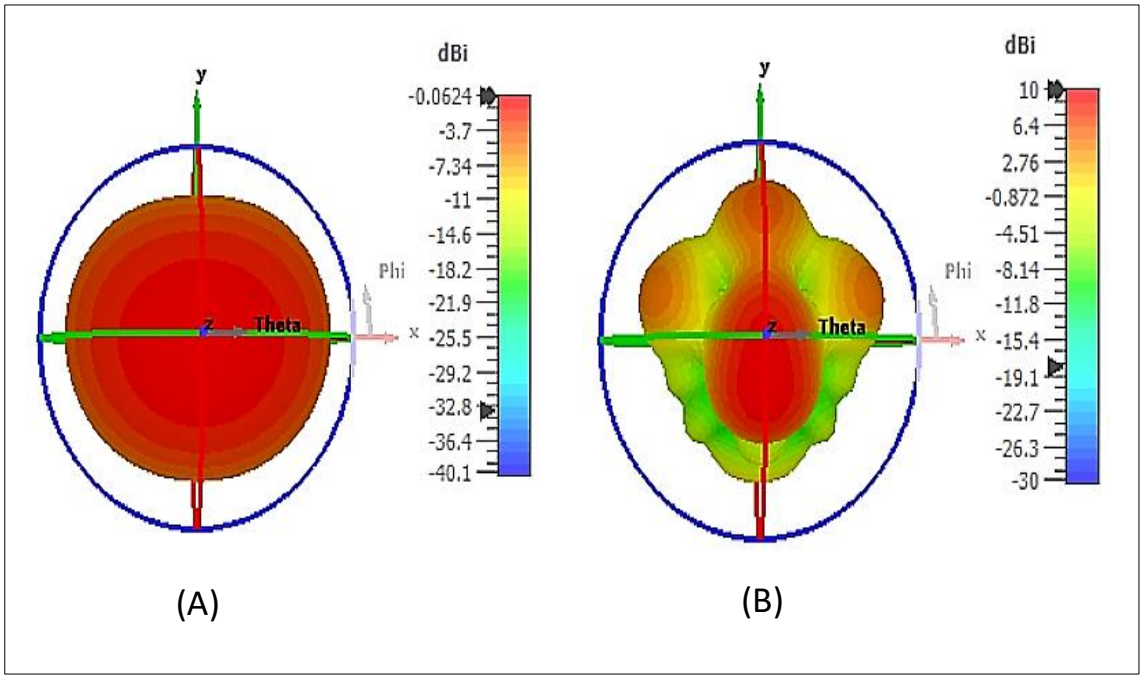

Figure 4.11: (A) The gain at frequency 6GHz, (B) The gain at frequency 28GHz. using Arlon AD 250C as substrate.

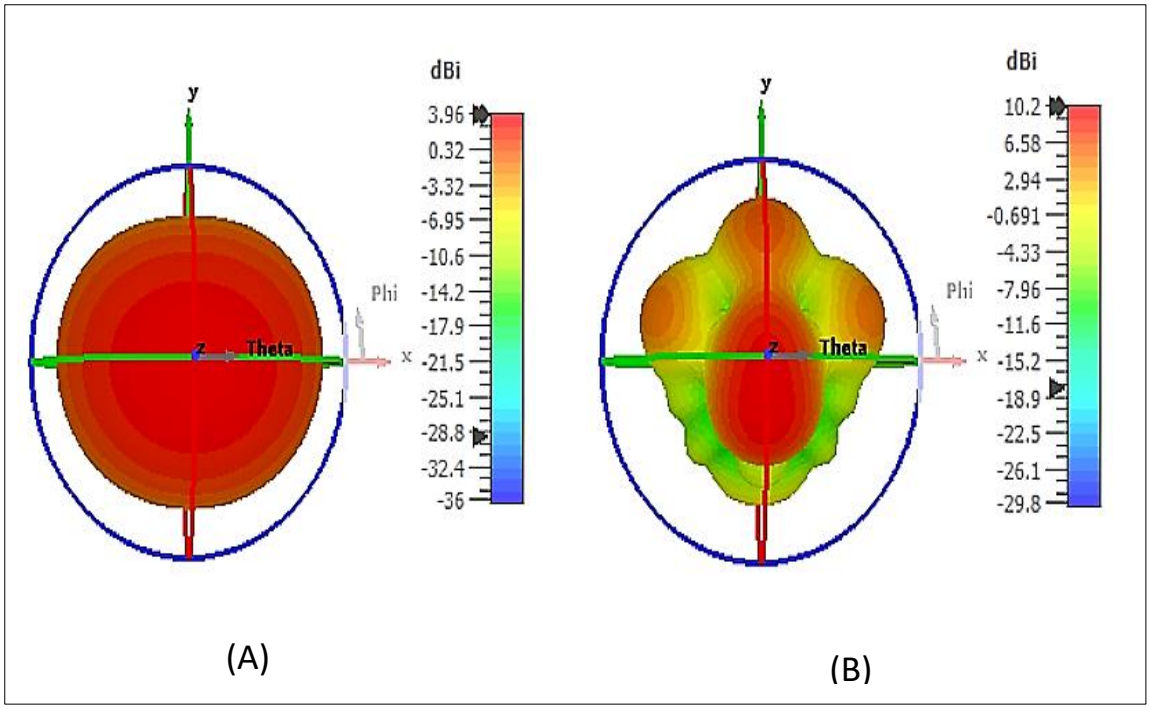

Figure 4.12: (A) The directivity at frequency 6 GHz, (B) The directivity at frequency 28 GHz. using Arlon AD 250C as substrate.

4.2.3.2 Model 2

Rogers RT/duroid 5880 (tm) is utilized in this model as a substrate, as mentioned earlier in the third chapter. The simulation result show that the values of the bandwidth are 4.3% (7-6.7) at 6 GHz and 14.18% (32.3 – 28.2) at 28 GHz as presented in Figure 4.13. Figure 4.14 shows the VSWR values of the proposed antenna

model These values are 1.1 at 6GHz and 1.06 dB at GHz, which are within the acceptable range of the good result because the ideal outcome is about one. The simulation results of model-2 show that the gain values are 3.54 dB at 6 GHz and 8.09 dB at 28GHz, as shown in Figure 4.15. In addition, the directivity values are 6.09 dB at 6 GHz and 8.19 dB at 28GHz as shown in Figure 4.16. By using the previous gain and directivity values, the radiation efficiency can be obtained as 58% at 6 GHz and 98% at 28 GHz.

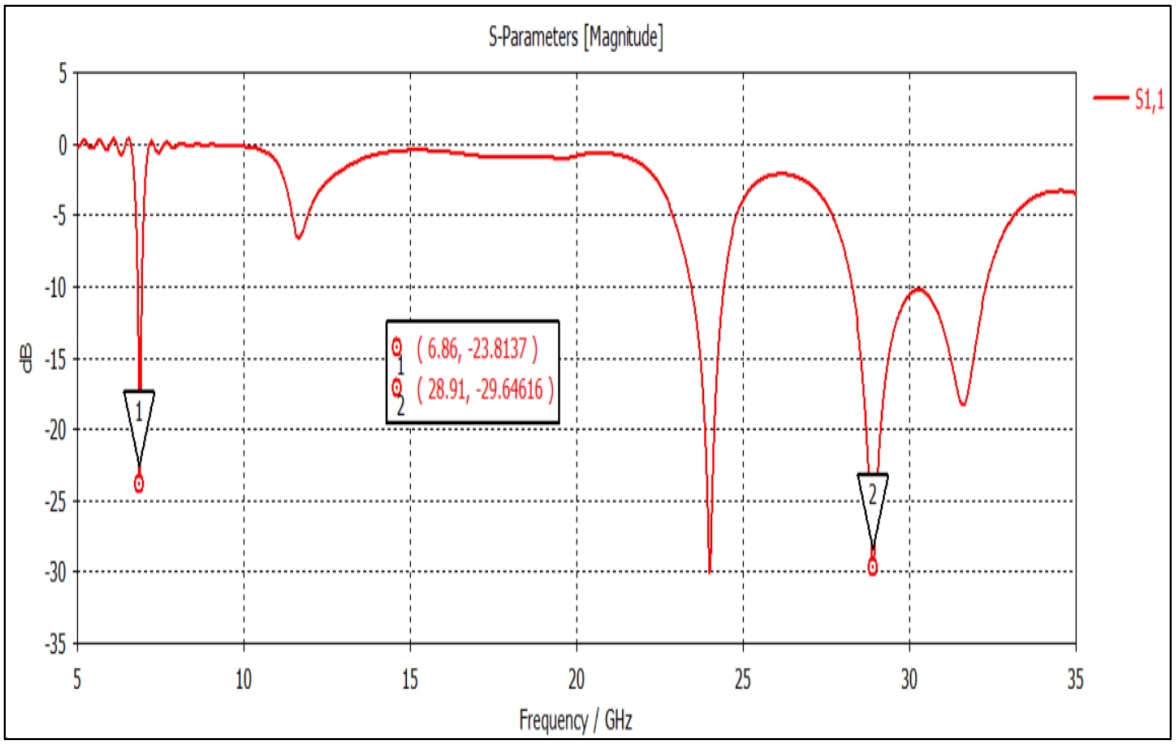

Figure 4.13: S11 for the proposed antenna before the optimization process using Rogers RT/duroid 5880 (tm) as a substrate

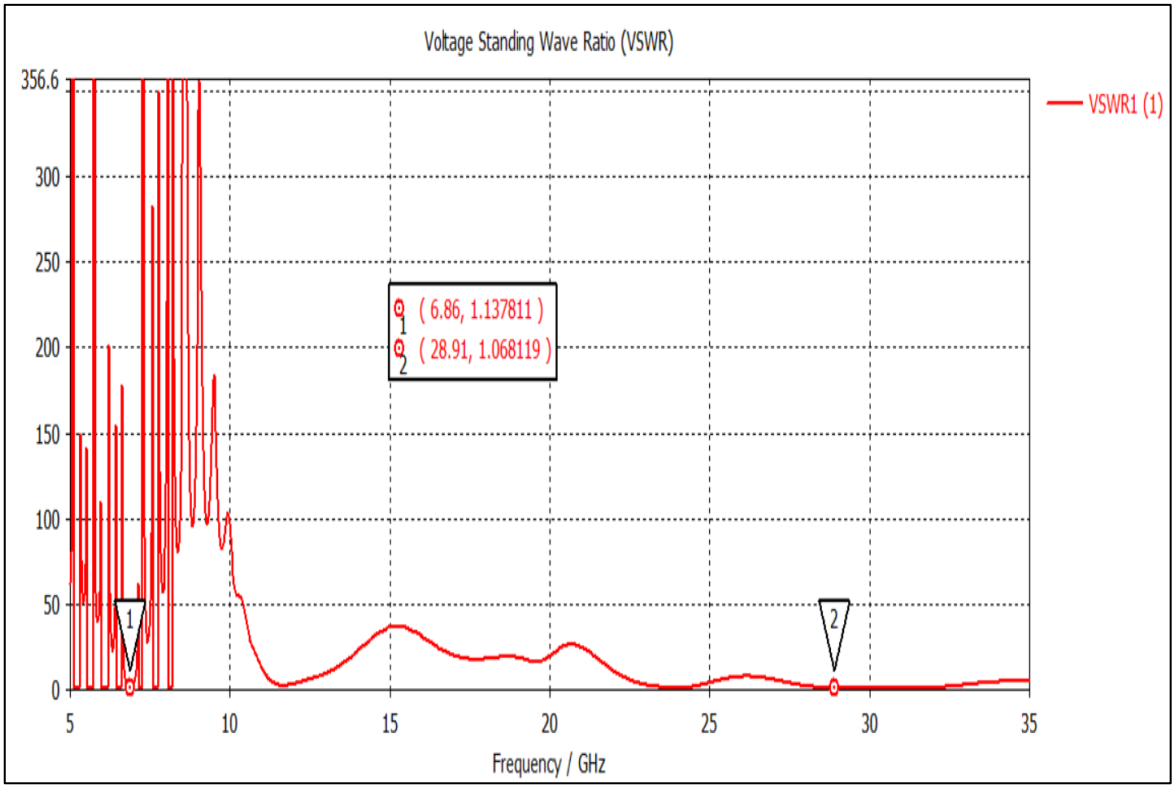

Figure 4.14: VSWR for the proposed antenna before the optimization process, using Rogers RT/duroid 5880 (tm) as a substrate.

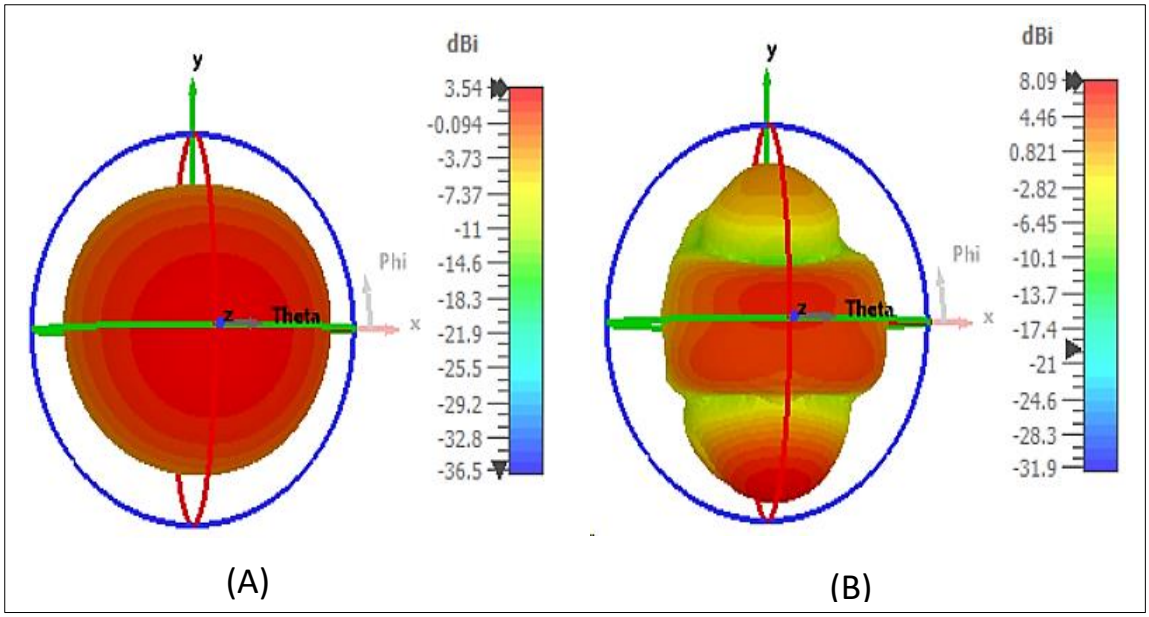

Figure 4.15: (A) The gain at frequency 6GHz, (B) The gain at frequency 28GHz , using Rogers RT/duroid 5880 (tm) as a substrate.

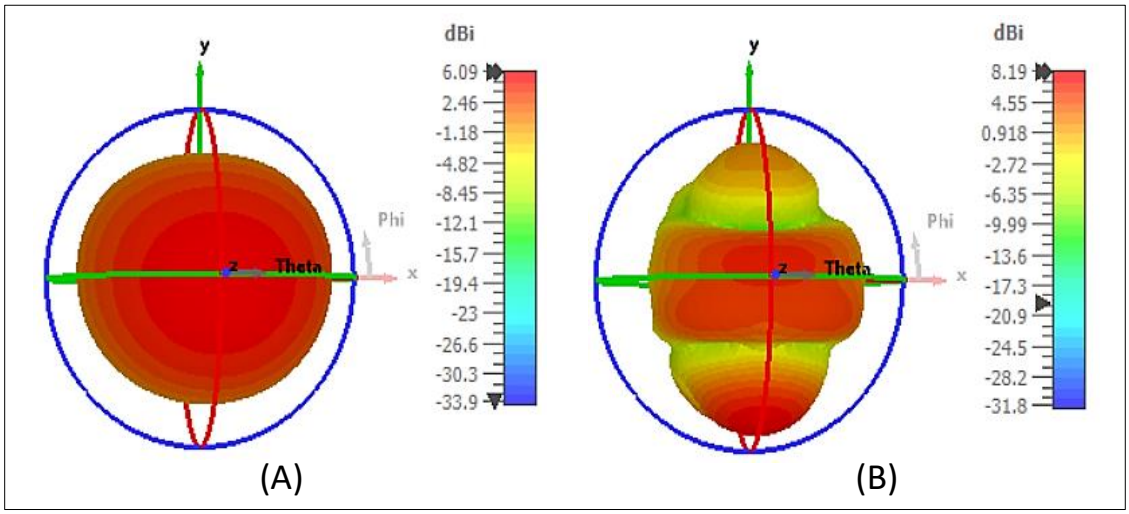

Figure 4.16: (A) The directivity at frequency 6 GHz, (B) The directivity at frequency 28 GHz, using Rogers RT/duroid 5880 (tm) as a substrate.

Table 4-1 shows the percentage of power reflected from the antenna. The reflected energy from the 6GHz antenna is 0.37%, calculated , thus the antenna can transmit 99.63% of the total power, that has been delivered to the antenna. In addition, in the 28GHz frequency, the percentage of energy reflected from the antenna is 0.08%, thus the transmitting power of the antenna is 99.92%, so the antenna performance is good.

Table 4.1: The reflected power percentage of the model 2.

Resonance Frequency	VSWR	Reflection Coefficient, Γ	Reflected Power (%)
6.86	1.1	0.06103	0.3725
28.91	1.06	0.029126	0.08483

A. First Developed Model 2

The second model has been improved by adjusting the dimensions of the proposed design to get a better result in terms of the S11, gain and bandwidth. Where the obtained bandwidth values are 4.3% (6.96-6.8 at 6 GHz and 14.18% (32.38 – 28.1) at 28 GHz as presented in Figure. 4.17. Figure 4.18 shows that the values of the VSWR of the proposed antenna model are 1.08 dB and 1.00003 dB at 6 GHZ and 28GHZ, respectively. Besides, the gains are 3.74 dB and 8.33dB at 6 GHZ and 28GHZ, respectively, as shown in Figure 4.19. The directivities are 5.9 dB and 8.4dB at 6 GHZ and 28 GHZ, respectively, as shown in Figure 4.20.The radiation efficiency values are (63% at 6 GHz and 99% at 28 GHz).

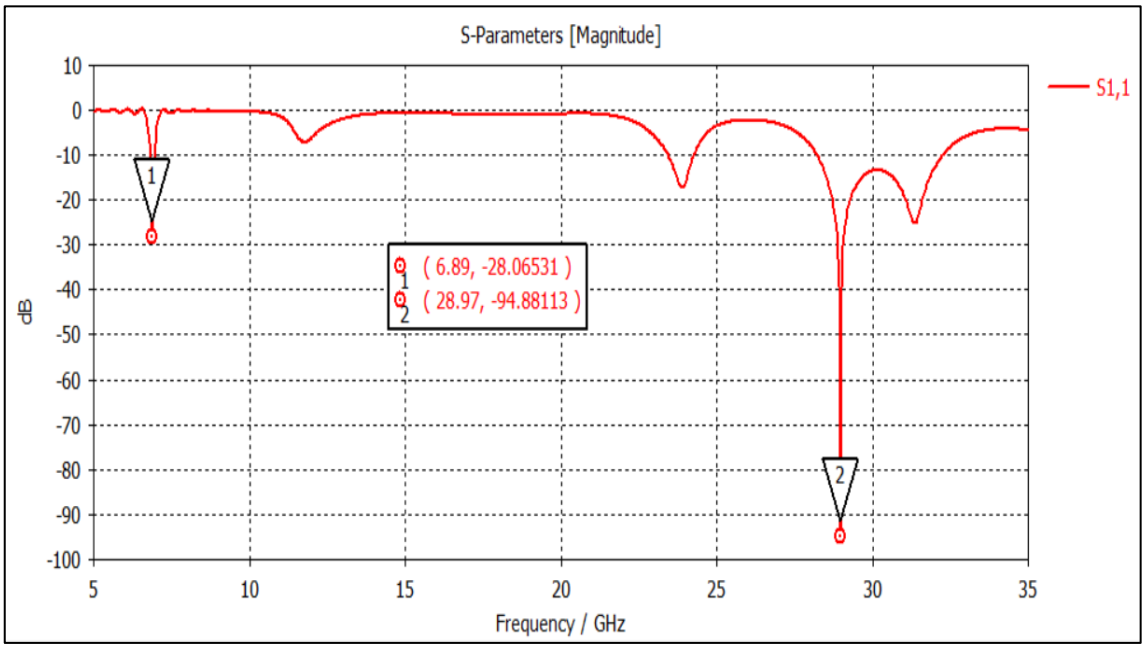

Figure 4.17:S11 for the proposed antenna, first development model 2.

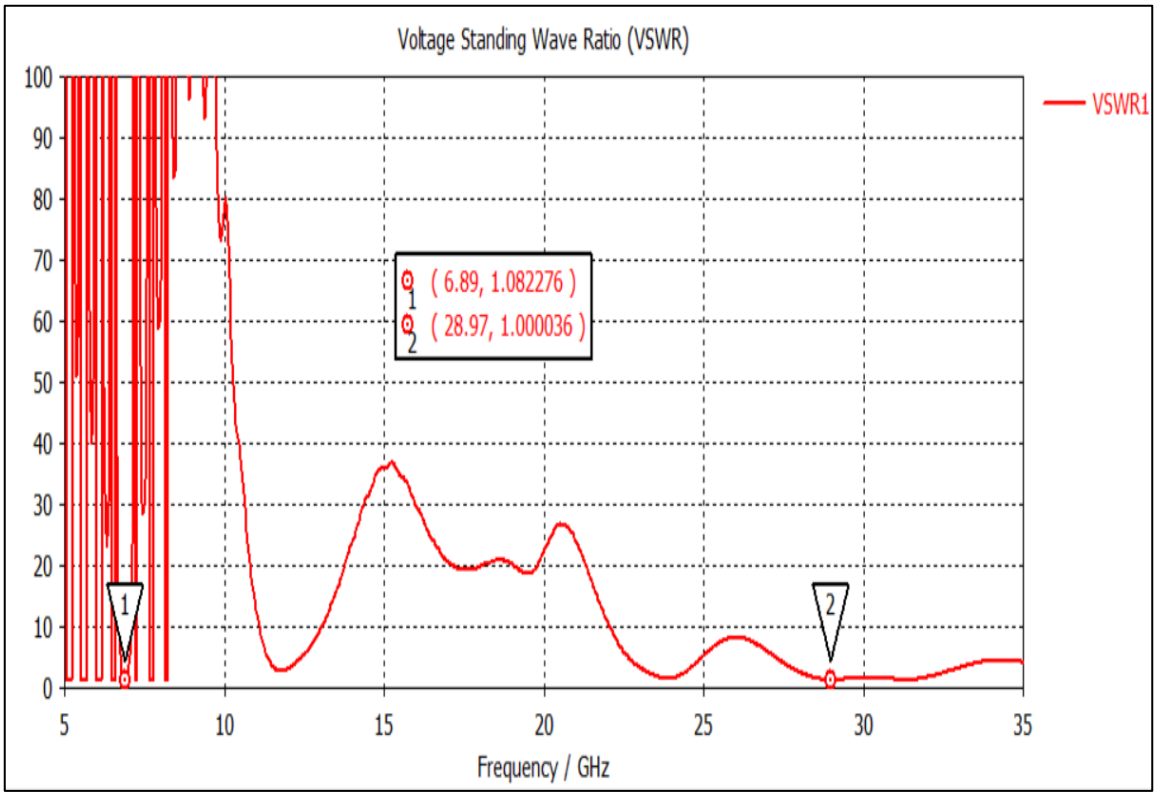

Figure 4.18: VSWR for the proposed antenna , first development model 2.

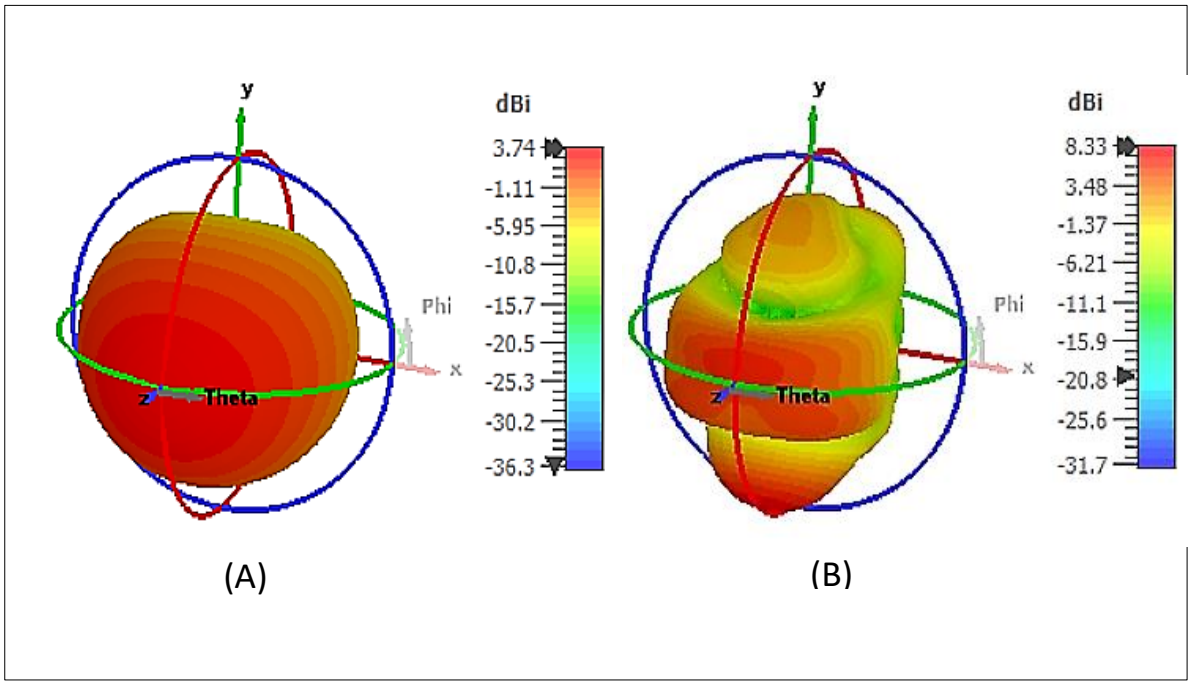

Figure 4.19:(A) The gain at frequency 6GHz, (B) The gain at frequency 28GHz , first development model 2.

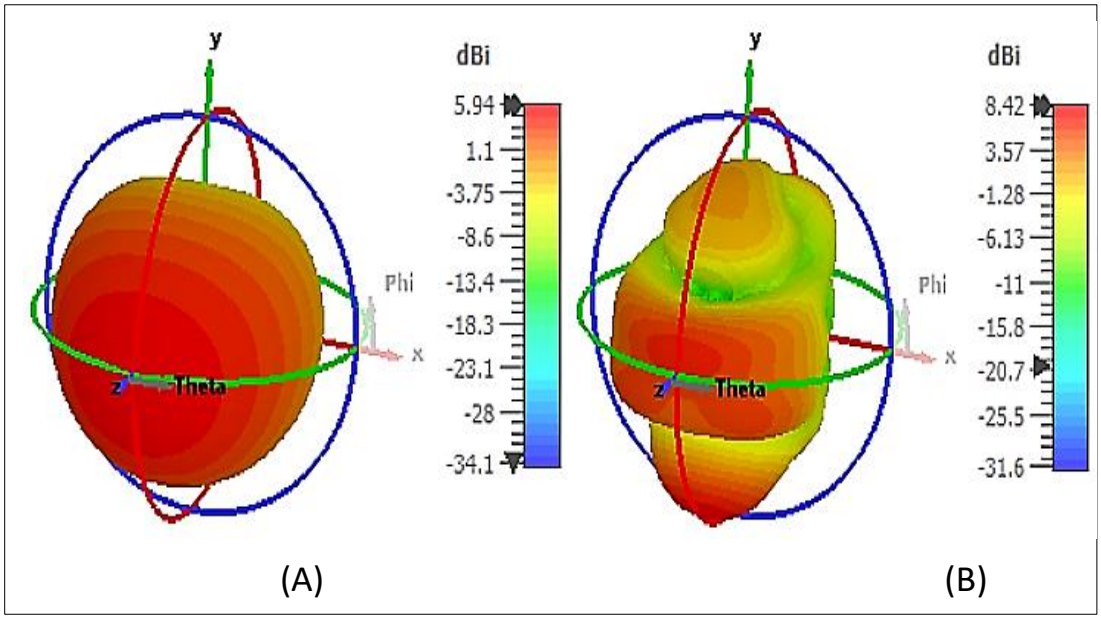

Figure 4.20: (A) The directivity at frequency 6 GHz, (B) The directivity at frequency 28 GHz, first development model 2.

Table 4-2 shows the percentage of the reflected power from the 6GHz antenna. The reflected energy from the 6GHz antenna is 0.14%, which means that the antenna can transmit 99.86% of the total power that has been delivered to the antenna. For the 28GHz frequency, the percentage of energy reflected from the antenna is 0.0000000225%, which means that almost all the power is transmitted.

Table 4.2: The reflected power percentage of the first development model 2.

Resonance Frequency	VSWR	Reflection Coefficient, Γ	Reflected Power (%)
6.89	1.08	0.03846	0.14793
28.97	1.00003	0.000015	0.0000000225

B. Second Developed Model 2

In this improvement, the apparent third frequency between frequencies 6 GHz and 28 GHz is eliminated, and the design becomes suitable for bending with different radii. The second model depends on

using Rogers RT/duroid 5880 (tm) as a substrate in the simulation process because it is suitable for the operation at the higher frequencies.

Figure 4.21 shows S11 of the proposed antenna model before bending (-69.2 dB and 23.2 dB on 6.74 GHz and 28.79 GHz, respectively). In addition, the VSWR values are (1.0006 and 1.14 dB on 6.74 GHz and 28.79 GHz, respectively) is shown in Figure 4.22.

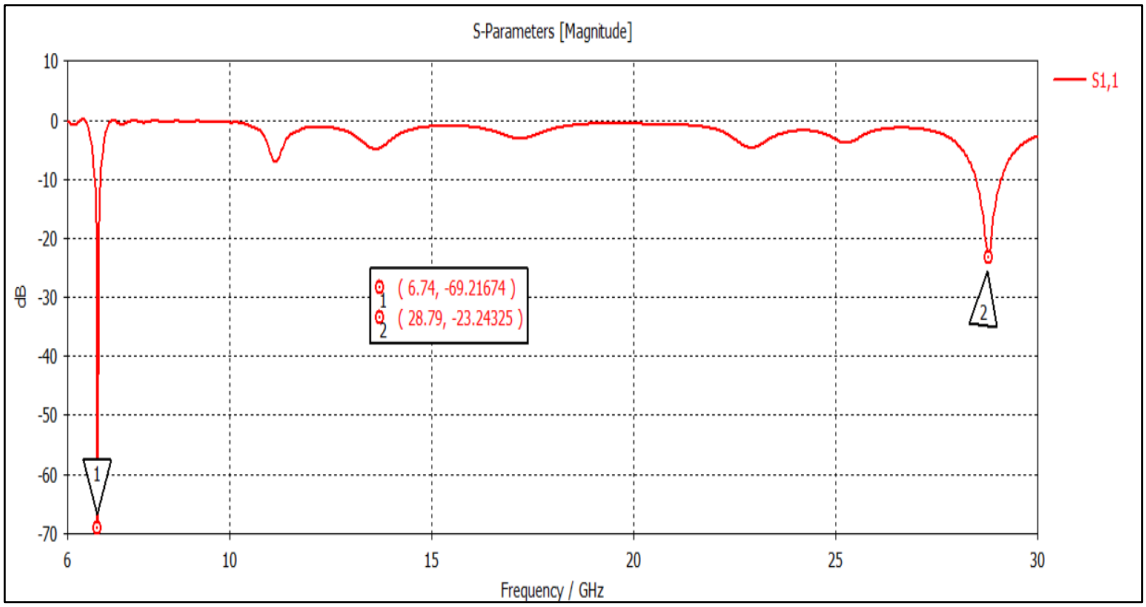

Figure 4.21: Reflection Coefficient (S11) for planar design, second development model 2.

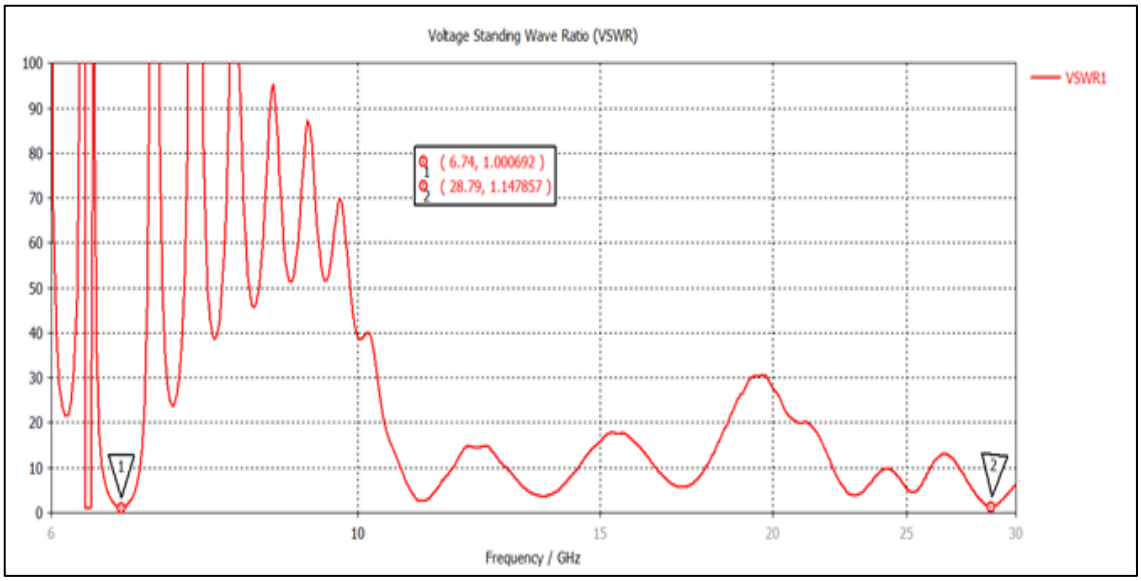

Figure 4.22: VSWR for Planar design, second development model 2.

Table 4-3 shows the percentage of power reflected from the antenna. The energy reflected from at 28GHz antenna is 0.42%, which means that 99.58% of the power has been delivered to the antenna. For the 6GHz frequency, the percentage of energy reflected from the antenna is 0.000008995%, thus transmitting power of the antenna is 99.99%, so the antenna's performance is very good. The transmitting power of the antenna is very high, and almost all the power is sent to the antenna.

Table 4.3: The reflected power percentage of the second development model 2.

Resonance Frequency	VSWR	Reflection Coefficient, Γ	Reflected Power (%)
6.74	1.0006	0.0002999	0.000008995
28.79	1.14	0.06542	0.428

Figure 4.23, 4.24 and Table 4.3 show that the proposed antenna with the second developed model2 out performance the original model2 and first developed model2 . where, the gain values are 3.73 dB and 6.96 dB at 6 GHz and 28GHz respectively .

Farther more , The directivity and VSWR values at 6 GHz 5.63 dB and 66% respectively, at 28 GHz 7.15 dB and 97% respectively.

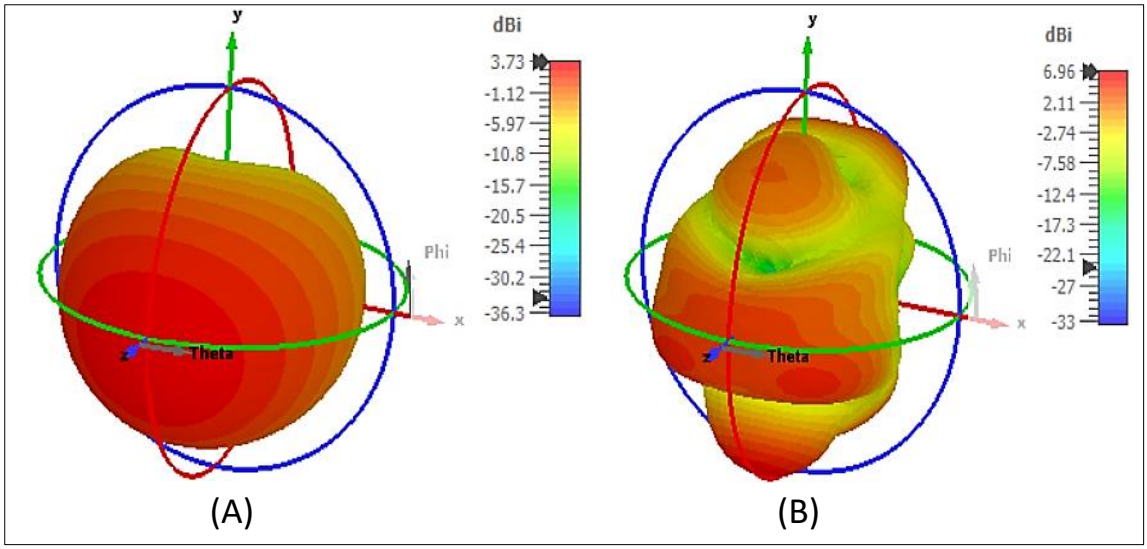

Figure 4.23: (A) The gain at frequency 6 GHz, (B) The gain at frequency 28 GHz , second development model 2.

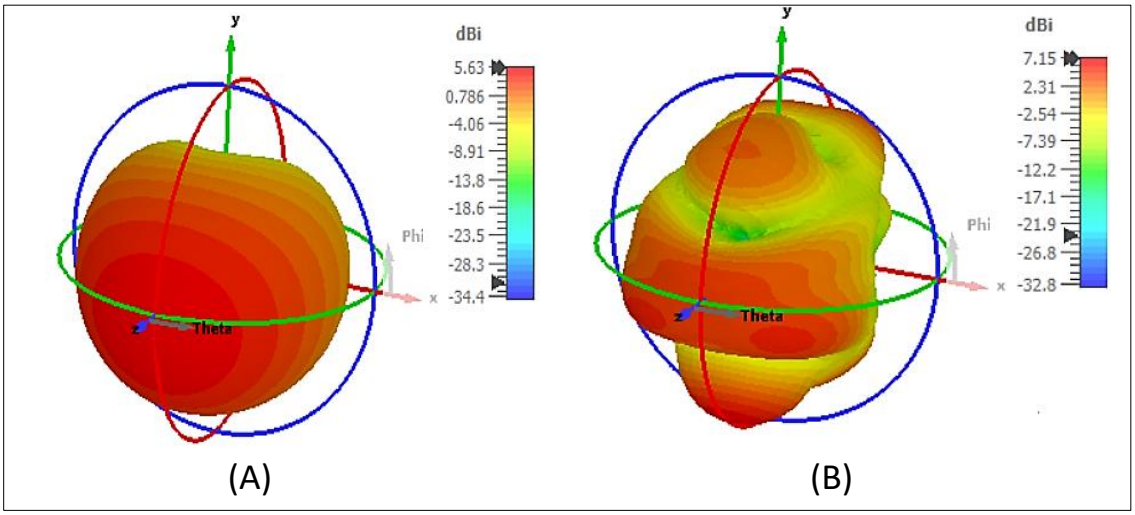

Figure 4.24: (A) The directivity at frequency 6 GHz, (B) The directivity at frequency 28 GHz , second development model 2.

Table 4.4 compares the results of the proposed antenna design and the other previous works. The proposed antenna achieves better gain than these antennas in [62] (at 28 GHz) and [63] (at 6 GHz). Where, the gain values of the proposed antenna are 3.72 dB and 7.07 dB at 6 GHz and 28GHz, respectively. Moreover, the proposed antenna at 6 GHz attained good percentage bandwidth compared to the antenna in [64] (at 6 GHz) and [27]

(at 28 GHz). Finally, the proposed antenna has efficiency better than the other works in the listed references.

Table 4.4: The parameters of the proposed design with a previous works.

Researcher	Frequency (GHz)	Bandwidth (%)	Gain (dB)	Efficiency (%)
[62]	28	5.5	4.47	94
[65]	28	2.7	9.33	87.2
[27]	28	2.2	8	N/R
[63]	6	8	3	N/R
[64]	6	2.1	3.9	58.4
[66]	6	8.44	9.94	58
Proposed antenna	6/ 28	2.5 / 2.3	3.72/7.07	65.7/97.5

4.2.3.3 Model 3

This model is designed and simulated for fabrication, where FR4 is the only available substrate material in the lab. It is used as a substrate to fabricate the proposed design of the dual-band antenna. The bandwidth values of this model are 4.8% (6.46-6.78) at 6 GHz and 3.1% (24.7 – 25.5) at 25 GHz, as presented in Figure. 4.25. Figure.4.26 shows that the VSWR values are 1.006 at 6 GHz and 1.2 dB at 25 GHz.

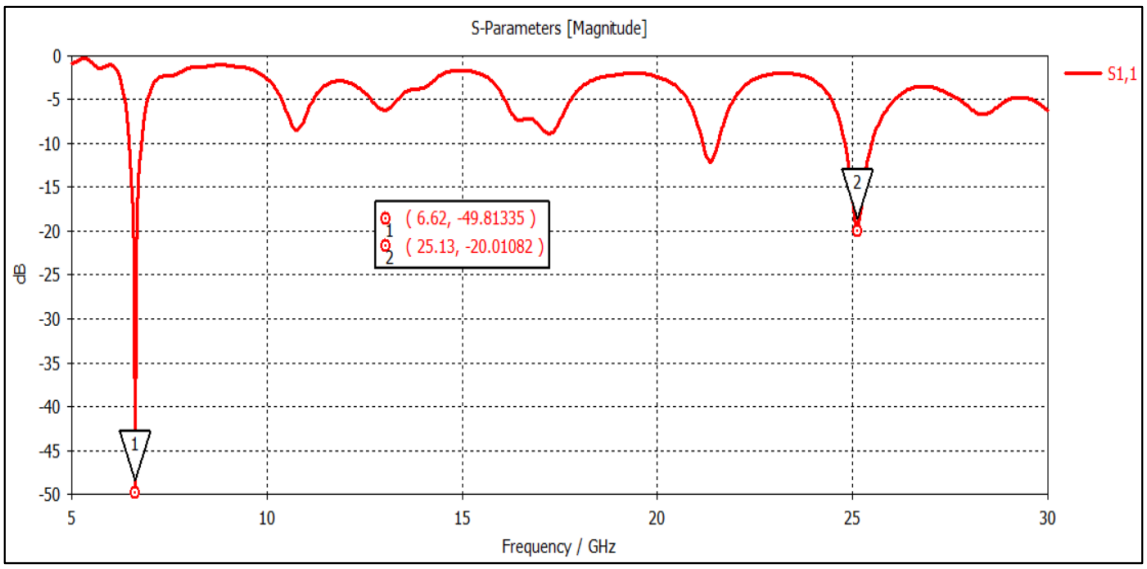

Figure 4.25: S11 for the proposed antenna using FR4 as squbstrate**.**

4.3 Results Of The Design Steps For The Proposed Antenna

As mentioned in Chapter 3, the proposed antenna design is firstly resonated at the frequency of 10 GHz, and to reduce the frequency to 6 GHz, part of the patch is cut out, and two strips of metal are added to both sides of the patch as shown in Figure 4.27.

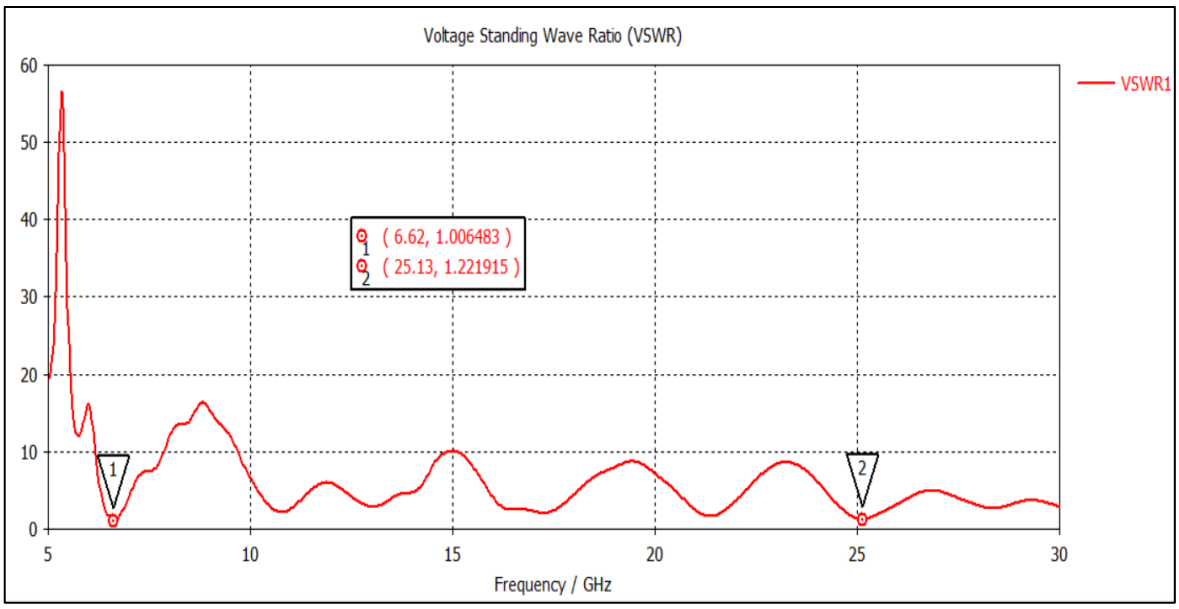

Figure 4.26: VSWR for the proposed antenna using FR4 as substrate.

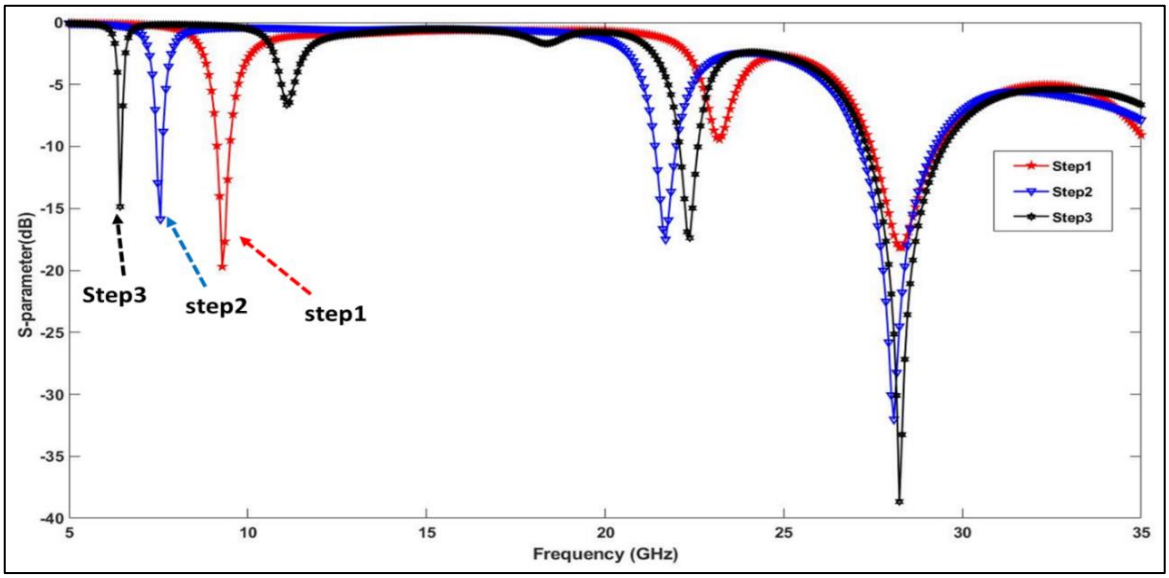

Figure 4.27: The effect of design modification on the reflection coefficient (S11) of the proposed patch antenna

To confirm the validity of the calculated results for the proposed design, the model is re-designed using the HFSS program. The obtained results of the simulated proposed design match with the calculated results of the fake model when using CST, which indicates the validity of the results for the proposed antenna model. Figure 4.28 presents the calculated (S11) model simulation for both software.

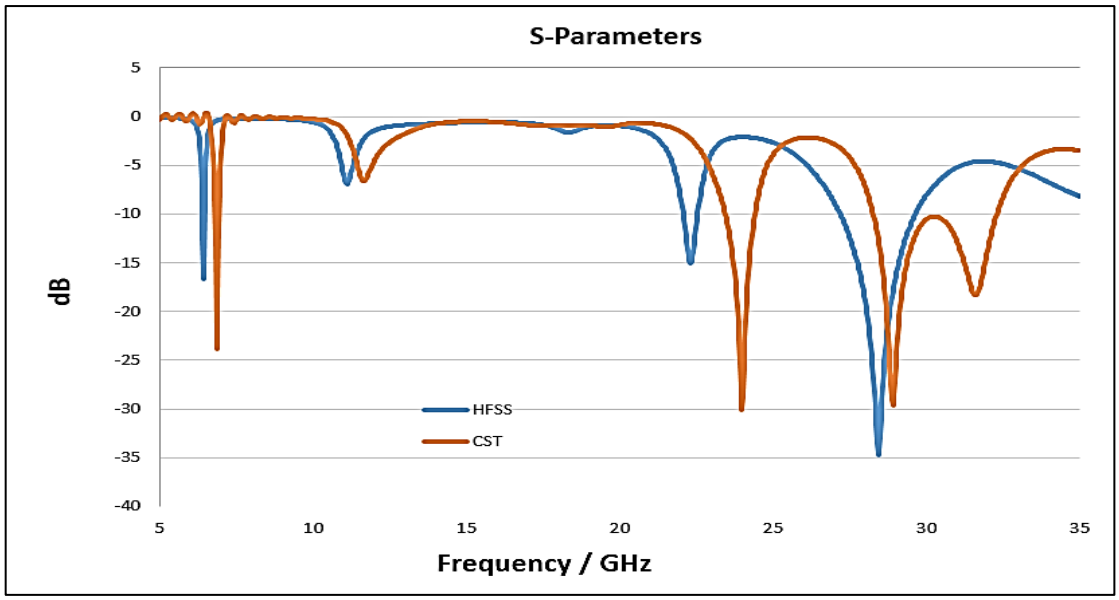

Figure 4.28: Combination between S-parameters when design in CST and HFSS program design.

4.4 The Results of Bending the Proposed Design

In this part, the effect of bending on antenna parameters will be demonstrated:

4.4.1 Effect of design folding on return loss and bandwidth

Figure 4.29 presents the Effect of folding on the antenna when folded with different radii, 5 mm, 10 mm, 15 mm, and 20 mm, compared with a non-folded patch antenna. Figure 4.30 and Table 4.5 show that at the increase of bending for the proposed antenna, the antenna's effective length decreases, and the resonant frequency shifts to a higher band than the frequency of the planar antenna[38] At the resonant frequency of 6 GHz, the return losses decrease with increasing bending but within acceptable limits. While at the millimeter wave frequencies, the return losses range (from -27 to -30), which means that the antenna works normally with bending. Although there is a frequency shift, it operates in the desired range: millimeter waves and microwaves.

Figure 4.30 shows a close-up of the 6GHz and 28GHz frequencies at the planar antenna, its bending process, and the effect of bending with different diameters on return losses and bandwidth.

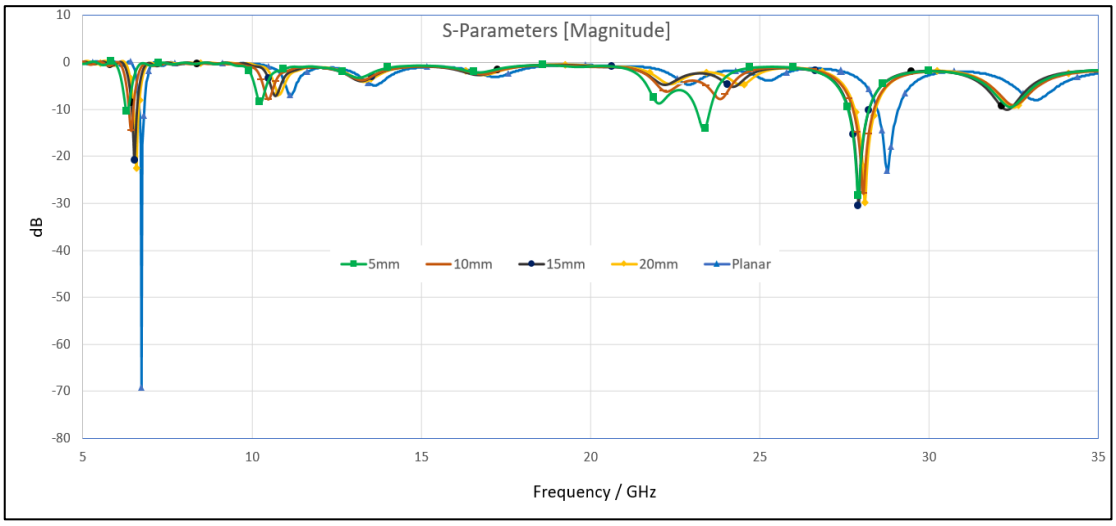

Figure 4. 29: Comparison in terms of S11 between a planar antenna and a bent antenna**.**

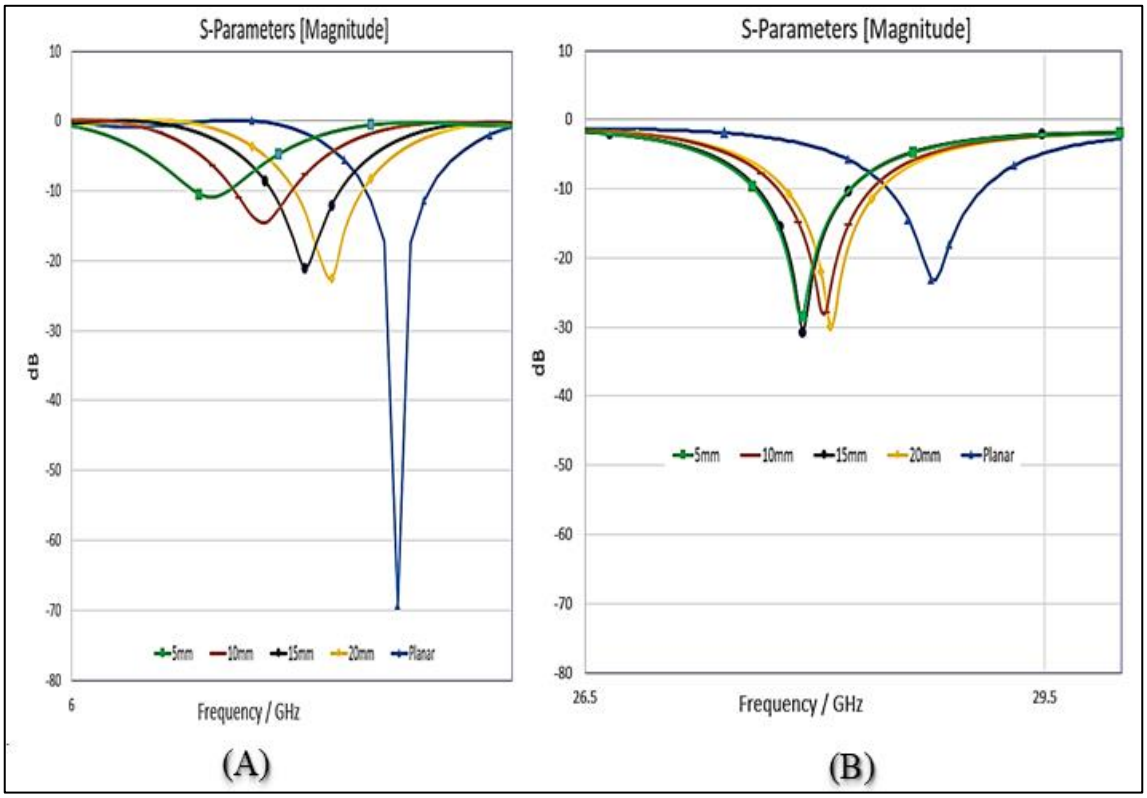

Figure 4.30: (A) Close-up image of the frequency 6GHz (B) Close-up image of the frequency 28GHz.

4.4.2 The Effect Of Folding on the Voltage Standing Wave Ratio(VSWR), Gain, Directivity, and Radiation Efficiency

Figure 4.31 shows a comparison of the VSWR for the planer (non-folded) antenna and the folded antenna with different radii. Where it is found that the folded antenna has a direction similar to the plane antenna in terms of VSWR, the VSWR of the millimeter wave and microwave frequency is within the acceptable range of less than two. Table 4-6 also shows the values of VSWR, the gain, and the directivity and efficiency for each frequency. The efficiency appears better than the flat antenna, This indicates that it can be used in a wearable antenna application.

Table 4.5: Comparison of return losses between a plane antenna and a bending antenna.

Cylindrical Bend [mm]	Resonance Frequency	Return Loss for Each Resonance Frequency	Bandwidth (%) For Each Resonance Frequency
r=0 (planar)	6.74 / 28.79	-69.21 / -23.24	2.18 / 4.66
r=5	6.32 / 27.92	-10.8 / -28.36	1.58 / 2.22
r=10	6.44 / 28.07	-14.5 / -27.96	2.1 / 2.85
r=15	6.53 / 27.92	-21 / -30.65	2.6 / 2.86
r=20	6.59 / 28.1	-22.4 / -29.92	2.9/ 2.4

4.4.3 Effect of design folding on the Reflection Coefficient Γ, Reflected Power (%).

Table 4-7 shows the percentage of the reflected power from the receiving antenna, the maximum reflected power is 8.163% at a frequency of 6 GHz, This indicates that the energy reaching the antenna is 91.38%, and the minimum reflected influence from the antenna is 0.000008995% at 6 GHz .Almost all the power is passed to the antenna, which indicates that the antenna has good performance in both cases when it is plane and bent.

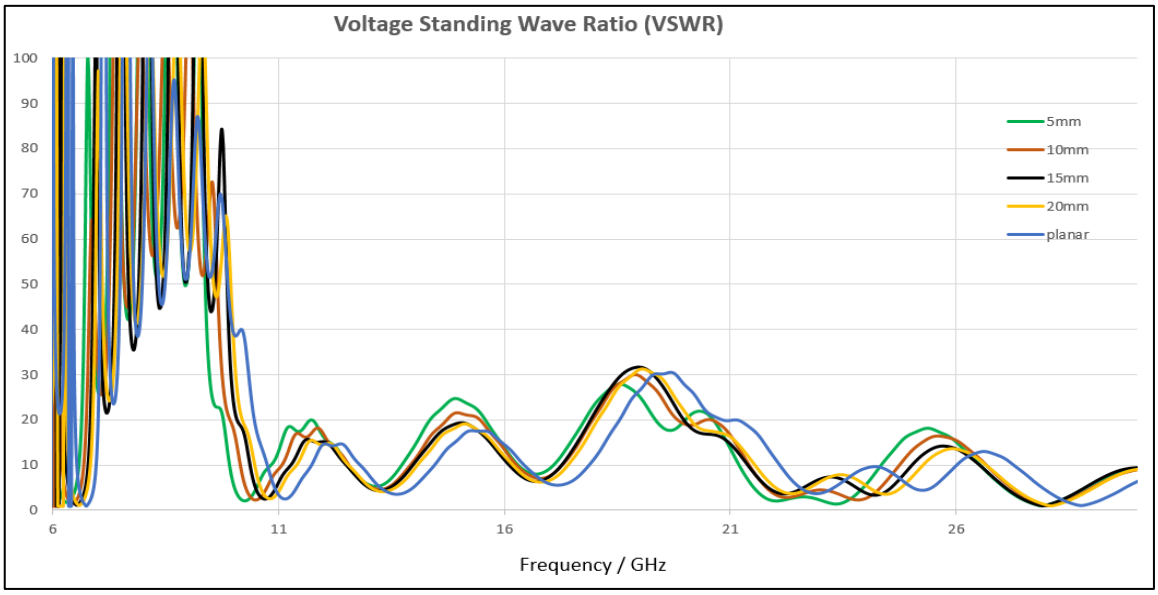

Figure 4. 31:Comparison in terms of voltage standing wave ratio between a planar antenna and a bent antenna.

Table 4.6: Comparison of VSWR and return losses between plane antenna and bent antenna.

Cylindrical Bend [mm]	Resonance Frequency	(VSWR)	Gain	Directivity	Radiation Efficiency (%)
r=0 (planar)	6.74 / 28.79	1.0006 / 1.14	3.7 / 6.9	5.6 / 7.1	66 / 97
r=5	6.32 / 27.92	1.8 / 1.07	3.69 / 6.85	5.2 / 7	70 / 97
R=10	6.44 / 28.07	1.4 / 1.08	3.8 / 6.7	5.5 / 6.9	69 / 97.1
R=15	6.53 / 27.92	1.1 / 1.06	3.9 / 7	5.7 / 7.2	68 / 97
R=20	6.59 / 28.1	1.1 / 1.06	4 / 7	5.8 /7.2	70 / 97

4.5 The Results of The Fabricated Model

In the fabrication process, the third model is used, FR4, utilized as a substrate because it is the only available material in the lab for fabricating. This material can be used at 6GHz frequency only, which is unsuitable for use at higher frequencies; the maximum frequency that can be tested via the available VNR is 20GHz, which cannot be used here for the 28GHz frequency. Furthermore, the hardness of FR4 that is used for two layers of the substrate leads to an air gap between these two layers that should be reduced to the minimum distance to reduce the thickness of the air gap layer, which has a dielectric constant (ε_r) equal to 1 between the ground layer and the substrate of the feed line, which firstly shifted the frequency from 6GHz to 7.23GHz, and return losses -9.896528, and after adjustment to slightly reduce the air gap via applying more compressing force on the two layers of the antenna during the check process. Then the frequency shifted in the 6 GHz direction at 7.17 GHz, with return losses of -14.49784, and this difference is shown in Figure 4.34. The output of VSWR is less than 2, that is, within the acceptable limits, and it is equal to 1.53, as shown in Figure 4-32.

The proposed antenna is redesigned by adding the air gap between the two layers, and the new model is simulated using the CST software. Moreover, the effect of thickness variation is also studied, as shown in Figure 4-33. The distance between the two substrates after the compression process turns out to be 0.06 mm.

Table 4.7: Comparison of Reflected Power between plane antenna and bend antenna.

Cylindrical Bend [mm]	Resonance Frequency	VSWR	Reflection Coefficient Γ	Reflected Power (%)
r=0 (planar)	6.74 / 28.79	1.0006 / 1.14	0.0002999 / 0.06542	0.000008995 / 0.428
r=5	6.32 / 27.92	1.8 / 1.07	0.2857 / 0.033816	8.163/ 0.11436
R=10	6.44 / 28.07	1.4 / 1.08	0.16667/ 0.03846	2.778 / 0.14793
R=15	6.53 / 27.92	1.19 / 1.08	0.04762 / 0.03846	0.22676 / 0.14793
R=20	6.59 / 28.1	1.16 / 1.07	0.04762 / 0.033816	0.22676 / 0.11436

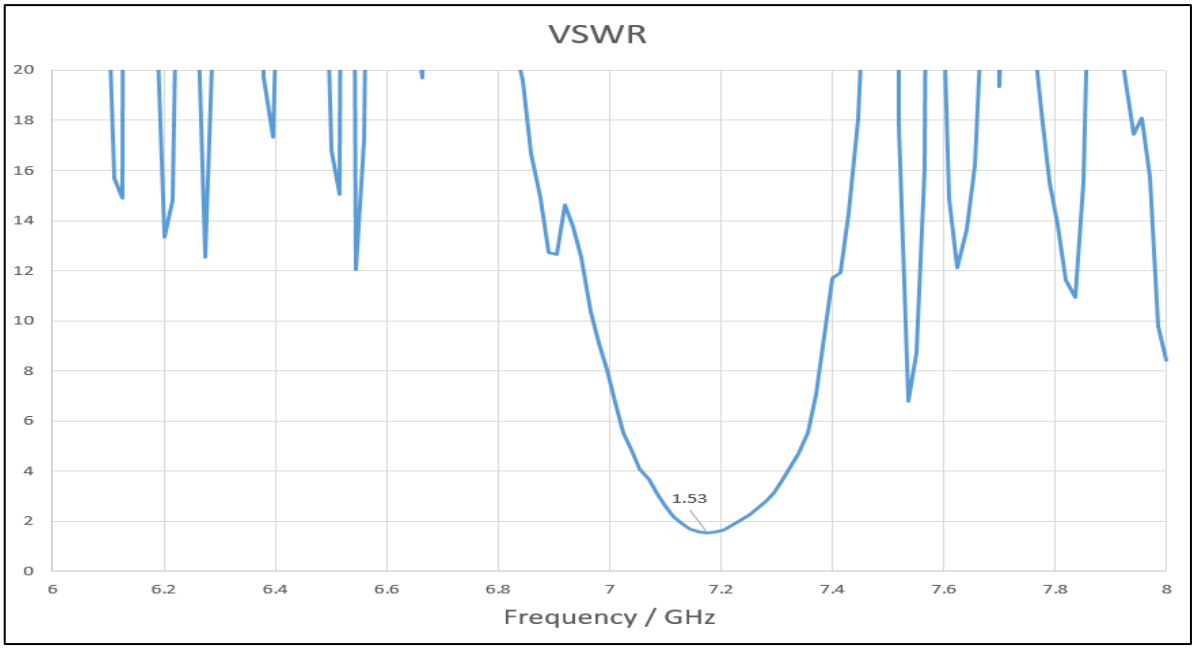

Figure 4.32: VSWR after the compression process of two antenna substrate.

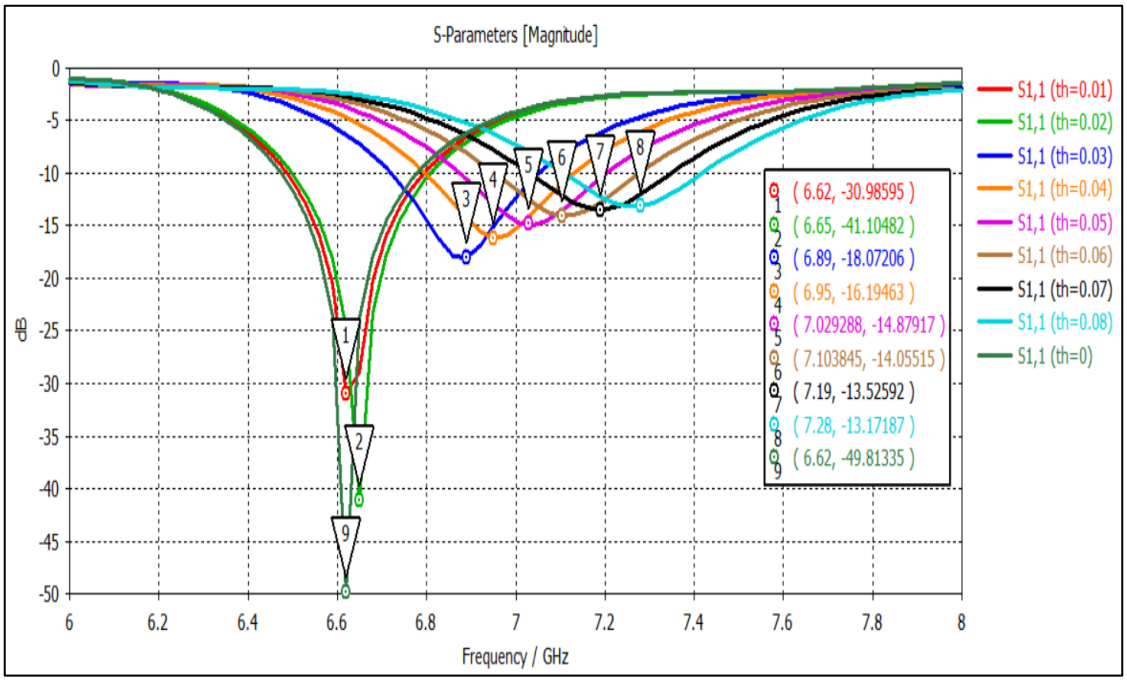

Figure 4.33: S-Parameter using different thicknesses for air.

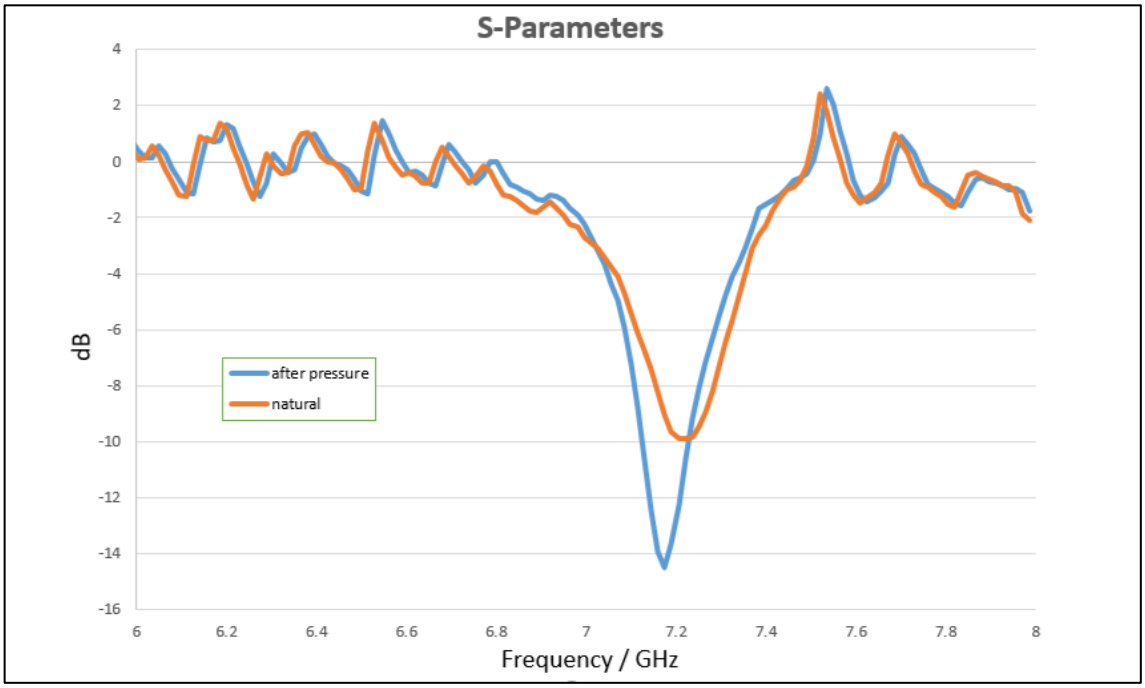

Figure 4.34: S-Parameter before the compression process of the two substrates and after the compression process.

Chapter Five Conclusion and Suggestions for Future Work

CHAPTER 5

Conclusions & Suggestions for Future Work

5.1 Conclusion

During the simulation and fabrication processes, there are a lot of problems and challenges that are encountered. Thus, some solutions and conclusions are listed in this section as follows:

1. The proposed antenna design operates in the dual bands of frequencies suggested for 5G applications.
2. Millimeter dimensions are used in the proposed antenna design. Therefore the antenna size is very small, which helps to wear it on clothes without disturbance, where the antenna dimensions are 20 * 22 * 1.355 mm.
3. The proposed antenna is designed using four feeding methods: microstrip line feed, proximity-coupled feed ,coaxial, and aperture-coupled feed.
4. The aperture-coupled method is adopted in this thesis because this method offers better performance in terms of S11, VSWR, gain , directivity, and efficiency
5. The proposed antenna is designed with three materials are(Arlon AD 250C, Rogers RT/droid 5880(tm) ,and FR4) .
6. The simulation results show that the Rogers RT/droid 5880(tm) offers the best results.
7. The FR4 is used in the fabrication process because it is the only one that is available in the Iraqi markets.

8. Due to the hardness of the FR4 material, the fabrication process left a gap between the substrates. This gap deteriorates the performance of the proposed antenna, this problem has been reduced by the compression of both substrates during the test process.
9. The folding process shows that the proposed antenna is suitable for wearable applications. Where the proposed antenna has the same performance after the folding process.

5.2 Future Work

In future work, the antenna can be further improved by using different substrates in the design of antenna design and bending with radii of less than 5mm. The distance between the two substrates can be investigated by filling the space of different adhesive materials with varying dielectric constant values (ε_r) more than (ε_r) of air and the Simulated results from the simulation before the fabrication.

REFERENCES

[1] S. Parasuraman, S. Yogeeswaran, and G. P. Ramesh, “Design of Microstrip Patch Antenna with improved characteristics and its performance at 5.1GHz for Wireless Applications,” *IOP Conf. Ser. Mater. Sci. Eng.*, vol. 925, no. 1, 2020, doi: 10.1088/1757-899X/925/1/012005.

[2] Douglas H. Werner Zhi Hao Jiang, *Electromagnetics of Body-Area Networks*. New Jersey: John Wiley & Sons, Inc., 2016.

[3] Kitur Stanley Kibet, “Design and Fabrication of Aperture Coupled Microstrip Patch Antennas With Arbitrarily Shaped Apertures,” Kenyatta University, 2013.

[4] J. G. Andrews *et al.*, “What will 5G be?,” *IEEE J. Sel. Areas Commun.*, vol. 32, no. 6, pp. 1065–1082, 2014, doi: 10.1109/JSAC.2014.2328098.

[5] I. Ahmad, H. Sun, Y. Zhang, and A. Samad, “High gain rectangular slot microstrip patch antenna for 5G mm-wave wireless communication,” *2020 5th Int. Conf. Comput. Commun. Syst. ICCCS 2020*, pp. 723–727, 2020, doi: 10.1109/ICCCS49078.2020.9118602.

[6] Zhi Ning Chen, *ANTENNAS FOR PORTABLE DEVICES*. Singapore: John Wiley & Sons, Ltd, 2014.

[7] H. H. M. Ghouz, M. F. Aboee, and M. Aly Ibrahim, “Novel wideband microstrip monopole antenna designs for WiFi/LTE/WiMax devices,” *IEEE Access*, vol. 8, pp. 9532–9539, 2020, doi: 10.1109/ACCESS.2019.2963644.

[8] A. Bansal and R. Gupta, “A review on microstrip patch antenna and feeding techniques,” *Int. J. Inf. Technol.*, vol. 12, no. 1, pp. 149–154, 2020, doi: 10.1007/s41870-018-0121-4.

[9] C. A. Balanis, *Antenna Theory Analysis and Design*, Third Edit. John Wiley & Sons, Inc., 2005.

[10] T. MIKULÁŠEK, “Microstrip Patch Antennas Fed by Substrate Integrated Waveguide,” Brno University of Technology, 2013.

[11] N. Sakib, S. N. Ibrahim, and M. Ibrahimy, “Development of Wearable Patch Antennas Using Rubber Development of Wearable Patch Antennas Applications By,” no. July, 2021, doi: 10.13140/RG.2.2.36524.39040.

[12] A. Balanis, *Antenna theory; analysis and design*, Third edit. New Jersey: John Wiley & Sons, Inc., 2005.

[13] Luyi Chen, “Dual Frequency Patch Antenna Design for Global Navigation Satellite System,” Ohio University, 2007.

[14] A. F. Alsager, “Design and Analysis of Microstrip Patch Antenna Arrays,” University College of Borås, 2011.

[15] M. A. R. Osman, M. K. A. Rahim, M. Azfar, N. A. Samsuri, F. Zubir, and K. Kamardin, “Design, implementation and performance of ultra-wideband textile antenna,” *Prog. Electromagn. Res. B*, vol. 27, no. 27, pp. 307–325, 2011, doi: 10.2528/PIERB10102005.

[16] A. A. Eldek, “Analysis and design of wideband slot and printed antennas for phased array antenna systems,” University of Mississippi, 2004.

[17] T. M. Macnamara, *Handbook ofAntennas for EMC*, Second Edi. Norwood, MA: Artech House, 2018.

[18] P. J. Soh, M. K. A. Rahim, A. Asrokin, and M. Z. A. Abdul Aziz, “Design, Modeling, and performance Comparison of feeding techniques for a Microstrip Patch Antenna,” *J. Teknol.*, vol. 47, no. 1, 2007, doi: 10.11113/jt.v47.270.

[19] V. Paraforou, “Design and full-wave analysis of supershaped patch antennas,” Delft University of Technology, 2013.

[20] Francisco A. Rivera-Abreu, “DUAL BAND OCTAGONAL MICROSTRIP PATCH ANTENNA DESIGN METHOD FOR

ENERGY HARVESTING," Faculty of Purdue University, 2018.

[21] M. Sarkar, A. Singh, S. Gupta, and A. E. Hassanien, "Smart antenna design for high-speed moving vehicles with minimum return loss," *Int. J. Commun. Syst.*, vol. 33, no. 11, pp. 1–22, 2020, doi: 10.1002/dac.4414.

[22] N. R. Ccoillo-Ramos, N. Aboserwal, Z. Qamar, and J. L. Salazar-Cerreno, "Improved analytical model for a proximity coupled microstrip patch antenna (pc-mspa)," *IEEE Trans. Antennas Propag.*, vol. 69, no. 10, pp. 6244–6252, 2021, doi: 10.1109/TAP.2021.3082570.

[23] J. Zhang, S. Yan, and G. A. E. Vandenbosch, "A Miniature Feeding Network for Aperture-Coupled Wearable Antennas," *IEEE Trans. Antennas Propag.*, vol. 65, no. 5, pp. 2650–2654, 2017, doi: 10.1109/TAP.2017.2677262.

[24] C. Hertleer, A. Tronquo, H. Rogier, L. Vallozzi, and L. Van Langenhove, "Aperture-coupled patch antenna for integration into wearable textile systems," *IEEE Antennas Wirel. Propag. Lett.*, vol. 6, pp. 392–395, 2007, doi: 10.1109/LAWP.2007.903498.

[25] A. S. B. Mohammed *et al.*, "Mathematical model on the effects of conductor thickness on the centre frequency at 28 GHz for the performance of microstrip patch antenna using air substrate for 5G application," *Alexandria Eng. J.*, vol. 60, no. 6, pp. 5265–5273, 2021, doi: 10.1016/j.aej.2021.04.050.

[26] R. Hussain *et al.*, "A Multiband Shared Aperture MIMO Antenna for Millimeter-Wave and Sub-6GHz 5G Applications," *Sensors*, vol. 22, no. 5, 2022, doi: 10.3390/s22051808.

[27] M. A. A. Rahim, I. M. Ibrahim, R. A. A. Kamaruddin, Z. Zakaria, and N. Hassim, "Characterization of microstrip patch array antenna at 28 GHz," *J. Telecommun. Electron. Comput. Eng.*, vol. 9, no. 2–8,

pp. 137–141, 2017.

[28] M. Buravalli, T. Kumar, G. D. Shilpa, and S. Anuradha, “Simulation study of 2x3 microstrip patch antenna array for 5G applications,” *Proc. 2020 Int. Conf. Comput. Commun. Secur. ICCCS 2020*, no. 1, 2020, doi: 10.1109/ICCCS49678.2020.9276831.

[29] J. O. Abolade, D. B. O. Konditi, and V. M. Dharmadhikary, “Compact hexa-band bio-inspired antenna using asymmetric microstrip feeding technique for wireless applications,” *Heliyon*, vol. 7, no. 2, p. e06247, 2021, doi: 10.1016/j.heliyon.2021.e06247.

[30] V. L. Pham, S. X. Ta, K. K. Nguyen, C. Dao-Ngoc, and N. Nguyen-Trong, “Single-Layer, Dual-Band, Circularly Polarized, Proximity-Fed Meshed Patch Antenna,” *IEEE Access*, vol. 10, pp. 94560–94567, 2022, doi: 10.1109/ACCESS.2022.3204685.

[31] M. V. Mokal, P. S. R. Gagare, and D. R. P. Labade, “Analysis of Micro strip patch Antenna Using Coaxial feed and Micro strip line feed for Wireless Application,” *IOSR J. Electron. Commun. Eng.*, vol. 12, no. 03, pp. 36–41, 2017, doi: 10.9790/2834-1203033641.

[32] D. K. Kong, J. Kim, D. Woo, and Y. J. Yoon, “Broadband Modified Proximity Coupled Patch Antenna with Cavity-Backed Configuration,” *J. Electromagn. Eng. Sci.*, vol. 21, no. 1, pp. 8–14, 2021, doi: 10.26866/jees.2021.21.1.8.

[33] N. Aboserwal, N. R. Ccoillo Ramos, Z. Qamar, and J. L. Salazar-Cerreno, “An Accurate Analytical Model to Calculate the Impedance Bandwidth of a Proximity Coupled Microstrip Patch Antenna (PC-MSPA),” *IEEE Access*, vol. 8, pp. 41784–41793, 2020, doi: 10.1109/ACCESS.2020.2976750.

[34] S. N. Ariffah, W. A. Mustafa, S. Z. S. Idrus, and A. Muhammad, “Point to Point Communication: 5.8 GHz Circular Polarized Proximity-Coupled Feeding Antenna,” *J. Phys. Conf. Ser.*, vol. 1529,

no. 4, 2020, doi: 10.1088/1742-6596/1529/4/042018.

[35] K. A. Malar and R. S. Ganesh, “Novel aperture coupled fractal antenna for Internet of wearable things (IoWT),” *Meas. Sensors*, vol. 24, p. 100533, 2022, doi: 10.1016/j.measen.2022.100533.

[36] G. Ghione and M. Pirola, *Microwave Electronics Measurement and Materials Characterization*. Southern Gate: John Wiley & Sons Ltd, 2017. doi: 10.1017/9781316756171.

[37] H. Khaleel, *Innovation in Wearable and Flexible Antennas*. Sonoma: WIT Press, 2015.

[38] L. Zheng Tung, G. Amouzed Mahdiraji, and L. Chia Ping, “Comparative Study between Planar and Bent Antenna Characterization,” *MATEC Web Conf.*, vol. 152, pp. 1–11, 2018, doi: 10.1051/matecconf/201815203002.

[39] J. Khan, “Design of Microstrip Patch Antenna on Liquid Crystal Polymer (LCP) for Applications at 70GHz,” University of Gävle, 2008.

[40] Z. Shen and W. Zhiwei, “Design of 5G antenna arrays based on Multi-directivity,” Linnaeus University, 2020.

[41] D. S. Bhatti *et al.*, “A Survey on Wireless Wearable Body Area Networks: A Perspective of Technology and Economy,” *Sensors*, vol. 22, no. 20, pp. 1–47, 2022, doi: 10.3390/s22207722.

[42] E. L. M. Wissem, I. Sfar, L. Osman, and J. M. Ribero, “A textile EBG-based antenna for future 5G-IoT millimeter-wave applications,” *Electron.*, vol. 10, no. 2, pp. 1–12, 2021, doi: 10.3390/electronics10020154.

[43] W. S. H. M. W. Ahmad *et al.*, “5G Technology: Towards Dynamic Spectrum Sharing Using Cognitive Radio Networks,” *IEEE Access*, vol. 8, pp. 14460–14488, 2020, doi: 10.1109/ACCESS.2020.2966271.

[44] S. P. Sreenilayam, I. Ul Ahad, V. Nicolosi, and D. Brabazon, “MXene materials based printed flexible devices for healthcare, biomedical and energy storage applications,” *Mater. Today*, vol. 43, pp. 99–131, 2021, doi: 10.1016/j.mattod.2020.10.025.

[45] A. S. Sayem *et al.*, “Flexible and Transparent Circularly Polarized Patch Antenna for Reliable Unobtrusive Wearable Wireless Communications,” pp. 1–22, 2022.

[46] R. Negra, I. Jemili, and A. Belghith, “Wireless body area networks: Applications and technologies,” *Procedia Comput. Sci.*, vol. 83, pp. 1274–1281, 2016.

[47] M. Fawaz *et al.*, “3D printed patch Antenna for millimeter wave 5G wearable applications”.

[48] J. O. Abolade, D. B. O. Konditi, and V. M. Dharmadhikary, “Comparative study of textile material characterization techniques for wearable antennas,” *Results Mater.*, vol. 9, p. 100168, 2021, doi: 10.1016/j.rinma.2021.100168.

[49] A. Yadav, V. K. Singh, M. Chaudhary, and H. Mohan, “A Review on Wearable Textile Antenna,” no. December, 2015.

[50] C. Mendes, “A Dual-Mode Single-Band Wearable Microstrip Antenna for Body Area Networks,” vol. 16, pp. 3055–3058, 2017.

[51] L. Xu, Y. Guo, and W. Wu, “Miniaturized Circularly Polarized loop Antenna for Biomedical Applications,” no. c, 2014, doi: 10.1109/TAP.2014.2387420.

[52] M. L. Scarpello, I. Kazani, C. Hertleer, H. Rogier, and S. Member, “Stability and Ef fi ciency of Screen-Printed Wearable and Washable Antennas,” vol. 11, pp. 838–841, 2012.

[53] P. M. Potey and K. Tuckley, “Design of wearable textile antenna for low back radiation,” *J. Electromagn. Waves Appl.*, vol. 0, no. 0, pp. 1–11, 2019, doi: 10.1080/09205071.2019.1699170.

[54] S. Yan, P. J. Soh, and G. A. E. Vandenbosch, “Wearable Dual-Band Magneto-Electric Dipole Antenna for WBAN/WLAN Applications,” *IEEE Trans. Antennas Propag.*, vol. 63, no. 9, pp. 4165–4169, 2015, doi: 10.1109/TAP.2015.2443863.

[55] J. Tak, S. Member, J. Choi, and S. Member, “An All-textile Louis Vuitton Logo Antenna,” vol. 1225, no. c, pp. 3–6, 2015, doi: 10.1109/LAWP.2015.2398854.

[56] R. B. V. B. Simorangkir, S. Member, Y. Yang, L. Matekovits, S. Member, and K. P. Esselle, “Dual-Band Dual-Mode Textile Antenna on PDMS Substrate for Body-Centric Communications,” vol. 1225, 2016, doi: 10.1109/LAWP.2016.2598729.

[57] S. Yan, P. J. Soh, and G. A. E. V. Fellow, “Dual-Band Textile MIMO Antenna Based on Substrate Integrated Waveguide (SIW) Technology,” 2015, doi: 10.1109/TAP.2015.2477094.

[58] P. Transfer, “A Printed Wearable Dual-Band Antenna for Wireless Power Transfer,” 2019, doi: 10.3390/s19071732.

[59] I. Munteanu and I. Hänninen, “Recent advances in CST STUDIO SUITE for antenna simulation,” *Proc. 6th Eur. Conf. Antennas Propagation, EuCAP 2012*, pp. 1301–1305, 2012, doi: 10.1109/EuCAP.2012.6206600.

[60] Dassault Systèmes, “CST Studio Suite High Frequency Simulation,” 2020.

[61] Dassault Systèmes, “Discover CST studio suite,” 2018.

[62] W. Ahmad, A. Ali, and W. T. Khan, “Small form factor PIFA antenna design at 28 GHz for 5G applications,” *2016 IEEE Antennas Propag. Soc. Int. Symp. APSURSI 2016 - Proc.*, pp. 1747–1748, 2016, doi: 10.1109/APS.2016.7696580.

[63] A. Abhishek and P. Suraj, “Design of Patch Antenna for 5G Communication at 6 GHz (WRC-23) with WLAN Application,” *2021*

6th Int. Conf. Converg. Technol. I2CT 2021, pp. 6–10, 2021, doi: 10.1109/I2CT51068.2021.9418211.

[64] C. Supratha and S. Robinson, “Design and Analysis of Microstrip Patch Antenna for WLAN Application,” *Proc. 2018 Int. Conf. Curr. Trends Towar. Converging Technol. ICCTCT 2018*, 2018.

[65] A. Abdelaziz and E. K. I. Hamad, “Design of a Compact High Gain Microstrip Patch Antenna for Tri-Band 5G Wireless Communication,” *Frequenz*, vol. 73, no. 1–2, pp. 45–52, 2019, doi: 10.1515/freq-2018-0058.

[66] H. El Omari El Bakali, A. Zakriti, A. Farkhsi, A. Dkiouak, and M. El Ouahabi, “Design and realization of dual band notch uwb mimo antenna in 5g and wi-fi 6e by using hybrid technique,” *Prog. Electromagn. Res. C*, vol. 116, pp. 1–12, 2021, doi: 10.2528/PIERC21080701.

APPENDIX A

A1 -SMA COAXIAL CONNECTORS

The Connex SMA connectors are semi-precision, sub-miniature, high-frequency connectors which offer reliable broadband performance DC to 18GHz with low reflection and constant 50 ohm impedance. The main features are high mechanical strength, high durability and low VSWR. Matured design principles, careful manufacturing at all stages and a thorough quality assurance organization are the bases for the well-known quality of Connex SMA Connectors.

ELECTRICAL SPECIFICATIONS

Impedance	50 ohm
Frequency range	*Semi–rigid cable for .141" or .085" O.D. copper jacket: 0–18 GHz *Flexible cable: 0–12.4 GHz
Voltage rating	*RG–58, 141, 142, 223: 500v peak *RG–174, 188, 316: 375V peak
Dielectric withstanding voltage	*.141" & RG–58 cable group: 1000V RMS * .085" & RG–316 cable group: 750V RMS
VSWR–straight Connectors *f in GHz	*.141" semi–rigid cable group: 1.05 + .005f *RG–58 cable group: 1.15 + .01f *RG–174 cable group: 1.15 + .02f *RG–178 cable group: 1.20 + .025f
Contact resistance	Center: 2.0 milliohms Body: 2.0 milliohms Braid to body: 0.5 milliohms
Insulation resistance	5000 Megohms
RF leakage	-90 db min. at 2–3 GHz
Insertion loss	db max. = .06$\sqrt{\text{freq. GHz}}$.. Test frequency @6.0 GHz

MILITARY SPECIFICATIONS
MIL–C–39012 & MIL–C–83517 SMA

MATERIAL SPECIFICATIONS

PARTS NAME		*MIL STANDARD*	*ECONOMIC TYPE*
Body, coupling nut, other metal parts		Non-magnetic stainless steel per QQ–S–764 #303 finish: passivated	Brass per QQ–B–626 finish: nickel or gold per requirement
Contacts	Male	Brass per QQ–B–626	Brass per QQ–B–626
	Female	Beryllium copper per QQ–C–530 heat treated per MIL–H–7199	Beryllium copper per QQ–C–530 heat treated per MIL–H–7199
		Finish: .00005" min gold plated per MIL–G–45204 type 1, Grade C.	Finish: .00005" min gold plated per MIL–G–45204 type 1, Grade C.
Insulator		PTFE	PTFE
Gasket		Silicone rubber	Silicone rubber
Crimp ferrule		Seamless copper tubing alloy	Seamless copper tubing alloy
Selection Guide		*Suitable for direct mounting on aluminium panels *Lowest cost	*For commercial application only *Lower cost

SMA COAXIAL CONNECTORS

INTERFACE MATING DIMENSIONS

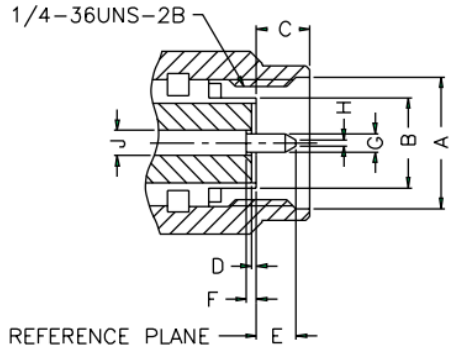

PLUG

Letter	Millimeters [Inches]	
	Minimum	Maximum
A	6.35 [.250]	6.73 [.265]
B	4.53 [.178]	4.59 [.181]
C	2.54 [.100]	3.43 [.135]
D	0.00	0.25 [.010]
E	1.91 [.075]	2.54 [.100]
F	0.00	0.25 [.010]
G	0.90 [.035]	0.94 [.037]
H	0.00	0.38 [.015]
J	1.24 [.049]	1.30 [.051]

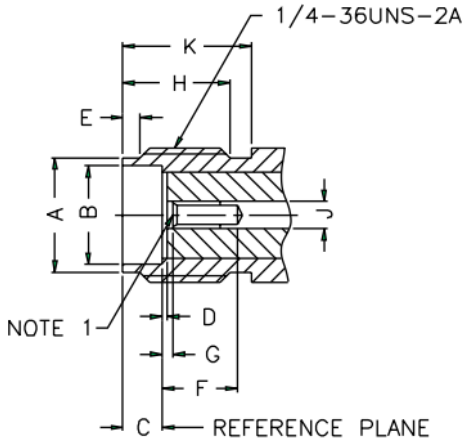

JACK

Letter	Millimeters [Inches]	
	Minimum	Maximum
A	5.28 [.208]	5.49 [.216]
B	4.60 [.181]	4.67 [.184]
C	1.88 [.074]	1.98 [.078]
D	0.00	0.25 [.010]
E	0.38 [.015]	1.14 [.045]
F	2.92 [.115]	–
G	0.00	0.25 [.010]
H	4.32 [.170]	–
J	1.24 [.049]	1.30 [.051]
K	5.54 [.218]	–

NOTE: 1. I.D. TO MEET VSWR AND CONTACT RESISTANCE WHEN MATED WITH 1.32/1.37 MM DIA. PIN.

SMA COAXIAL CONNECTORS

All connectors listed, unless otherwise noted, are Commercial Grade construction, gold-plated brass bodies with 50µ" gold contacts. All insulators are teflon. All other parameters are equal to Mil Standard construction.

Mil Standard connectors, i.e. Stainless Steel body, available upon request as per material specifications listed in Material section on preceding page.

All dimensions in millimeters and [inches].

CABLE GROUP LEGEND

01	58/ 58A/ 58C/ 141/ 303/ LMR195™/ B7806A	06A	179/ U DOUBLE BRAIDED	09	B8227/ 89207
01A	55/ 142/ 223/ 400	07	8/ 8A/ 213/ 393	10	.141 SEMI-RIGID/ 402/U
01B	LMR200™/ B7807A	07A	214	11	.085 SEMI-RIGID/ 405/U
02	58 PLENUM/THINNET/ 122U/ B88240/ B89907	07B	8X/ LMR240™/ B7808A	12	.250 SEMI-RIGID
03	59/ 62/ 140/ 210	07C	B9913/ LMR400™/ B7810A/ B8214	13	.047 SEMI-RIGID/ B1674A
03A	59/ U-20AWG	07D	B89913	14	178/ 196
04	59/ U PLENUM	07E	11	15	B8281/ B9231/ B9141
04A	59/ U PLENUM-20AWG	07F	11/ U-14AWG/ B8213/ B9292/ B7731/ B1859A	15A	B88281
05	174/ 188A/ 316/ B7805A	08	6/ 143/ 212	16	180/ 195/ 122/ B8218/ B1865A/ B1855
05A	316/ U DOUBLE BRAIDED	08A	B1694A/ B9248	17	LMR600™
06	179/ 187/ B9221	08B	6 PLENUM/ B1695A	18	AT&T734A/ B1505A
				19	AT&T735A/ B735A1

DIRECT SOLDER FOR SEMI-RIGID .047", .085" AND .141" CABLE

PRINTED CIRCUIT BOARD/STRAIGHT TERMINALS

STRAIGHT PLUG FOR P.C. BOARD

P.N.	Cable Group	Finish	Insulation	Impedance	Crimp Tool
132133	N/A	Gold	Teflon	50	N/A

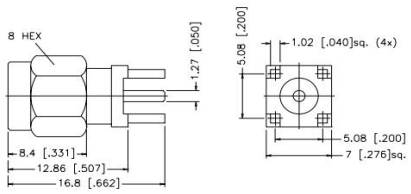

STRAIGHT JACK FOR P.C. BOARD

P.N.	Cable Group	Finish	Insulation	Impedance	Crimp Tool
132134	N/A	Gold	Teflon	50	N/A
132134-10 SURFACE MOUNT	N/A	Gold	Teflon	50	N/A
132319 EXTENDED BOCY	N/A	Gold	Teflon	50	N/A
132320 2-HOLE PCB MOUNT	N/A	Gold	Teflon	50	N/A
132291 BULKHEAD MOUNT	N/A	Gold	Teflon	50	N/A

132134

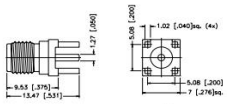

132319

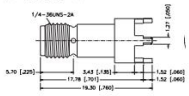

132320

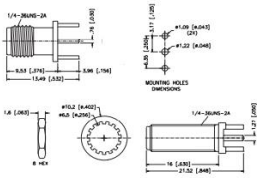

132291

RIGHT ANGLE PLUG FOR P.C. BOARD

P.N.	Cable Group	Finish	Insulation	Impedance	Crimp Tool
132135	N/A	Gold	Teflon	50	N/A

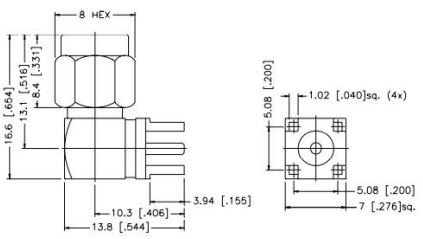

RIGHT ANGLE JACK FOR P.C. BOARD

P.N.	Cable Group	Finish	Insulation	Impedance	Crimp Tool
132136	N/A	Gold	Teflon	50	N/A
132225 DIECAST BODY	N/A	Gold	Teflon	50	N/A

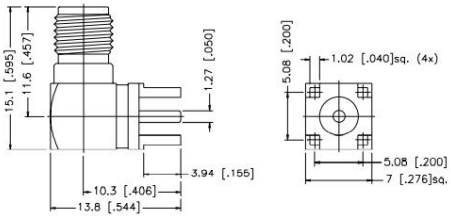

PRINTED CIRCUIT BOARD/STRAIGHT TERMINAL

RIGHT ANGLE BULKHEAD JACK FOR P.C. BOARD

P.N.	Cable Group	Finish	Insulation	Impedance	Crimp Tool
132203	N/A	Gold	Teflon	50	N/A

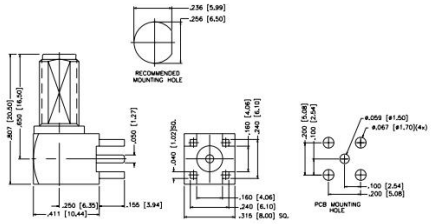

END LAUNCH JACK RECEPTACLE

P.N.	Cable Group	Finish	Insulation	Impedance	Crimp Tool
132255	N/A	Gold	Teflon	50	N/A
132289 BULKHEAD MOUNT	N/A	Gold	Teflon	50	N/A
132322	N/A	Gold	Teflon	50	N/A
132270 BULKHEAD MOUNT	N/A	Gold	Teflon	50	N/A

132255

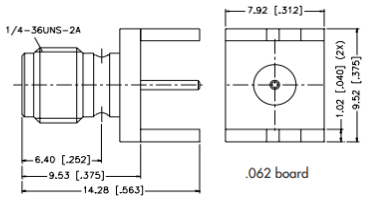

132289

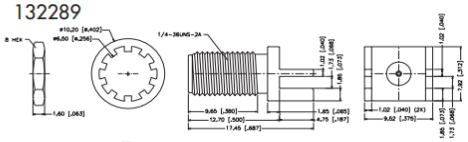

132322

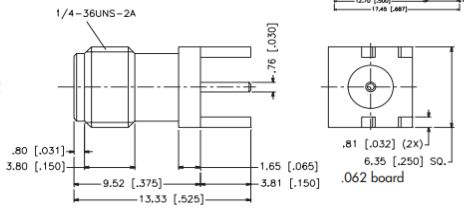

132270

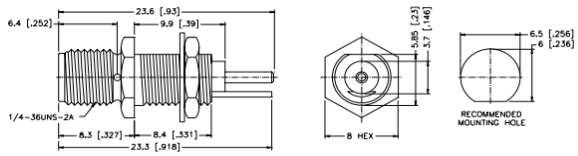

PRESS FIT RECEPTACLE

P.N.	Cable Group	Finish	Insulation	Impedance	Crimp Tool
132264	N/A	Gold	Teflon	50	N/A
132264SS	N/A	S/S	Teflon	50	N/A
132264-10SS	N/A	S/S	Teflon	50	N/A
SOLDER POT CONTACT					

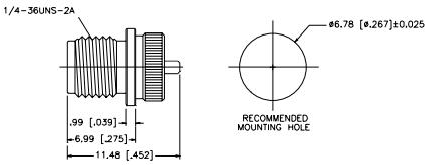

BULKHEAD MOUNT/SOLDER POT TERMINALS

BULKHEAD JACK RECEPTACLE — FRONT MOUNT

P.N.	Cable Group	Finish	Insulation	Impedance	Crimp Tool
132137	N/A	Gold	Teflon	50	N/A
132271	N/A	Gold	Teflon	50	N/A
EXTENDED BODY, BLUNT POST					

132137

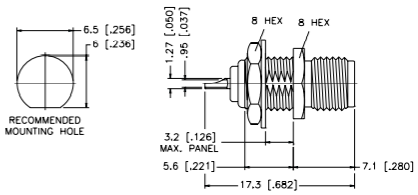

132271

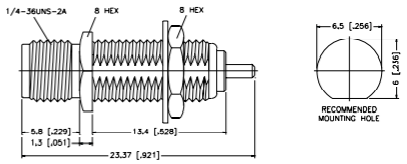

BULKHEAD JACK RECEPTACLE — REAR MOUNT

P.N.	Cable Group	Finish	Insulation	Impedance	Crimp Tool
132138	N/A	Gold	Teflon	50	N/A

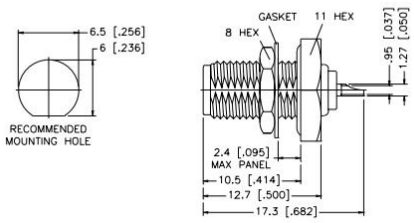

BULKHEAD JACK RECEPTACLE — REAR MOUNT

P.N.	Cable Group	Finish	Insulation	Impedance	Crimp Tool
132139	N/A	Gold	Teflon	50	N/A
132227	N/A	Gold	Teflon	50	N/A
	FLATWASHER				

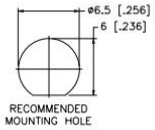

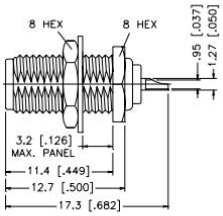

A2- MS4640 Series Microwave Vector Network Analyzers

Introduction This document provides the specifications for the MS4640A series microwave Vector Network Analyzers (VNAs) listed below, including all related options, and accessories.

Instrument Models and Operating Frequenciesa

• MS4642A – 10 MHz to 20 GHza

• MS4644A – 10 MHz to 40 GHza

• MS4645A – 10 MHz to 50 GHza

• MS4647A – 10 MHz to 70 GHza

Main Options

• MS4640A-002 – Time Domain

• MS4640A-007 – Receiver Offset

• MS464xA-041 – Noise Figure

• MS464xA-051 – Direct Access Loops

• MS464xA-061 – Active Measurements Suite, 2 Attenuators

• MS464xA-062 – Active Measurements Suite, 4 Attenuators

• MS4640A-070 – 70 kHz Low-End Frequency Extension

• MS4647A-080/081 – Broadband/Millimeter-Wave System

• MS464xA-082/083 – 110 GHz and Millimeter-Wave Extensions.

Separate documents found on the Anritsu web site (www.anritsu.com/VectorStar) provide specifications for 110 GHz Broadband Coaxial,

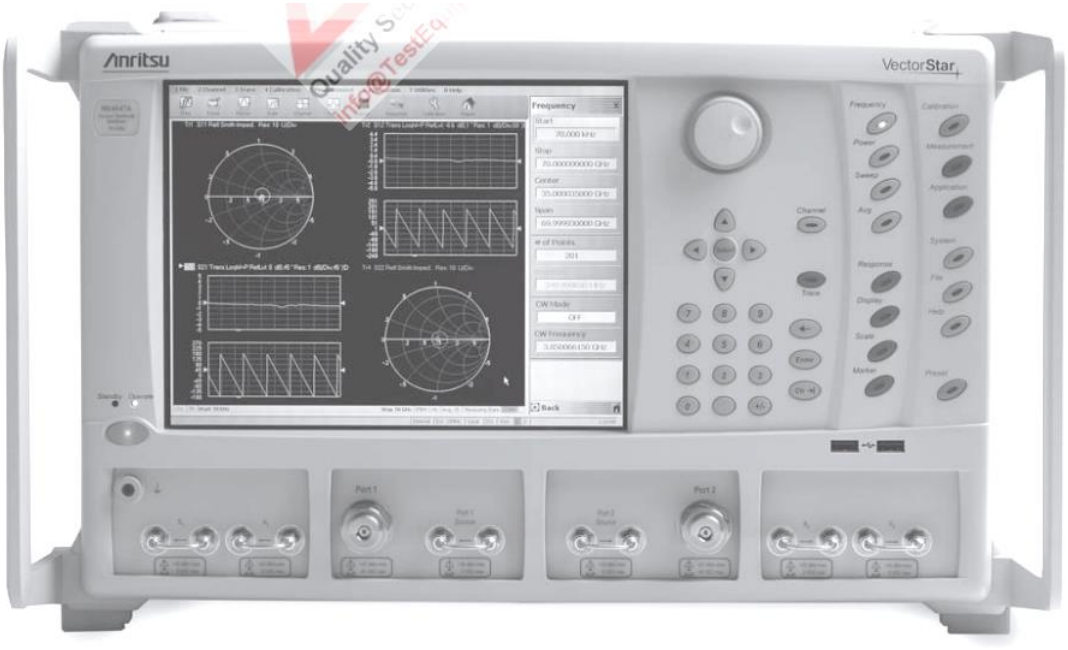

VectorStar MS4640A VNA Front Panel

1. Definitions

All specifications and characteristics apply under the following conditions, unless otherwise stated:

Warm-Up Time	After 90 minutes of warm-up time, where the instrument is left in the ON state.
Temperature Range	Over the 25 °C ± 5 °C temperature range.
Error-Corrected Specifications	For error-corrected specifications, over 23 °C ± 3 °C, with < 1 °C variation from calibration temperature. Error-corrected specifications are warranted and include guard-bands, unless otherwise stated.
User Cables	Specifications do not include effects of any user cables attached to the instrument.
Discrete Spurious Responses	Specifications may exclude discrete spurious responses.
Internal Reference Signal	All specifications apply with internal 10 MHz Crystal Oscillator Reference Signal.
Specifications Subject to Change	All specifications subject to change without notice. For the most current data sheet, please visit the Anritsu web site: www.anritsu.com
Typical Performance	"Typical" specifications describe expected, but not warranted, performance based on sample testing. They do not guarantee the performance of any individual product. No measurement uncertainty value is accounted for in the specification.
Characteristic Performance	Characteristic performance indicates a performance designed-in and verified during the design phase. It does include guard-bands and is not covered by the product warranty.
Below 300 kHz	All uncertainties below 300 kHz are typical.
Recommended Calibration Cycle	12 months

2. System Dynamic Range

Calculated as the difference between the maximum rated source power and the specified noise floor at the specified location.

MS4642A, 20 GHz Model, System Dynamic Range (dB)

	at Ports 1 or 2			at b1 or b2	
Frequency Range	**Standard**	**Option 051**	**Option 061 [a] or 062**	**Option 051**	**Option 061 [a] or 062**
0.07 to 0.3 MHz	85	83	81	114	112
0.3 to 2 MHz	102	100	98	126	124
2 to 10 MHz	115	113	111	134	132
0.01 to 2.5 GHz	122	119	114	140	135
2.5 to 20 GHz	123	119	115	134	130

a. The Option 061 Dynamic Range reported in this column applies for S_{21} measurements. For S_{12} Dynamic Range, use the figures from the Option 051 column.

MS4644A, 40 GHz Model, System Dynamic Range (dB)

	at Ports 1 or 2			at b1 or b2	
Frequency Range	**Standard**	**Option 051**	**Option 061 [a] or 062**	**Option 051**	**Option 061 [a] or 062**
0.07 to 0.3 MHz	85	83	81	114	112
0.3 to 2 MHz	102	100	98	126	124
2 to 10 MHz	115	113	111	134	132
0.01 to 2.5 GHz	122	119	114	140	135
2.5 to 40 GHz	119	115	110	130	125

a. The Option 061 Dynamic Range reported in this column applies for S_{21} measurements. For S_{12} Dynamic Range, use the figures from the Option 051 column.

MS4645A & MS4647A, 50 & 70 GHz Models, System Dynamic Range (dB)

	at Ports 1 or 2			at b1 or b2	
Frequency Range	**Standard**	**Option 051**	**Option 061 [a] or 062**	**Option 051**	**Option 061 [a] or 062**
0.07 to 0.3 MHz	85	83	81	114	112
0.3 to 2 MHz	102	100	98	126	124
2 to 10 MHz	115	113	111	134	132
0.01 to 2.5 GHz	122	119	114	140	135
2.5 to 5 GHz	116	112	106	127	121
5 to 20 GHz	115	111	105	126	120
20 to 38 GHz	116	111	105	126	120
38 to 50 GHz	115	109	104	124	119
50 to 65 GHz	107	101	97	116	112
65 to 67 GHz	103	97	91	112	106
67 to 70 GHz	100	91	84	106	99

a. The Option 061 Dynamic Range reported in this column applies for S_{21} measurements. For S_{12} Dynamic Range, use the figures from the Option 051 column.

3. Receiver Dynamic Range

Calculated as the difference between the maximum receiver input level for 0.1 dB compression and the specified noise floor at the specified location. Characteristic Performance.

All Models, Receiver Dynamic Range (dB)

	at Ports 1 or 2			at b1 or b2	
Frequency Range	**Standard**	**Option 051**	**Option 061[a] or 062**	**Option 051**	**Option 061[a] or 062**
0.07 to 0.3 MHz	80	79	78	90	89
0.3 to 2 MHz	102	102	102	107	107
2 to 10 MHz	115	115	115	115	115
0.01 to 2.5 GHz	120	119	116	119	116
2.5 to 5 GHz	120	118	115	117	114
5 to 20 GHz	120	118	115	118	115
20 to 40 GHz[b]	120	118	115	118	116
38 to 50 GHz	120	118	117	117	117
50 to 65 GHz	117	115	115	113	114
65 to 67 GHz	115	113	111	110	109
67 to 70 GHz	113	110	109	107	108

a. The Option 061 Dynamic Range reported in this column applies for S21 measurements. For S12 Dynamic Range, use the figures from the Option 051 column.

b. 20 to 38 GHz for MS4647A

4. Receiver Compression

Port power level beyond which the response may be compressed more than 0.1 dB relative to the normalization level. 10 Hz IF bandwidth used to remove any trace noise effects. Match not included. Performance is characteristic.

All Models, Compression Levels (dBm)

	0.1 dB Compression Levels in dBm relative to the Normalization Level[a]					
	at Ports 1 or 2			at a_x loops	at b_x loops	
Frequency Range	Standard	Option 051	Option 061[b] or 062	Option 051, 061, or 062	Option 051	Option 061 or 062
< 0.3 MHz	+5	+5	+5	−15	−15	−15
0.3 to 10 MHz	+10	+11	+12	−10	−10	−9
0.01 to 2.5 GHz	+10	+11	+12	−10	−10	−9
2.5 to 5 GHz	+10	+11	+12	−5	−5	−4
5 to 20 GHz	+10	+11	+12	−4	−4	−3
20 to 40 GHz[c]	+10	+11	+12	−4	−4	−2
38 to 50 GHz	+10	+12	+14	−4	−4	−1
50 to 65 GHz	+10	+12	+14	−5	−5	−2
65 to 67 GHz	+10	+13	+15	−5	−5	−2
67 to 70 GHz	+10	+13	+15	−5	−5	−1

a. 0.17 dB for < 0.3 MHz.

b. The Option 061 compression level reported in this column applies to Port 2 or b_2. For Port 1 or b_1 compression level, use the figures from the appropriate Port X or b_x "Option 051" column.

c. 20 to 38 GHz for MS4647A.

5. High Level Noise

Measured at 1 kHz IF bandwidth, at default power, with either full reflects or through transmission. RMS. Characteristic performance on MS4647A with either Option -051, -061, or -062. Trace noise magnitude may be degraded to 20 mdB RMS (typical) at particular frequencies, due to spurious receiver residuals.

Frequency (GHz)	Magnitude (dB)	Phase (degree)
< 500 kHz	< 0.04	< 0.4
500 kHz to 2.5	< 0.0045	< 0.05
2.5 to 5	< 0.0045	< 0.05
5 to 20	< 0.0045	< 0.05
20 to 40	< 0.006	< 0.06
40 to 67	< 0.006	< 0.08
67 to 70	< 0.008 (< 0.006)	< 0.08

6. Noise Floor

Measured at 10 Hz IF Bandwidth with no averaging, and at –10 dBm port power. RMS, no leakage correction applied. Measurement made with a through line connection, with its effects compensated for. Performance at a_x and b_x loops is characteristic.

All Models, Noise Floor (dBm)

	At Ports 1 or 2			At a_x Loops	At b_x Loops	
Frequency Range	Standard	Option 051	Option 061[a] or 062	Option 051, 061, or 062	Option 051	Option 061[a] or 062
0.07 to 0.3 MHz	−75	−74	−73	−105	−105	−104
0.3 to 2 MHz	−92	−91	−90	−117	−117	−116
2 to 10 MHz	−105	−104	−103	−125	−125	−124
0.01 to 2.5 GHz	−110	−108	−104	−129	−129	−125
2.5 to 40 GHz[b]	−110	−107	−103	−121	−122	−118
38 to 50 GHz	−110	−106	−103	−121	−121	−118
50 to 65 GHz	−107	−103	−101	−118	−118	−116
65 to 67 GHz	−105	−100	−96	−115	−115	−111
67 to 70 GHz	−103	−97	−94	−112	−112	−109

a. The Option 061 noise floor reported in this column applies to Port 2 or b_2. For Port 1 or b_1 noise floor, use the figures from the appropriate $Port_x$ or b_x Option 051 column.

b. 2.5 to 38 GHz for the MS4647A VNA.

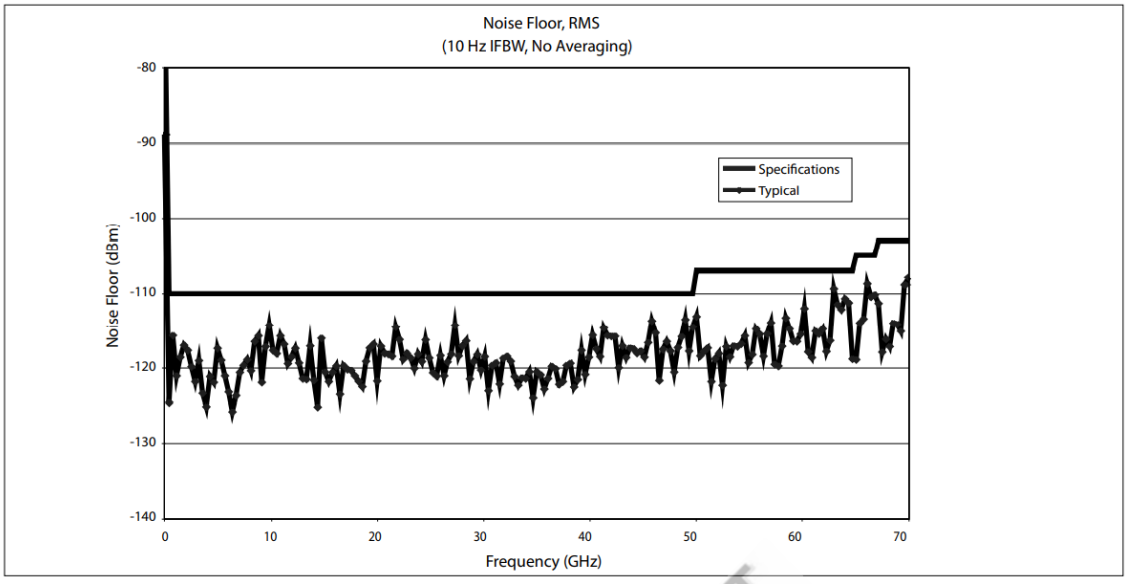

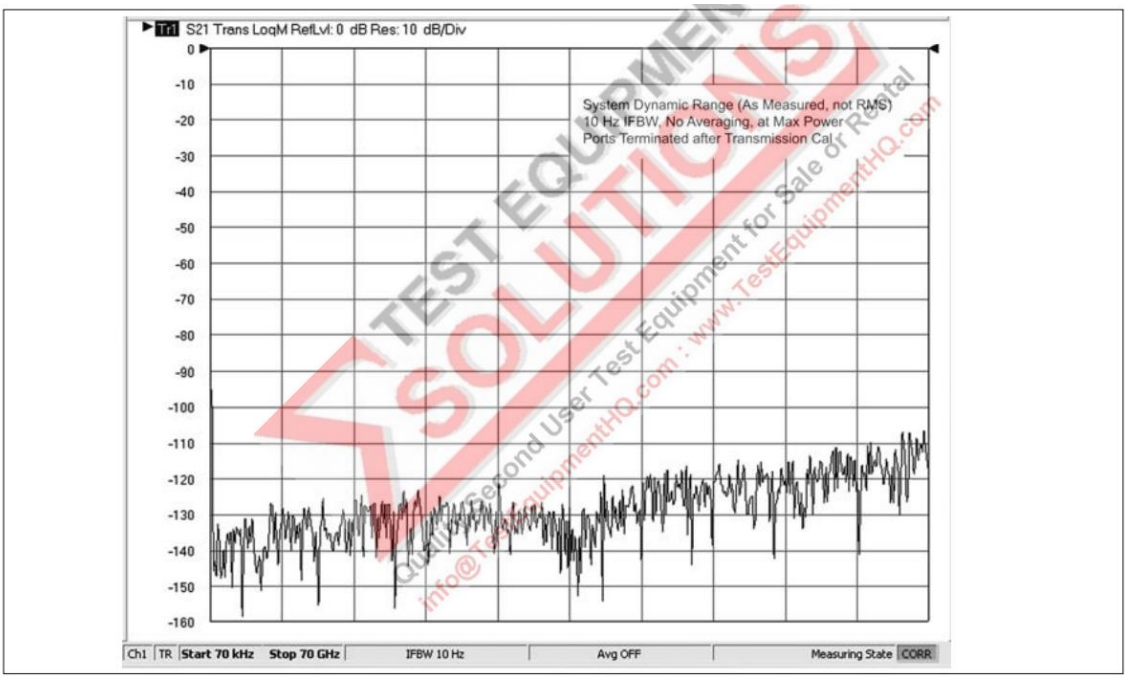

7. Power Range

Maximum Rated Power to minimum level. The difference reflects the ALC range for standard models or with Option 051, and the ALC + Attenuator Range for models with Options 061 or 062.

MS4642A, 20 GHz Model, Power Range (dBm to dBm)

Frequency	Standard (No Options)	Option 051	Option 061[a] or 062
< 0.01 GHz	+10 to –25	+9 to –25	+8 to –95
0.01 to 2.5 GHz	+12 to –25	+11 to –25	+10 to –95
2.5[a] to 20 GHz	+13 to –20	+12 to –20	+11 to –90

a. Typical between 2.5 and 2.7 GHz

MS4644A, 40 GHz Model, Power Range (dBm to dBm)

Frequency	Standard (No Options)	Option 051	Option 061[a] or 062
< 0.01 GHz	+10 to −25	+9 to −25	+8 to −95
0.01 to 2.5 GHz	+12 to −25	+11 to −25	+10 to −95
2.5 to 20 GHz	+9 to −20	+8 to −20	+7 to −90
20 to 40 GHz	+9 to −25	+8 to −25	+7 to −95

a. The Option 061 power range reported in this column applies to Port 1. For Port 2, use the figures from the Option 051 column.

MS4645A & MS4647A, 50 & 70 GHz Models, Power Range (dBm to dBm)

Frequency	Standard (No Options)	Option 051	Option 061[a] or 062
< 0.01 GHz	+10 to −25	+9 to −25	+8 to −85
0.01 to 2.5 GHz	+12 to −25	+11 to −25	+10 to −85
2.5 to 5 GHz	+6 to −20	+5 to −20	+3 to −80
5 to 20 GHz	+5 to −20	+4 to −20	+2 to −80
20 to 38 GHz	+6 to −25	+4 to −25	+2 to −85
38 to 50 GHz	+5 to −25	+3 to −25	+1 to −85
50 to 65 GHz	0 to −25	−2 to −25	−4 to −85
65 to 67 GHz	−2 to −25	−3 to −25	−5 to −85
67 to 70 GHz	−3 to −25	−6 to −25	−10 to −85

a. The Option 061 power range reported in this column applies to Port 1. For Port 2 Power Range, use the figures from the Option 051 column.

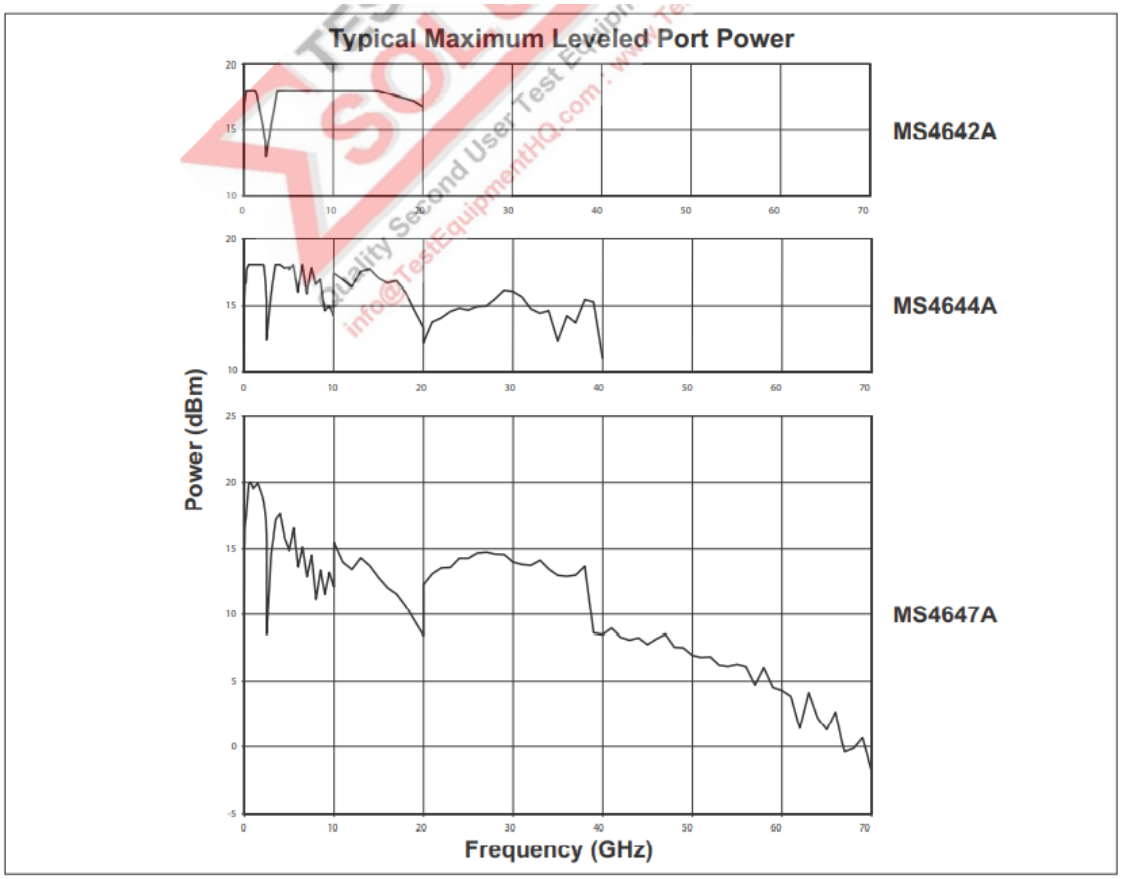

8. Output Default Power

Instrument default power. For maximum rated power, see section **7. Power Range** on page 7 above.

Model	Standard (No Options)	Option 051, 061 or 062
MS4642A, 20 GHz	+5 dBm	+5 dBm
MS4644A, 40 GHz	+5 dBm	+5 dBm
MS4645A, 50 GHz	–3 dBm	–10 dBm
MS4647A, 70 GHz	–3 dBm	–10 dBm

9. Power Accuracy, Linearity, and Resolution

Frequency (GHz)	Accuracy[a] (dB)	Linearity[b] (dB)	Resolution (dB)
< 0.01	± 1.5	± 1.5	0.01
0.01 to 40	± 1.5	± 1.0	0.01
40 to 67	± 3.0	± 1.0	0.01
67 to 70	± 4.0 (± 3.0)	± 2.0 (± 1.0)	0.01

a. Measured at default power

b. Measured between default and 5 dB below default port power.

10. Measurement Stability

Ratio measurement, with ports shorted. Characteristic.

Frequency (GHz)	Magnitude (dB/°C)	Phase (degree/°C)
< 0.01	< 0.04	< 0.4
0.01 to 20	< 0.02	< 0.2
20 to 40	< 0.03	< 0.5
40 to 67	< 0.03	< 0.7
67 to 70	< 0.04	< 0.8

11. Frequency Resolution, Accuracy, and Stability

Resolution	Accuracy	Stability
1 Hz	± 5 x 10^{-7} Hz/Hz (at time of calibration)	< 5 x 10^{-9}/°C over 0 °C to 50 °C temperature < 1 x 10^{-9}/day aging, instrument on

12. Phase Noise, Harmonics, and Non-Harmonics (Spurious)

Measured at default power. Non-Harmonics are characteristic performance.

Frequency (GHz)	SSB Phase Noise (dBc/Hz) at 10 kHz offset	Harmonics (dBc) (second and third)	Non-Harmonic Spurious (dBc) at > 1 kHz offsets
< 0.01	–78	–20	–20
0.01 to 2.5	–84	–20	–30
2.5 to 5	–84	–20[a]	–30
5 to 10	–78	–20	–30
10 to 20	–72	–20	–30
20 to 40	–66	–20	–30
40 to 67	–61	–20	–30
67 to 70	–61	–20	–30

a. May degrade by 3 dB (typical) between 2.5 and 2.7 GHz.

13. Uncorrected (Raw) Port Characteristics

Characteristic performance with either Option -051, -061, or -062.

Frequency Range (GHz)	Directivity (dB)	Port Match[a] (dB)
<0.01	> 10[b]	> 8
0.01 to 2.5	> 9[b]	> 10
2.5 to 5	> 20	> 10
5 to 20	> 17	> 9
20 to 40	> 14	> 7
40 to 65	> 11	> 7
65 to 67	> 11	> 7
67 to 70	> 5 (> 10)	> 7

a. Port Match is defined as the worst of source and load match.

b. Raw Directivity degraded to 4 dB (typical) below 300 kHz and in a 300 MHz window below 2.5 GHz.

14. MS4642A 20 GHz VNA System Performance

14.1 MS4642A – 12-Term SOLT – Sliding Load – 3652A-1 K Calibration Kit

MS4642A 20 GHz Model, with 12-term SOLT with Sliding Load Calibration, using the 3652A-1 K Calibration Kit.

Frequency Range (GHz)	Directivity (dB)	Source Match (dB)	Load Match[a] (dB)	Reflection Tracking (dB)	Transmission Tracking (dB)
< 0.01 GHz	> 38	> 36	> 38	± 0.02	± 0.05
0.01 to 2.5 GHz	> 42	> 41	> 42	± 0.005	± 0.03
2.5 to 20 GHz	> 43	> 39	> 43	± 0.006	± 0.07

a. Since Residual Load Match is limited by Residual Directivity and the user test port cable, it can only be specified as Residual Directivity. For practical considerations, derate it by ≈ 8 dB for a 3670 Series test port cable, to compensate for effects such as match, repeatability, bend radius, and similar parameters.

A3-FR-4

FR-4 glass epoxy is a popular and versatile high-pressure thermoset plastic laminate with good strength to weight ratio. With near zero water absorption, FR-4 is most commonly used as an electrical insulator possessing considerable mechanical strength. "FR" is an abbreviation for Flame Retardant, and Type "4" indicates woven glass reinforced epoxy resin. The material is known to retain its high mechanical values and electrical insulating qualities in both dry and humid conditions. These attributes, along with good fabrication characteristics offer many options for a wide variety of electrical and mechanical applications.

Benefits
Electrically insulative
Can be fabricated
Good strength to weight ratio
Near zero water absorption

Applications
Printed circuit boards (PCB)
Electrical insulation
Relays
Switches
Standoffs
Busbars

SHAPES AVAILABLE

FR-4 Glass Epoxy Technical Product Information

Property	Units	Value	Condition
Tg, min. (DSC)	°C	135	
CTE x-axis	ppm/°C	14	Ambient to Tg
CTE y-axis	ppm/°C	13	Ambient to Tg
CTE z-axis	ppm/°C	175	Ambient to 288 °C
Solder Float, 288 °C	seconds	>120	Condition A

Electrical Properties

Property	Units	Value	Condition
Permittivity (DK) max.		4.7	C-24/23/50
@ 500 Mhz		4.35	
@1 GHz (HP4291)		4.34	
Loss Tangent (DF), max. @			
1 MHz (2 Fluid Cell)		0.020	
500 Mhz		0.017	
1 GHz (2 Fluid Cell)		0.016	
Surface Resistivity, min.	megohms	2 X 10^5	Condition F
		1 X 10^8	E-24/125
Volume Resistivity, min.	min.	8 X 10^7	Condition F
	megohm-cm	2 X 10^7	E-24/125
Dielectric Breakdown, min	kV	55	D-48/50
Arc Resistance, min.	seconds	100	

Physical Properties

Property	Units	Value	Condition
Peel Strength, 1 oz.	lb./in.	9.0	Condition A
		9.0	After Thermal Stress
		9.0	E-1/125
Flexural Strength - LW	psi	80000	Condition A
Flexural Strength - CW	psi	60000	Condition A
Warp & Twist	%	0.5	Condition
Flammability		V-0	UL94
Moisture Absorption	%	< 0.25	D-24/23
Tensil Strength - LW	psi	50000	Condition A
Tensil Strength - CW	psi	40000	Condition A
Tensil Modulus (Young's) - LW	psi	3.5 X 10^6	Condition A
Tensil Modulus (Young's) - CW	psi	3.0 X 10^6	Condition A
Flexural Modulus (Taylor's) - LW	psi	2.7 X 10^6	Condition A
Flexural Modulus (Taylor's) - CW	psi	2.4 X 10^6	Condition A
Poisson's Ratio - LW		0.136	Condition A
Poisson's Ratio - CW		0.118	Condition A

الخلاصة

أدى التطور السريع للتطبيقات القابلة للارتداء المعتمدة على شبكات الجيل الخامس إلى الحاجة الملحة لأنواع محددة من الهوائيات. يجب أن تتمتع هذه الهوائيات باستهلاك منخفض للطاقة وصغر الحجم ومرونة كبيرة وميزات أخرى. وبالتالي ، فإن هوائي microstrip هو الخيار الأفضل لهذه التطبيقات. في هذه الرسالة، تم تقديم هوائي مزدوج النطاق لتطبيقات الجيل الخامس القابلة للارتداء. يعمل الهوائي المقترح بترددات 6 جيجاهرتز و 28 جيجاهرتز ، والتي تقع ضمن نطاق ترددات الجيل الخامس. يتم محاكاة تصميم الهوائي والتحقق من صحته من خلال برنامجين: تقنية محاكاة الكمبيوتر (CST-Studio) وبرنامج محاكاة التردد العالي (HFSS) .

تُستخدم المواد Arlon AD 250C و Rogers RT / droid 5880 (tm) و FR4 كعوازل ، بالإضافة إلى النحاس للرقعة والأرض. تُظهر نتائج المحاكاة أن مادة Rogers RT / droid 5880 (tm) تتمتع بأداء أفضل مقارنة بالمواد الأخرى. ومع ذلك ، يتم استخدام مادة FR4 في عملية التصنيع بسبب عدم توفر Rogers RT / droid 5880 (tm) في الاسواق العراقية.

تم تصميم الهوائي المقترح بأربع طرق تغذية Microstrip line, Coaxial (coplanar feed), Proximity coupled, and Aperture coupled. تظهر نتائج المحاكاة أن طريقة ال Aperture coupled تمتلك نتائج أفضل من الطرق الأخرى. حيث تم حساب معاملات الهوائي المعتمد على طريقة ال Aperture coupled على النحو التالي: قيم S11 هي 69.2- ديسيبل و 23.2 ديسيبل عند ترددات 6 جيجا هرتز و 28 جيجا هرتز على التوالي ،ر بالإضافة إلى ان قيم VSWR هي 1.006 ديسيبل و 1.14 ديسيبل عند ترددات 6 جيجا هرتز و 28 جيجا هرتز على التوالي. علاوة على ذلك ، فإن قيم الكسب والكفاءة هي (3.72 ديسيبل و ٪ 65.7) و (7.07 ديسيبل و ٪ 97.5) لـترددات 6 جيجا هرتز و 28 جيجا هرتز على التوالي, تمت مقارنة هذه

النتائج مع بعض نتائج الاعمال السابقة وهذه المقارنة تبين أن الهوائي المقترح يتفوق على هذه الاعمال .

تم اختبار قدرة الانحناء للهوائي المقترح عن طريق ثنيه على أسطوانات ذات أنصاف أقطار مختلفة. حيث تُظهر نتائج المحاكاة أن نسخ الهوائي المنحني تمتلك نفس اداء الهوائي الاصلي. في الختام، تُظهر نتائج التصنيع أن الهوائي المصنع لديه مشكلة بسبب الفجوة الهوائية الموجودة بين عوازل الهوائي، والتي تُركت بسبب صلابة مادة ال FR4. ومع ذلك ، فقد تم تصحيح أداء الهوائي المصنع بضغط كلا الركيزتين أثناء عملية

.

جمهوريـــة العراق
وزارة التعليم العالي والبحث العلمي
جامعـــــة بابـــل
كليـــة الهندســـة / قسم الهندســـة
الكهربائية

تصميم هوائي ثنائي الحزمة قابل للارتداء

لتطبيقات الجيل الخامس

رسالة

مقدمـــة إلى كليـــة الهندســـة في جامعـــــة بابـــل

كجزء من متطلبات نيل درجـــــة الماجستير

الهندسة الكهربائية/ اتصالات في علوم

من قبل

شهلاء ياسين يونس العبادي

بأشراف

الدكتور

أ.م.د. محمد تايه كاطع

2023 م **1444 هـ**